ISSN 1881-7831 Online ISSN 1881-784X

DD&T

Drug Discoveries & Therapeutics

Volume 6, Number 1
February, 2012

IRCA BSSA

IACMHR

www.ddtjournal.com

DD&T
Drug Discoveries & Therapeutics

ISSN: 1881-7831
Online ISSN: 1881-784X
CODEN: DDTRBX
Issues/Year: 6
Language: English
Publisher: IACMHR Co., Ltd.

Drug Discoveries & Therapeutics is one of a series of peer-reviewed journals of the International Research and Cooperation Association for Bio & Socio-Sciences Advancement (IRCA-BSSA) Group and is published bimonthly by the International Advancement Center for Medicine & Health Research Co., Ltd. (IACMHR Co., Ltd.) and supported by the IRCA-BSSA and Shandong University China-Japan Cooperation Center for Drug Discovery & Screening (SDU-DDSC).

Drug Discoveries & Therapeutics publishes contributions in all fields of pharmaceutical and therapeutic research such as medicinal chemistry, pharmacology, pharmaceutical analysis, pharmaceutics, pharmaceutical administration, and experimental and clinical studies of effects, mechanisms, or uses of various treatments. Studies in drug-related fields such as biology, biochemistry, physiology, microbiology, and immunology are also within the scope of this journal.

Drug Discoveries & Therapeutics publishes Original Articles, Brief Reports, Reviews, Policy Forum articles, Case Reports, News, and Letters on all aspects of the field of pharmaceutical research. All contributions should seek to promote international collaboration in pharmaceutical science.

Editorial Board

Editorial and Head Office:

Pearl City Koishikawa 603,
2-4-5 Kasuga, Bunkyo-ku,
Tokyo 112-0003, Japan
Tel.: +81-3-5840-9697
Fax: +81-3-5840-9698
E-mail: office@ddtjournal.com

Drug Discoveries & Therapeutics

Editorial and Head Office

Pearl City Koishikawa 603, 2-4-5 Kasuga, Bunkyo-ku,
Tokyo 112-0003, Japan

Tel: +81-3-5840-9697, Fax: +81-3-5840-9698
E-mail: office@ddtjournal.com
URL: www.ddtjournal.com

Editorial Board Members

CONTENTS

Volume 6, Number 1, 2012

Review

Brief Reports

Original Articles

CONTENTS (*Continued*)

Mini-Review

DOI: 10.5582/ddt.2012.v6.1.1

Evidence-based research on traditional Japanese medicine, Kampo, in treatment of gastrointestinal cancer in Japan

Jianjun Gao[1,2], Peipei Song[1], Fanghua Qi[1], Norihiro Kokudo[1], Xianjun Qu[2], Wei Tang[1,2,*]

[1] *Hepato-Biliary-Pancreatic Surgery Division, Department of Surgery, Graduate School of Medicine, The University of Tokyo, Tokyo, Japan;*
[2] *Shandong University China-Japan Cooperation Center for Drug Discovery & Screening, Ji'nan, Shandong, China.*

ABSTRACT: Gastrointestinal cancer is a great threat to human health in Japan. Conventional anti-cancer therapies including surgery, radiation, and chemotherapy are the main strategies and play important roles in curing this disease or extending the life of patients with these cancers. On the other hand, patients undergo great suffering induced by these treatments. Kampo, the Japanese traditional medicine, has been used in clinics to reduce side effects and to improve the quality of life of gastrointestinal cancer patients in Japan. In order to testify to the efficacy and safety of these Kampo medicines and to clarify the underlying mechanisms, a number of clinical and basic studies were implemented in the past several decades. These studies suggested the benefits of Kampo medicine as an adjuvant to conventional anti-cancer therapies in treating gastrointestinal cancer. Since the safety and efficacy as well as quality control of traditional medicine have long been focused worldwide, the development course of Kampo medicine may provide reference to other countries in the world.

Keywords: Kampo, traditional medicine, gastrointestinal cancer, side effects, quality of life

1. Introduction

Traditional medicine, defined in contrast to Western medicine, is the sum total of knowledge, skills and practices based on theories, beliefs and experiences indigenous to different cultures that are used to maintain health, as well as to prevent, diagnose, improve or treat physical and mental illnesses (*1*). In the world, traditional medicine is generally available, affordable, and commonly used in large parts of Asia, Africa, and Latin America (*2*). In some of the African countries such as Uganda, Tanzania and Ethiopia, 60-90% of the population depends on traditional medicine for primary health care at the present time (*3*). Moreover, the use of traditional medicine as complementary/alternative medicine (CAM) has been reported in 70-90% of populations in developed countries such as Canada, France, Germany and Italy (*3*). In Asia, the use of traditional medicine in Japan (Kampo) has a history of thousands of years and plays an important role to insure human health. Indeed, it is reality that traditional medicine can treat various chronic conditions (*4*). However, evidence of safety and efficacy as well as quality control of traditional medicine have long been focused and highlighted by policy-makers, medical professionals and/or the public in many countries in the world (*5-9*).

Cancer has been the leading cause of death in Japan since 1981 (*10*). In 2010, a total of 353,000 people died of this disease, accounting for one in every three deaths, according to the statistics published by the Japan Ministry of Health, Labor and Welfare. Among causes of cancer deaths in 2009, stomach, colon, rectum, liver, gallbladder and bile ducts, and pancreas cancers lead to 169,932 deaths which make up 49.4% of all deaths induced by malignant tumors (*11*). Thus gastrointestinal tumors are extremely serious cancer types and the most common causes of cancer-related death in Japan at the present stage. Due to early detection by mass screening and application of modern cancer treatment strategies including surgery, radiation, and chemotherapy, the 5-year survival rates of patients with gastrointestinal cancers have shown steady improvement since 1962 according to the hospital-based cancer registry of Japan National Cancer Center Hospital (*12*). On the other hand, those conventional therapies inflict great suffering and require stoic endurance on the part of the patients. In this context, Kampo was introduced into gastrointestinal tumortherapy, aiming to deal with problems such as the side effects of radiotherapy and chemotherapy and various types of general malaise (*13-15*).

**Address correspondence to:*
Dr. Wei Tang, Hepato-Biliary-Pancreatic Surgery Division, Department of Surgery, Graduate School of Medicine, The University of Tokyo, 7-3-1 Hongo, Bunkyo-ku, Tokyo, Japan.
E-mail: TANG-SUR@h.u-tokyo.ac.jp

2. Research on Kampo medicine in treatment of gastrointestinal cancer

Kampo medicine plays an important role in cancer prevention in high-risk groups, enhancement of tumor immunity, improvement of general condition after operations, and attenuation of adverse reactions to chemotherapy and radiation. Although several herbs were supposed to have direct antitumor activity, Kampo medicine mainly acts as a kind of adjuvant to conventional antitumor treatments in clinical practice, contributing to the maintenance of a good quality of life for cancer patients (*16*). In this regard, Kampo formulas such as Juzentaihoto, Ninjin'yoeito, Hochuekkito, Shosaikoto, Daikenchuto, and Hangeshashinto are often prescribed to patients with gastrointestinal cancers in Japan (Table 1) (*17-21*).

2.1. *Clinical studies on Kampo medicine used for care of gastrointestinal cancer*

The approval of the currently used Kampo for application in clinics is without rigorous clinical trials from phases I to III but simply based on that Kampo medicine had passed the test of a thousand years of historical experience in Japan (*22*). Although the efficacy of Kampo is believed by many prescribers and patients, objective evaluation of those Kampo medicines to attain scientific evidence is trend-driven. In this regard, a number of clinical trials were carried out to testify to the efficacy and safety of Kampo in Japan. In order to disseminate evidence-based medicine in Kampo products, the Japan Society for Oriental Medicine established the Special Committee for Evidence-based Medicine (EBM) in 2001, aiming to present evidence from "good" studies of Kampo products such as randomized controlled trials (RCTs) published from 1986 when the quality of Kampo formulations reached the present levels. According to their studies, based on the criteria that *i*) studies that employed Kampo formulations are approved by Japan government as a research object, *ii*) studies that used rational methods for experimental design including randomized controlled trials (RCTs), quasi-randomized controlled trials (quasi-RCTs), crossover trials, and meta-analyses, it was demonstrated that there are a total of 359 randomized controlled clinical trials and 1 meta-analysis on Kampo products from the year 1986 (including 1986) to June 2010 (*23*). Based on that evidence, fifty nine Kampo medicines were recommended and included in Japanese Clinical Practice Guidelines by March 31, 2011 (*24*).

The efficacy of Kampo medicine in preventing cancer occurrence, enhancing the immune system, and/or reducing the side effects of conventional therapies has been testified through EBM based clinical trials (Table 2). The combination of operations with chemotherapy is the most common treatment strategy

Table 1. Kampo medicines that are currently used for treatment of gastrointestinal cancers in Japan

Kampo	Formulation*	Composition of crude drugs**	Approved indications
Juzentaihoto	Granules	Astragalus Root, Cinnamon Bark, Rehmannia Root, Peony Root, Cnidium Rhizome, Atractylodes Lancea Rhizome, Japanese Angelica Root, Ginseng, Poria Sclerotium, Glycyrrhiza	Relief of declined constitution after recovery from disease, fatigue and malaise, anorexia, perspiration during sleep, cold limbs, and anemia.
Ninjin'yoeito	Granules	Rehmannia Root, Japanese Angelica Root, Atractylodes Rhizome, Poria Sclerotium, Ginseng, Cinnamon Bark, Polygala Root, Peony Root, Citrus Unshiu Peel, Astragalus Root, Glycyrrhiza, Schisandra Fruit	Relief of declined constitution after recovery from disease, fatigue and malaise, anorexia, perspiration during sleep, cold limbs, and anemia.
Hochuekkito	Granules	Astragalus Root, Atractylodes Lancea Rhizome, Ginseng, Japanese Angelica Root, Bupleurum Root, Jujube, Citrus Unshiu Peel, Glycyrrhiza, Cimicifuga Rhizome, Ginger	Indicated for the symptoms/conditions of patients having delicate constitution, reduced digestive functions, and severe fatigability of limbs.
Shosaikoto	Granules	Bupleurum Root, Pinellia Tuber, Scutellaria Root, Jujube, Ginseng, Glycyrrhiza, Ginger	Relief of the following symptoms of those patients with moderately strong constitution, right upper abdominal tenderness accompanied by fullness and discomfort, coated tongue, oral cavity discomfort, anorexia, and/or those with slight fever and nausea; Improvement of liver dysfunction due to chronic hepatitis.
Daikenchuto	Granules	Processed Ginger, Ginseng, Zanthoxylum Fruit	Relief of abdominal cold feeling and pain accompanied by abdominal flatulence.
Hangeshashinto	Granules	Pinellia Tuber, Scutellaria Root, Processed Ginger, Glycyrrhiza, Jujube, Ginseng, Coptis Rhizome	Relief of the symptoms of those patients with blocked feeling in the stomach pit and occasional nausea, vomiting, anorexia, borborygmus, and a tendency to loose stools or diarrhea.

* Granules are a mixture of extract of crude drugs indicated and certain medicinal accessory materials.
** All the crude drugs comply with the Japanese Pharmacopoeia.

Table 2. Clinical trials of Kampo in treatment of gastrointestinal cancer in Japan

Kampo Formula	Tumor	Study Design	Study Purpose	Conclusion	*Ref.*
Juzentaihoto	Gastric cancer	RCT-envelope 33 patients	Improvement effect on host-immunity in patients undergoing postoperative adjuvant chemo-therapy (tegafur/uracil (UFT) 300 mg/day).	Juzentaihoto is useful in gastric cancer patients undergoing postoperative adjuvant UFT.	*27*
Juzentaihoto	Gastric cancer	RCT 94 patients	Efficacy of Juzentaihoto combined with oral 5-fluorouracil (5-FU) as postoperative adjuvant chemotherapy in patients with surgically treated gastric cancer.	Combination of Juzentaihoto with oral 5-FU is effective for patients with surgically treated stage III or IV gastric cancer.	*28*
Juzentaihoto	Colorectal cancer	RCT-envelope 44 patients	To elucidate the mechanism by which Juzentaihoto reduces the adverse reaction to treatment with 5-FU (hepatopathy) by determining the distribution of 5-FU in tissues of patients with colorectal cancer receiving slow-release tegafur preoperatively.	Administration of Juzentaihoto in patients receiving slow-release tegafur capsules increases 5-FU concentration in tumor tissues but decreases 5-FU concentration in normal tissues, enhancing the tumor selectivity of tegafur. This effect may be partly due to the modulation by Juzentaihoto of thymidine phosphorylase activity in tissues and of cytochrome P-450.	*36*
Juzentaihoto	Colorectal cancer	RCT 168 patients	To evaluate the clinical efficacy of Juzentaihoto for the prevention of postoperative recurrence of colorectal cancer.	Juzentaihoto may have a metastasis-suppressive effect, but since these are interim reports, the follow-up is still ongoing.	*37* *38*
Juzentaihoto	Hepatocellular carcinoma	RCT 20 patients	To evaluate the effect of Juzen-taihoto for reducing adverse effects of spongel + lipiodol + phosphatidyl choline + cisplatin treatment in transarterial embolization (TAE) for hepatocellular carcinoma.	Juzentaihoto significantly suppresses nausea/vomiting after TAE with spongel + lipiodol + phosphatidyl choline + cisplatin for hepatocellular carcinoma.	*34*
Juzentaihoto	Esophageal, gastric, or colorectal cancer	RCT-envelope 174 patients	Effect on the cell-mediated immunity of postoperative patients with esophageal, gastric, or colorectal cancer.	Juzentaihoto postoperatively administered for treatment of esophageal, gastric, or colorectal cancer may act as a biological response modifier (BRM).	*39*
Juzentaihoto	Gastric and colorectal cancer	RCT-envelope 284 patients	To evaluate the efficacy of Juzentaihoto for reducing adverse effects and improving quality of life (QOL) in postoperative patients undergoing chemotherapy (UFT 4 capsules/day) for gastric, colorectal, or breast cancer (curative resection/ non-curative resection).	Juzentaihoto reduces the number of adverse drug reactions and improves QOL in postoperative patients on chemotherapy (UFT 4 capsules/day) for gastric, colorectal, or breast cancer.	*29* *30*
Ninjin'yoeito	Gastric cancer	RCT-envelope 46 patients	Efficacy for reducing adverse effects and improving performance status in patients undergoing postoperative adjuvant chemotherapy (fluoropyrimidine anticancer drug).	Ninjin'yoeito tends to suppress the decreases in RBC count and platelet count but not the decrease in WBC count and does not improve performance status in patients undergoing postoperative adjuvant fluoropyrimidine-based chemotherapy for gastric cancer.	*31*
Ninjin'yoeito	Colorectal cancer	RCT-envelope 23 patients	Immunostimulation and improvement of nutritional status in postoperative patients with colorectal cancer.	Ninjin'yoeito significantly promotes improvement of lymphocyte count and PHA-stimulated lymphocyte proliferation in postoperative patients with colorectal cancer, suggesting its role as a possible biological response modifier.	*40*
Shosaikoto	Colorectal cancer	RCT 20 patients	Immunostimulation and suppression of liver metastasis in postoperative patients with colorectal cancer.	Saiko agents increased PHA-stimulated lymphocyte proliferation and NK cell activity, evaluated by CD57 and CD16, suggesting its immunostimulating effect.	*41*
Shosaikoto	Liver cancer	quasi-RCT 95 patients	Preventive effect on the progression of cirrhosis to liver cancer.	While not significant, the Shosaikoto treatment tends to lower the incidence of liver cancer and AFP.	*33*
Hochuekkito	Large intestine carcinoma	RCT-envelope 20 patients	To evaluate the efficacy of 1-week preoperative treatment with Hochuekkito for improving pre- and post-operative nutritional status and immune function in patients scheduled to undergo laparotomy for large intestine carcinoma.	Preoperative treatment with Hochuekkito may be useful for early recovery from surgery for large intestine carcinoma.	*42*

Continued

Hochuekkito	Gastric/colon cancer	RCT 51 patients	To evaluate the efficacy of pre-operative administration of Hochuekkito for postoperative systemic inflammatory response syndrome (SIRS) in gastric/colon cancer.	Preoperative administration of Hochuekkito significantly suppresses the postoperative inflammatory response to surgical wounding.	*25*
Hochuekkito	Gastric or colorectal cancer	RCT 48 patients	To evaluate whether preoperative administration of Hochuekkito relieves surgical stress in patients with gastric or colorectal cancer.	Preoperative administration of Hochuekkito extract granules reduces the response to surgical stress and may be helpful for accelerating postoperative recovery.	*26*
Daikenchuto	Large intestine carcinoma	RCT 30 patients	To evaluate the reduction in the number of days to post-operative flatulence and the anti-inflammatory efficacy of Daikenchuto in patients who underwent laparotomy for large intestine carcinoma.	Daikenchuto is useful in promoting flatulence and inhibiting inflammation after surgery for large intestine carcinoma.	*35*
Daikenchuto	Colorectal cancer	RCT 175 patients	To evaluate the effects of Daikenchuto on intestinal obstruction following colorectal cancer surgery.	Daikenchuto extract fine granules do not prevent ileus following colorectal cancer surgery, but do result in the reduction of postoperative abdominal pain and irregular bowel movements.	*43*
Daikenchuto	Liver carcinoma	RCT 20 patients	To evaluate the anti-inflammatory efficacy of Daikenchuto in postoperative patients with liver carcinoma.	Daikenchuto may be useful in inhibiting early postoperative inflammation after surgery for liver carcinoma.	*35*
Daikenchuto	Gastric and colorectal cancer	RCT-envelope 20 patients	To evaluate the efficacy of Hangeshashinto for delayed diarrhea induced by irinotecan in patients with metastatic gastric and colorectal cancer.	Hangeshashinto is a useful supportive therapy from the viewpoint of QOL in patients treated for advanced gastric and colorectal cancer with S-1/irinotecan combination therapy.	*32*

Abbreviations: RCT-envelope, randomized controlled trial using sealed envelopes for allocation; RCT, randomized controlled trial; quasi-RCT, quasi-randomized controlled trial.

for gastric cancer. It was demonstrated that preoperative administration of the Kampo medicine Hochuekkito could be helpful in suppressing the postoperative inflammatory response to surgical wounding and accelerating postoperative recovery (*25,26*). In addition, Juzentaihoto, Ninjin'yoeito, and Hangeshashinto were exhibited to have abilities in improving host-immunity and reducing side effects in gastric cancer patients undergoing postoperative adjuvant chemotherapy including tegafur-uracil (UFT), 5-FU, fluoropyrimidine, and irinotecan treatments (*27-32*). The application of Kampo medicine in treatment of liver cancer were also studied (*33-35*). For example, Juzentaihoto was found to suppresses nausea/vomiting after transarterial embolization (TAE) with spongel + lipiodol + phosphatidyl choline + cisplatin for hepatocellular carcinoma (*34*). In addition, Daikenchuto may be useful in inhibiting early postoperative inflammation after surgery for liver carcinoma (*35*). The efficacy of Kampo medicine in treating large intestine cancer and colorectal cancer were extensively investigated. A series of Kampo products including Juzentaihoto, Ninjin'yoeito, Shosaikoto, Hochuekkito, Daikenchuto, and Hangeshashinto were proved to be effective in stimulating immune system, improving nutritional status, acting as biological response modifier, enhancing the tumor selectivity of chemotherapy drugs, or improving the quality of life of cancer patients (Table 2). These clinical studies suggested the benefits of Kampo medicine in combination with conventional anti-cancer strategies in treatment of gastrointestinal cancers.

2.2. *Basic studies on the mechanisms underlying the effects of Kampo medicine*

Mechanisms underlying the effects of those Kampo medicines have been extensively investigated. Studies indicated that the immunity regulation effects of **Juzentaihoto** and **Hochuekkito** were related with enhancement of humoral immunity, cell-mediated immunity, natural killer (NK) activity, macrophage activity, and production of immunity related cytokines. It was found that oral administration of Juzentaihoto inhibited liver metastasis of colon cancer cells implanted in mice. However, this inhibitory effect was not observed in mice pretreated with 2-chloroadenosine which had an effect to inactivate macrophages. Hochuekkito enhanced the *in vitro* cytotoxic activity of activated T lymphocytes from healthy volunteers and cancer patients (*44*). In a mouse cancer metastasis model prepared by implanting mouse colon cancer cells (Colon 26-L5), removal of NK cells led to the disappearance of the inhibitory effects of Hochuekkito on cancer metastasis (*45*). In addition, oral administration of Hochuekkito to mice enhanced the anti-tumor cytotoxic activity of peritoneal exudate

cells (*46*) and inhibited restraint of a stress-induced decrease of serum interleukin (IL)-12 in tumor bearing mice (*47*). These studies indicated that Juzentaihoto and Hochuekkito may exhibit indirect antitumor activity through enhancing the organism's antineoplastic immune response.

Shosaikoto was shown to lower the incidence of liver cancer in clinical studies (*33*). Basic studies indicated that Shosaikoto has ability to prevent hepatopathy. In hepatocytes isolated from rats, Shosaikoto inhibited antibody-dependent cellular cytotoxicity (ADCC) responses and cell impairment induced by the culture supernatant of activated macrophages (*48*). In addition, Shosaikoto could inhibit liver fibrosis, which may decrease the risk of liver cancer. In rat liver stellate cells, Shosaikoto inhibited proliferation and transformation to myofibroblast-like cells, and suppressed type I/III procollagen mRNA expression (*49*). In another study, a diet containing Shosaikoto was given to a rat fibrosis model induced by dimethylnitrosamine or porcine serum. It inhibited an increase in the malondialdehyde level *in vivo*. Furthermore, it inhibited oxidative stress in rat liver stellate cells and hepatocytes *in vitro* (*50*). These studies illustrated the direct protective effects of Shosaikoto on liver cells. Also, Shosaikoto was found to exhibit an immune stimulatory effect. Oral administration of Shosaikoto to mice and rats activated macrophages (*48*). Other studies demonstrated that Shosaikoto showed a regulatory effect on production of cytokines. For example, oral administration of Shosaikoto increased the production of IL-1, IL-2, IL-1β, IL-6, IL-10, GM-CSF, TNF-α, and IFN-γ and decreased the excessive production of IL-4 and IL-5 in peripheral blood mononuclear cells derived from healthy individuals or chronic hepatitis patients (*48,51-53*). The activities of lymphokine-activated killer (LAK) cells and NK cells in human peripheral blood mononuclear cells were also enhanced after oral administration of Shosaikoto (*48*). All these experimental studies elucidated the mechanisms underlying the anti-tumor effects of Shosaikoto.

Daikenchuto showed benefits to patients with ileus following colorectal cancer surgery in clinical studies. The pharmacological effects of Daikenchuto are displayed in two aspects (*54*). First, oral administration of Daikenchuto promoted gastrointestinal motility through enhancing the contraction of stomach/duodenum in the resting phase in healthy subjects. Second, oral administration of Daikenchuto increased the plasma motilin, gastrin, plasma vasoactive intestinal polypeptide (VIP), calcitonin gene related peptide (CGRP), substance P, and serotonin levels in healthy subjects or patients with paralytic ileus after extensive hysterectomy with pelvic lymphadenectomy (*55-57*). Mechanisms behind the pharmacological actions of Daikenchuto were illustrated in animal studies. Daikenchuto improved chlorpromazine-induced decrease of small intestinal and distal colonic transit in mice. It was found that atropine and a cholecystokinin receptor antagonist, lorglumide, could antagonize the activities of Daikenchuto (*58*). In isolated rabbit jejunum, Daikenchuto also enhanced spontaneous contractions and reversed the decrease of spontaneous contractions inhibited by atropine. In the longitudinal muscle of isolated guinea pig ileum, Daikenchuto induced contractions and acetylcholine (ACh) release. The contraction induction effect could be inhibited by pretreatment or concurrent use of atropine, tetrodotoxin, noradrenaline, substance P receptor antagonist, or one 5-HT_4 receptor inhibitor ICS205930, but not by pre-exposure to hexamethonium (*59,60*). These experimental studies on laboratory animals suggested that the contractile response induced by Daikenchuto is partially mediated by ACh released from cholinergic nerve endings and that 5-HT_4, substance P, and cholecystokinin receptors would be involved in this effect of Daikenchuto.

Hangeshashinto was found to be useful in relieving delayed diarrhea induced by irinotecan which is usually employed to treat metastatic gastric and colorectal cancer (*32*). Studies indicated that Hangeshashinto exhibits pharmacological effects *via* actions including protection of the gastric mucosa, anti-inflammatory actions, and enhancement of large intestinal water absorption. Oral administration of Hangeshashinto to rats inhibited taurocholic acid-induced decreases in the gastric mucosa levels of phospholipids, a reduction of gastric mucosal potential differences, and gastric mucosa back diffusion of H^+ (*61*). In addition, Hangeshashinto inhibited an ethanol-induced decrease in the volume of mucus in the superficial gastric mucosa and the deep mucosa of the gastric body (*61*). These results demonstrated the protective effects of Hangeshashinto on gastric mucosa. In regard to its anti-inflammatory actions, oral pretreatment with Hangeshashinto in rats inhibited irinotecan induced production of prostaglandin E_2 in the large intestinal mucosa (*62*). In terms of enhancement of large intestinal water absorption, oral administration of Hangeshashinto to rats enhanced water absorption in the large intestine (*63*). In another study, oral pre-treatment of this drug to rats inhibited the irinotecan induced reduction of water absorption in the large intestine (*62*). Thus, these studies suggested the efficacy of Hangeshashinto in reducing side effects induced by the chemotherapy drug irinotecan.

3. Quality control of Kampo medicine

Japan is currently the only developed country where traditional medicine, *i.e.* Kampo, is widely believed by the public, officially recognized by the Government, and mostly (148 of all 210 formulae) covered by the

national health insurance system. Thus far, much progress has been made in scientifically evaluating Kampo medicine. These achievements may be ascribed to, if not all, the standardization of Kampo products. In order to improve quality control of Kampo medicine, an Advisory Committee for Kampo Drugs which is in close association with the Ministry of Health, Labor and Welfare was established in 1982. Since the implementation of Good Manufacturing Practice Law in 1986, equal standards were applied to all pharmaceutical drugs including Western drugs and Kampo drugs. Moreover, guidelines for ethical extract products in oriental medicine formulations were developed in 1985 (*64*). One characteristic of Kampo is that every formulation has consisted of fixed combinations of herbs in standardized proportions, which is different from traditional Chinese medicine with modifying formulas. Although each Kampo product may be produced by various manufacturers, it is composed of exactly the same ingredients under the Ministry's standardization methodology. Moreover, the herbs used in the formulas must have the required levels of at least two marker components in order for the formula to be approved as a medicament (*65*). Because of that, the quality of crude drugs receives a high degree of attention. Since the majority of crude drugs are imported from different countries, they were subjected to rigorous checks such as quantification of the possible active ingredients to guarantee consistency in quality. The herbs also undergo tests for any possible contaminants of agricultural pesticides or environmental pollutants, especially heavy metals. Microbial tests for bacteria, yeast and mold are also carried out. These measures ensure the quality of Kampo products from the very beginning. It is the high and consistent quality of Kampo products that have prepared the groundwork for clinical and basic studies on the therapeutic value of Kampo medicine.

4. Prospects and conclusions

The evaluation of the efficacy and safety of traditional medicine including Kampo is not without challenges. The clinical application of Kampo medicine has long been based on its own diagnosis theory called 'Sho' in Japanese which refers to a particular pathological status of a patient and is patterned according to the patient's constitution and symptoms. The term 'Sho' is different from the disease entities understood in terms of modern Western medicine. However, the currently used evaluation model employed in clinical studies are nearly based on the disease terms defined by Western medicine. Considering the characteristics of Kampo medicine, *i.e.* the uncertainty of active ingredients, the combination of diagnosis theories of Kampo medicine and Western medicine would be more rational in patients selected and grouped in clinical trials in the future. Despite all of this, in terms of scientific evaluation and quality control of traditional medicine, some meaningful conclusions on Kampo medicine are put forward as an exploration for reducing the side effects and improving the quality of gastrointestinal cancer patients subjected to conventional anti-cancer therapies. These achievements may provide reference for the development and dissemination of other traditional medicines in the world.

Acknowledgements

This study was supported in part by Japan-China Medical Association and Grants-in-Aid from the Ministry of Education, Science, Sports, and Culture of Japan.

References

1. World Health Organization (WHO). *http://www.who.int/medicines/areas/traditional/definitions/en/index.html* (accessed October 21, 2011).
2. World Health Organization (WHO). *http://www.who.int/dg/speeches/2008/20081107/en/index.html* (accessed October 21, 2011).
3. World Health Organization (WHO). THE WORLD MEDICINES SITUATION 2011. *http://www.who.int/medicines/areas/policy/world_medicines_situation/WMS_ch18_wTraditionalMed.pdf* (accessed December 01, 2011).
4. World Health Organization (WHO). *http://www.who.int/mediacentre/factsheets/fs134/en/index.html* (accessed October 21, 2011).
5. Song PP, Gao JJ, Kokudo N, Tang W. Standardization of traditional Chinese medicine and evaluation of evidence from its clinical practice. Drug Discov Ther. 2011; 5:261-265.
6. Xu HL, Tang W, Du GH, Kokudo N. Targeting apoptosis pathways in cancer with magnolol and honokiol, bioactive constituents of the bark of *Magnolia officinalis*. Drug Discov Ther. 2011; 5:202-210.
7. Cui XY, Wang YL, Kokudo N, Fang DZ, Tang W. Traditional Chinese medicine and related active compounds against hepatitis B virus infection. BioSci Trends. 2010; 4:39-47.
8. Qi FH, Li AY, Inagaki Y, Gao JJ, Li JJ, Kokudo N, Li XK, Tang W. Chinese herbal medicines as adjuvant treatment during chemo- or radio-therapy for cancer. BioSci Trends. 2010; 4:297-307.
9. Mishra M, Huang J, Lee YY, Chua DSK, Lin X, Hu JM, Heese K. Gastrodia elata modulates amyloid precursor protein cleavage and cognitive functions in mice. BioSci Trends. 2011; 5:129-138.
10. History of Cancer Control in Japan. National Cancer Center. *http://ganjoho.jp/public/statistics/backnumber/2010_en.html* (accessed November 21, 2011).
11. Japan Cancer Society. *http://www.jcancer.jp/english/cancerinjapan/* (accessed November 11, 2011).
12. National Cancer Institute. Cancer statistics in Japan (2005). *http://ganjoho.jp/data/public/statistics/backnumber/odjrh3000000h332-att/fig11.pdf* (accessed November 21, 2011).
13. Sakata Y, Suzuki H, Kamataki T. Preventive effect of

TJ-14, a kampo (Chinese herb) medicine, on diarrhea induced by irinotecan hydrochloride (CPT-11). Gan To Kagaku Ryoho. 1994; 21:1241-1244.
14. Endo S, Nishida T, Nishikawa K, Nakajima K, Hasegawa J, Kitagawa T, Ito T, Matsuda H. Dai-kenchu-to, a Chinese herbal medicine, improves stasis of patients with total gastrectomy and jejunal pouch interposition. Am J Surg. 2006; 192:9-13.
15. Takegawa Y, Ikushima H, Ozaki K, Furutani S, Kawanaka T, Kudoh T, Harada M. Can Kampo therapy prolong the life of cancer patients? J Med Invest. 2008; 55:99-105.
16. Motoo Y. Japanese herbal medicine in Western-style modern medical system. In: Botanical Medicine in Clinical Practice (Watson RR, Preedy VR, eds.). Cromwell Press, Trowbridge, UK, 2008; pp. 105-111.
17. Morimoto S, Shimada M, Kurita N, Iwata T, Nishioka M, Yoshikawa K, Miyatani T, Mikami C, Kashihara H. Effect of Kampo medicine Juzen-taiho-to on adverse events induced by cetuximab. J Clin Oncol. 2011; 29 (suppl 4; abstr 396).
18. Takano F, Ohta Y, Tanaka T, Sasaki K, Kobayashi K, Takahashi T, Yahagi N, Yoshizaki F, Fushiya S, Ohta T. Oral administration of Ren-Shen-Yang-Rong-Tang 'Ninjin'yoeito' protects against hematotoxicity and induces immature erythroid progenitor cells in 5-fluorouracil-induced anemia. Evid Based Complement Alternat Med. 2009; 6:247-256.
19. Yoshikawa K, Shimada M, Nishioka M, Kurita N, Iwata T, Morimoto S, Miyatani T, Komatsu M, Kashihara H, Mikami C. The effects of the Kampo medicine (Japanese herbal medicine) "Daikenchuto" on the surgical inflammatory response following laparoscopic colorectal resection. Surg Today. 2011.
20. Ikegami F, Sumino M, Fujii Y, Akiba T, Satoh T. Pharmacology and toxicology of Bupleurum root-containing Kampo medicines in clinical use. Hum Exp Toxicol. 2006; 25:481-494.
21. Kawashima K, Fujimura Y, Makino T, Kano Y. Pharmacological properties of traditional medicine (XXXII): Protective effects of hangeshashinto and the combinations of its major constituents on gastric lesions in rats. Biol Pharm Bull. 2006; 29:1973-1975.
22. Terasawa K. Evidence-based reconstruction of Kampo medicine: Part I – Is Kampo CAM? Evid Based Complement Alternat Med. 2004; 1:11-16.
23. The Japan Society for Oriental Medicine (JSOM). *http://www.jsom.or.jp/medical/ebm/index.html* (accessed January 15, 2012).
24. The Japan Society for Oriental Medicine (JSOM). *http://www.jsom.or.jp/medical/ebm/cpg/index.html* (accessed January 18, 2012).
25. Iwagaki H, Saito S. Regulation of post-operative systemic inflammatory response syndrome (SIRS) by preoperative administration of hochuekkito (a Japanese herbal medicine). Nihon Toyo Igaku Zqsshi. 2010; 61:78-83. (in Japanese)
26. Saito S, Iwagaki H, Kobayashi N, Tanaka N, Kawashima R, Takeuchi Y, Miyake M, Takiue T, Shimamura H, Watanabe T, Mitsuoka N, Maeda T. Effects of a Japanese herbal medicine (TJ-41) on surgical stress of patients with gastric and colorectal cancer. Nihon Rinsho Geka Gakkai Zasshi. 2006; 67:568-574. (in Japanese)
27. Konno H, Maruo Y, Baba S, *et al*. Improvement of host-immunity by Juzen-taiho-to in the postoperative adjuvant chemotherapy for patients with gastric cancer. Biotherapy. 1997; 11:193-199. (in Japanese)
28. Yamada T. Randomized controlled trial of the efficacy of juzentaihoto (TJ-48) combined with oral 5-FU for gastric cancer. Progress in Medicine. 2004; 24:2746-2747. (in Japanese)
29. Kosaka A, Kamiya T, Sumiyama M, *et al*. Usefulness of TSUMURA Juzentaihoto (TJ-48) for reducing adverse effects of anticancer drugs and improving QOL. Progress in Medicine. 1994; 14:2259-2264. (in Japanese)
30. Kosaka A, Hojyo M, Osaku M, *et al*. The value of TSUMURA Juzentaihoto (TJ-48) in reducing adverse effects of anticancer drugs from the perspective of QOL improvement. Progress in Medicine. 1993; 13:1072-1079. (in Japanese)
31. Sugimachi K. A study of the usefulness of ninjin'yoeito in the postoperative adjuvant chemotherapy for gastric cancer. Rinsho to Kenkyu. 1995; 72:454-458. (in Japanese)
32. Hibi S, Ina K, Furuta R, Kataoka T, Kojima S, Kawai M. Clinical effects of Hange-shashin-to on combination therapy of S-1/irinotecan against the for patients with metastatic gastric and colorectal cancer. Gan To Kagaku Ryoho. 2009; 36:1485-1488.
33. Ayukawa K, Sato T, Nagase S, *et al*. Preventive effect of shosaikoto on liver carcinogenesis. Rinsho to Kenkyu. 1994; 71:1874-1876. (in Japanese)
34. Nagatomo H, Shigehira M. Efficacy of TSUMURA Juzentaihoto for reducing the adverse effects of the anticancer drug cisplatin. Kampo Igaku. 1992; 16:116-119. (in Japanese)
35. Yoshikawa K. Evaluation of anti-inflammatory efficacy of daikenchuto – A study in a fasted rat model and a randomized controlled trial in postoperative patients with colorectal cancer. 5th Annual Meeting of the Japanese Gastroenterological Association (Workshop 5). 2009; pp. 9-10.
36. Toda T, Matsuzaki K, Kawano T, *et al*. Preoperative and postoperative combination therapy with slow-release tegafur capsules and Juzen-taiho-to in patients with colorectal cancer – Tissue concentrations and thymidine phosphorylase activity. Gan No Rinsho. 1998; 44:317-323. (in Japanese)
37. Sasaki K, Ezoe E, Araya J, *et al*. Effects of Kampo medicine on the immune functions in gastroenteric cancer patients. Kampo to Saishin-chiryo. 2006; 15:9-14. (in Japanese)
38. Sasaki K, Takasaka H, Furuhata T, *et al*. Effect of Kampo medicine on cancer chemotherapy. Geka Chiryo. 2007; 97:504-510. (in Japanese)
39. Yamada T. Clinical study of Juzen-taiho-to administration for postoperative esophageal carcinoma, gastric carcinoma, and colorectal carcinoma – Influence of surgical intervention and postoperative chemotherapy on cell mediated immunity. Wakan Iyaku Gakkaishi. 1992; 9:157-164. (in Japanese)
40. Araki Y, Tanaka T, Ogata Y, *et al*. Immunological evaluation of the efficacy of Kampo prescription for postoperative patients with colorectal cancer. Shinyaku to Rinsho. 1992; 41:1670-1676. (in Japanese)
41. Sasaki K, Takashima K, Kitagawa K, *et al*. Immuno-stimulation and suppression of liver metastasis by Kampo medicines in postoperative patients with colorectal cancer. Progress in Medicine. 1992; 12:1652-1655. (in Japanese)
42. Nishimura G. Evaluation of clinical efficacy of

hochuekkito in improving nutritional/immune status in patients with surgery for large intestine carcinoma. Progress in Medicine. 2009; 29:84-85. (in Japanese)
43. Takagi K, Nagata H, Horie T, *et al*. Effect of the preventive herbal therapy using Dai-kenchu-to on intestinal obstruction following curative resection for colorectal cancer: Prospective, randomized study. Kampo Kenkyu. 2007; 429:270-271. (in Japanese)
44. TSUMURA Hochuekkito Extract Granules for Ethical Use. *http://www.tsumura.co.jp/password/m_square/products/inta/pdf/tj-41.pdf* (accessed February 05, 2012).
45. Saiki I. A Kampo medicine "Juzen-taiho-to" – prevention of malignant progression and metastasis of tumor cells and the mechanism of action. Biol Pharm Bull. 2000; 23:677-688.
46. Harada M, Seta K, Ito O, Tamada K, Li T, Terao H, Takenoyama M, Kimura G, Nomoto K. Concomitant immunity against tumor development is enhanced by the oral administration of a kampo medicine, Hochu-ekki-to (TJ-41: Bu-Zhong-Yi-Qi-Tang). Immunopharmacol Immunotoxicol. 1995; 17:687-703.
47. Li T, Tamada K, Abe K, Tada H, Onoe Y, Tatsugami K, Harada M, Kubo C, Nomoto K. The restoration of the antitumor T cell response from stress-induced suppression using a traditional Chinese herbal medicine Hochu-ekki-to (TJ-41: Bu-Zhong-Yi-Qi-Tang). Immunopharmacology. 1999; 43:11-21.
48. TSUMURA Shosaikoto Extract Granules for Ethical Use. *http://www.tsumura.co.jp/english/products/pi/JPR_T009.pdf* (accessed February 05, 2012).
49. Kayano K, Sakaida I, Uchida K, Okita K. Inhibitory effects of the herbal medicine Sho-saiko-to (TJ-9) on cell proliferation and procollagen gene expressions in cultured rat hepatic stellate cells. J Hepatol. 1998; 29:642-649.
50. Shimizu I, Ma YR, Mizobuchi Y, Liu F, Miura T, Nakai Y, Yasuda M, Shiba M, Horie T, Amagaya S, Kawada N, Hori H, Ito S. Effects of Sho-saiko-to, a Japanese herbal medicine, on hepatic fibrosis in rats. Hepatology. 1999; 29:149-160.
51. Yamashiki M, Kosaka Y, Nishimura A, Takase K, Ichida F. Efficacy of a herbal medicine "sho-saiko-to" on the improvement of impaired cytokine production of peripheral blood mononuclear cells in patients with chronic viral hepatitis. J Clin Lab Immunol. 1992; 37:111-121.
52. Yamashiki M, Nishimura A, Sakaguchi S, Suzuki H, Kosaka Y. Effects of the Japanese herbal medicine 'Sho-saiko-to' as a cytokine inducer. Environ Toxicol Pharmacol. 1996; 2:301-306.
53. Yamashiki M, Nishimura A, Suzuki H, Sakaguchi S, Kosaka Y. Effects of the Japanese herbal medicine "Sho-saiko-to" (TJ-9) on *in vitro* interleukin-10 production by peripheral blood mononuclear cells of patients with chronic hepatitis C. Hepatology. 1997; 25:1390-1397.
54. TSUMURA Daikenchuto Extract Granules for Ethical Use. *http://www.tsumura.co.jp/english/products/pi/JPR_T100.pdf* (accessed February 05, 2012).
55. Nagano T, Itoh H, Takeyama M. Effect of Dai-kenchu-to on levels of 3 brain-gut peptides (motilin, gastrin and somatostatin) in human plasma. Biol Pharm Bull. 1999; 22:1131-1133.
56. Nagano T, Itoh H, Takeyama M. Effects of Dai-kenchu-to on levels of 5-hydroxytryptamine (serotonin) and vasoactive intestinal peptides in human plasma. Biol Pharm Bull. 2000; 23:352-353.
57. Sato Y, Katagiri F, Inoue S, Itoh H, Takeyama M. Dai-kenchu-to raises levels of calcitonin gene-related peptide and substance P in human plasma. Biol Pharm Bull. 2004; 27:1875-1877.
58. Satoh K, Kase Y, Yuzurihara M, Mizoguchi K, Kurauchi K, Ishige A. Effect of Dai-kenchu-to (Da-Jian-Zhong-Tang) on the delayed intestinal propulsion induced by chlorpromazine in mice. J Ethnopharmacol. 2003; 86:37-44.
59. Satoh K, Hayakawa T, Kase Y, Ishige A, Sasaki H, Nishikawa S, Kurosawa S, Yakabi K, Nakamura T. Mechanisms for contractile effect of Dai-kenchu-to in isolated guinea pig ileum. Dig Dis Sci. 2001; 46:250-256.
60. Satoh K, Hashimoto K, Hayakawa T, Ishige A, Kaneko M, Ogihara S, Kurosawa S, Yakabi K, Nakamura T. Mechanism of atropine-resistant contraction induced by Dai-kenchu-to in guinea pig ileum. Jpn J Pharmacol. 2001; 86:32-37.
61. TSUMURA Hangeshashinto Extract Granules for Ethical Use. *http://www.tsumura.co.jp/english/products/pi/JPR_T014.pdf* (accessed February 05, 2012).
62. Kase Y, Hayakawa T, Aburada M, Komatsu Y, Kamataki T. Preventive effects of Hange-shashin-to on irinotecan hydrochloride-caused diarrhea and its relevance to the colonic prostaglandin E_2 and water absorption in the rat. Jpn J Pharmacol. 1997; 75:407-413.
63. Kase Y, Hayakawa T, Ishige A, Aburada M, Komatsu Y. The effects of Hange-shashin-to on the content of prostaglandin E_2 and water absorption in the large intestine of rats. Biol Pharm Bull. 1997; 20:954-957.
64. International Agency for Research on Cancer, World Health Organization. In: IARC Monographs on the Evaluation of Carcinogenic Risks to Humans: Volume 82 Some Traditional Herbal Medicines, Some Mycotoxins, Naphthalene and Styrene. IARC Press, Lyon, France, 2002; p. 63.
65. Kenner D. Research in Japanese botanical medicine and immune modulating cancer therapy. Townsend Letter for Doctors and Patients. 2001.

(Received December 24, 2011; Revised February 6, 2012; Accepted February 8, 2012)

Brief Report

DOI: 10.5582/ddt.2012.v6.1.9

Synthesis of solasodine glycoside derivatives and evaluation of their cytotoxic effects on human cancer cells

Changzhi Cui[1], Xuesen Wen[1], Min Cui[1], Jian Gao[1], Bin Sun[1,2], Hongxiang Lou[1,*]

[1] *School of Pharmaceutical Sciences, Shandong University, Ji'nan, Shandong, China;*
[2] *National Glycoengineering Research Center, Shandong University, Ji'nan, Shandong, China.*

ABSTRACT: Solasodine glycosides, such as solamargine, have been proved to be very important anti-cancer agents. In order to discover more potent cytotoxic agents and explore the preliminary structure activity relationship, a new series of solasodine glycosides 2-9 were synthesized *via* a transglycosylation strategy, and their cytotoxic activity against a panel of human cancer cell lines (MCF-7, KB, K562, and PC3 cells) were evaluated by MTT assays. The results indicated that compounds 2, 8, and 9 with the substitute moiety of rhamnose, 2-hydroxyethoxymethyl, and 1,3-dihydroxypropan-2-yloxy-methyl, respectively, exhibited quite strong anticancer activity. The underlying mechanism tests demonstrated that these compounds could induce apoptosis detected by DAPI staining, and Annexin V and propidium iodide binding. Cell cycle analysis indicated that the cancer cells were predominantly arrested at the G2/M phase when exposure to these compounds was examined by flow cytometry. These compounds may serve as lead candidates in the development of novel chemotherapeutics for cancer treatment.

Keywords: Saponins, solasodine, cytotoxicity, apoptosis

1. Introduction

Natural derived products which belong to the traditional medicinal system are affluent resources for new drug development. Steroidal glycosides are a series of natural products and display a wide spectrum of structural diversity with versatile biological activities, such as anti-inflammatory, antibacterial, antiparasitic, antifungal, and anticancer activities (*1-5*). Both the sugar residue and aglycone in the structure play very important roles in their biological performance (*6-8*).

Solasodine, a solanum type of steroid alkaloid with a C27 cholestane skeleton, was first discovered from the fruit of the devil's apple in free and conjugated forms (*9*). Solasodine conjugates displayed uneventful anticancer activity, but the mixture of the solasodine glycosides (BEC: 33% solasonine, 33% solamargine, and 34% of their corresponding di- and monoglycosides) discovered from the Devil's Apple plant (*9-15*) have been clinically applied as an antineoplastic agent.

Solasodine glycosides exhibited obvious anticancer activities when compared with its aglycone (*9-14*). Meanwhile, the cytotoxic activities of solasodine glycosides were generally dependent on the presence of sugars, in particular rhamnose (*9-21*), and were mediated by the rhamnose-binding receptors that occur on the membrane of cancer cells (*21*).

In order to discover more potent cytotoxic agents for cancer therapy with the simplified structures which were facilitated for industrial preparation, six monosaccharides including rhamnose as well as two open-loop saccharide analogues were introduced to solasodine and compounds **2-9** were then prepared accordingly (Scheme 1).

2. Materials and Methods

2.1. *Chemicals*

Solasodine **1** (Scheme 1) was synthesized using five straightforward sequential reactions as reported previously (*22*). Six glycosyl bromide **10-15** (Scheme 1) was then employed to assemble a small library of solasodine glycosides using classic Koenigs-Knorr glycosylation. In addition, two open-loop saccharide analogues were transferred to the solasodine using 2-(1*H*-benzotriazole-1-yl)-1,1,3,3-tetramethyluronium tetrafluoroborate (DIEA) as a catalyst.

As shown in Scheme 1, glycosyl donors **10-14** were prepared from the corresponding benzoylated monosaccharide using a solution of 45% HBr/HOAc in CH_2Cl_2. Compound **15** was easily prepared from

**Address correspondence to:*
Dr. Hongxiang Lou, School of Pharmaceutical Sciences, Shandong University, Ji'nan, Shandong, China.
E-mail: louhongxiang@sdu.edu.cn

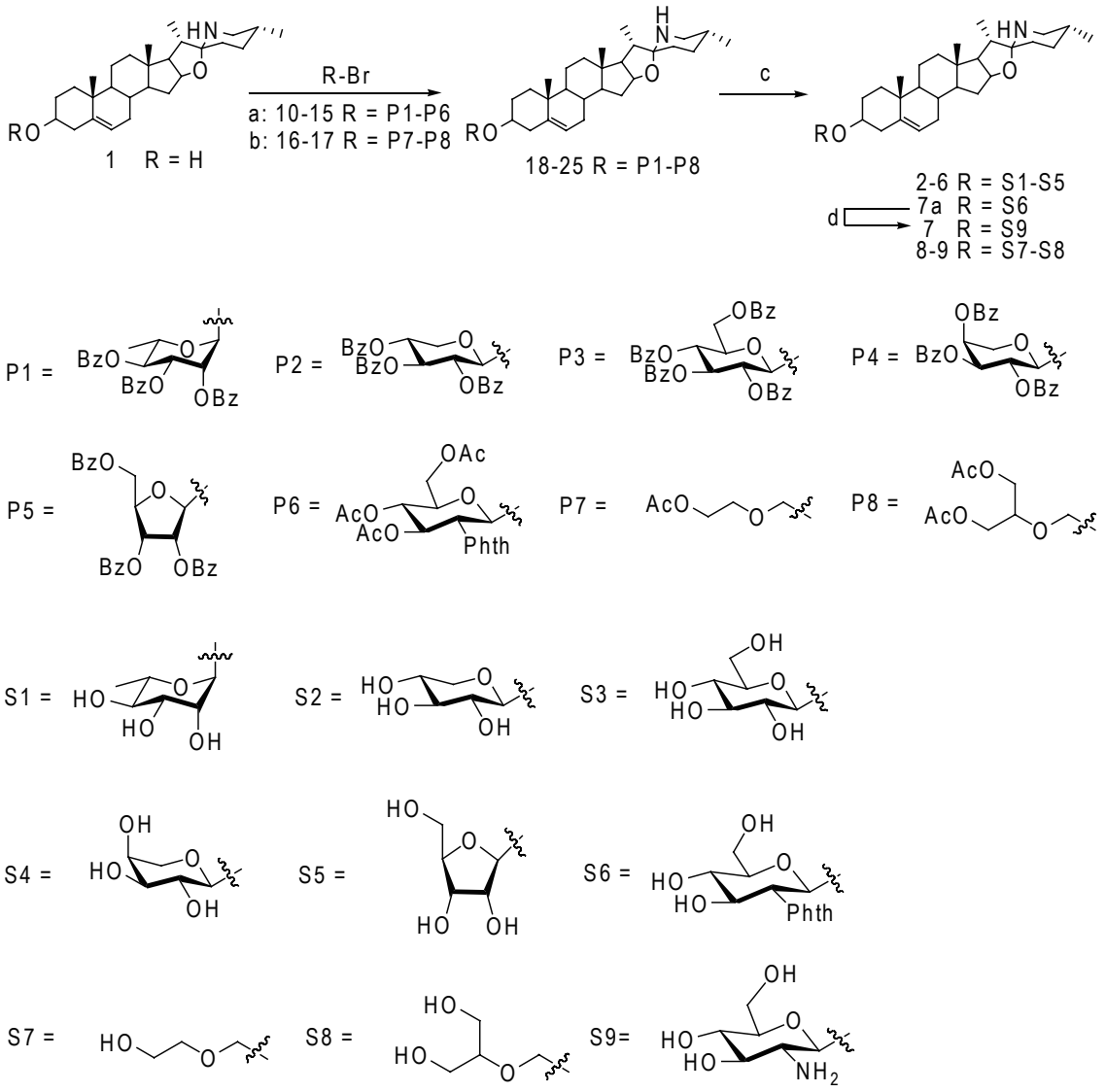

Scheme 1. Reagents and conditions. (a) AgOTf, 4 Å molecular sieve, −20°C, solasodine, 12 h; **(b)** DIEA, CH_2Cl_2, room temperature, 24 h; **(c)** CH_3OH/CH_3ONa, 4 h, 98%; **(d)** CH_3NH_2, 4 h, 97%.

commercial glucosamine hydrochloride (*23*). Compound **16** was synthesized from 1,3-dioxolane using AcBr, and **17** was prepared from 1,3-dioxolan-4-yl-methanol (*24*). And then each donor of **10-15** was condensed with solasodine **1**, respectively, with catalysis from silver trifluoromethanesulfonate (AgOTf) to provide protected **18-23**. Under the promotion of DIEA, coupling of open-loop donor **16** or **17** with solasodine **1** afforded the intermediates **24** and **25**, respectively. At last, MeOH/MeONa or CH_3NH_2 was used to hydrolyze the tosyl, acetyl and phthalic anhydride to provide target compounds **2-9**. The β-bond linkage between glycosyl and aglycone in compounds **2-7** was comfirmed. Specific information on synthesis of targeted compounds **2-9** is indicated in the Appendix.

2.2. *Cell lines and cell culture*

Human squamous cell carcinoma (KB), breast adenocarcinoma (MCF-7), myelogenous leukemia (K562), prostate cancer (PC3), human umbilical vein endothelial (ECV304), and human hepatocyte cells (HL7702) were maintained in RPMI 1640 medium (HyClone, Thermo Fisher Scientific Inc., Waltham, MA, USA). The medium was supplemented with 10% fetal bovine serum (FBS) (Gibco, Invitrogen, Carlsbad, CA, USA), 100 μg/mL penicillin and 100 μg/mL streptomycin. Cells were cultured in a humidified atmosphere of 5% CO_2 at 37°C.

2.3. *MTT assay*

Cells were seeded into 96-well culture plates at a density of 4-5 × 10^3 cells per well and cultured for 24 h. Thereafter the cells were treated with various concentrations of tested compounds and incubated for 24-48 h. Cell viability was assessed by MTT assay. The cells were incubated with 5 mg/mL MTT solution at 37°C for 4 h, and the resulting crystals were dissolved

in dimethyl sulfoxide (DMSO). The optical density (OD) was measured using a plate microreader (Bio-Rad 680, Bio-Rad Co., Hercules, USA). Cell viability was calculated as follows:

$$\text{Cell viability (\%)} = 100 \times (OD_{sample} - OD_{blank})/(OD_{control} - OD_{blank})$$

2.4. *Cell morphology examination*

To assess the effect of compounds **2**, **8**, and **9** on apoptosis, MCF-7 cells were seeded in 24-well plates. After treatment with compounds **2**, **8** and **9** for 24 h cells were washed twice with PBS, and were observed under the microscope. Images were processed with Adobe Photoshop 7.0.

2.5. *4',6-Diamino-2-phenylindole (DAPI) staining*

MCF-7 cells were seeded onto 12-mm round, glass cover slips in 24-well plates. After 24 h treatment with compounds **2**, **8**, and **9**, cells were stained with 4 μg/mL DAPI for 10 min at room temperature. The cover slips containing cells were then mounted on microscope slides using mounting medium and analyzed with fluorescence microscopy. Fluorescence images were processed using AutoQuant X 2.1 software from Cybernatics, Inc. (Bethesda, MD, USA).

2.6. *Apoptosis analysis*

Apoptosis was evaluated with Annexin V/propidium iodide (PI) staining using an FITC Annexin V Apoptosis Detection Kit purchased from BD Biosciences (San Jose, CA, USA). MCF-7 cells were seeded at a density of 1×10^5/mL into 6-well plates. After 24 h incubation with compounds **2**, **8**, and **9**, the cells were washed twice with ice-cold phosphate buffered saline (PBS). Each cell sample was transferred to individual tubes and centrifuged at 200 × g for 5 min. The supernatant was removed, and the cells were resuspended in 400 μL of annexin V-FITC binding buffer and incubated at room temperature in the dark for 15 min with 5 μL annexin V-FITC and PI 10 μL (50 μg/mL) was added for another 5 min. Apoptosis was measured using flow cytometry (Becton, Dickinson and Company, Franklin Lakes, NJ, USA) and WinMDI 2.9 analysis software.

2.7. *Cell-cycle analysis*

Cell cycle was analyzed using flow cytometry of PI-stained cells. MCF-7 cells were cultured in the presence of different concentrations of compounds **2**, **8**, and **9**. After designated time intervals, cells were fixed in 70% ethanol overnight at 4°C and washed once with PBS. Then, the cells were incubated with 1 U/mL of RNase A (DNase free) for 30 min at 37°C and 10 μg/mL of PI for 1 h at room temperature in the dark. Cell cycle distribution was examined by flow cytometry, and data was analyzed using the Modfit program (Becton, Dickinson and Company).

2.8. *Statistical analysis*

All experiments were performed at least three times. Statistical analysis was performed with an analysis of variance (ANOVA) followed by the Turkey's *t*-test. $p < 0.05$ were considered statistically significant.

3. Results and Discussion

3.1. *Cytotoxic effects of synthesized compounds on human cancer cells*

The anticancer effect of synthesized saponins **2-9** as well as solasodine **1** against human KB, K562, MCF-7, PC3, EVC304, and HL7702 cells were preliminarily evaluated by MTT assay (*25*). As shown in Table 1, compounds **2**, **3**, **8**, and **9** were found to possess relatively potent cytotoxic activity against PC3 cells, with IC_{50} values ranging from 7.2 to 18.4 μM. In K562 cells, compounds **2** and **9** with IC_{50} values of 18.8 and 17.0 μM showed obvious superiority to other synthesized compounds in suppressing cell proliferation. Similarly, compounds **2**, **8**, and **9** exhibited excellent proliferation inhibitory activity against MCF-7 cells, with IC_{50} values of 12.9 and 17 μM, respectively. On the other hand, compounds **2**, **8**, and **9** showed weak cytotoxicity in human normal cell lines ECV304 and HL7702 (Table 1). These results indicated that the saponins with rhamnose (*e.g.* compound **2**) or open-loop saccharide analogues (*e.g.* compounds **8** and **9**) exhibited more potent anticancer activity than the other derivatives synthesized in the current study.

3.2. *Compounds **2, 8, and 9** induced cell morphologic alteration in MCF-7 cells*

To examine the effect of compounds **2**, **8**, and **9** on cell morphology during cell death, MCF-7 cells were treated with various concentrations (0, 15, 30 μM) of these compounds for 24 h, respectively. As shown in Figure 1A, the morphological character of cells changed greatly. Cell shrinkage and membrane integrity loss appeared, which are typical features of apoptosis (*26,27*). Apoptotic cells were also defined on the basis of characteristic nuclear morphology including condensation of chromatin producing crescent shapes around the periphery of the nucleus and apoptotic bodies (*28,29*). As shown in Figure 1B, the non-treated cells had rounded and intact nuclei with diffuse DAPI staining, while the cells treated with compounds **2**, **8**, and **9** had nuclei that were smaller and brighter

Table 1. The cytotoxicity of compounds 1-9 on human cell lines

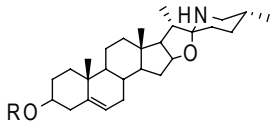

Compound	R	IC_{50} (μM)					
		KB	K562	MCF-7	PC3	ECV304	HL7702
Solamargine (*Ref. 30*)	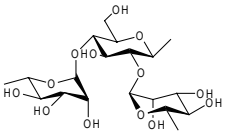	7.8	8.0	8.2	5.9	ND	ND
1	H-	ND	ND	ND	13.6	ND	ND
2	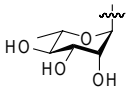	29.1	18.8	14.2	18.4	34.0	36.0
3	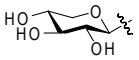	ND	51.0	53.0	16.5	ND	ND
4	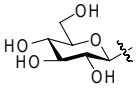	ND	43.0	77.0	27.9	ND	ND
5	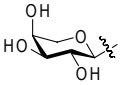	ND	44.0	64.0	23.1	ND	ND
6	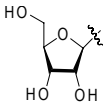	ND	ND	ND	66.9	ND	ND
7	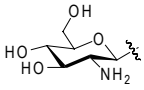	ND	37.0	98.0	21.9	ND	ND
8	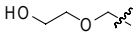	28.9	112.0	12.9	17.4	> 40	> 40
9	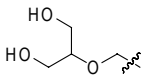	29.4	17.0	26.0	7.2	> 40	> 40

ND: not detected.

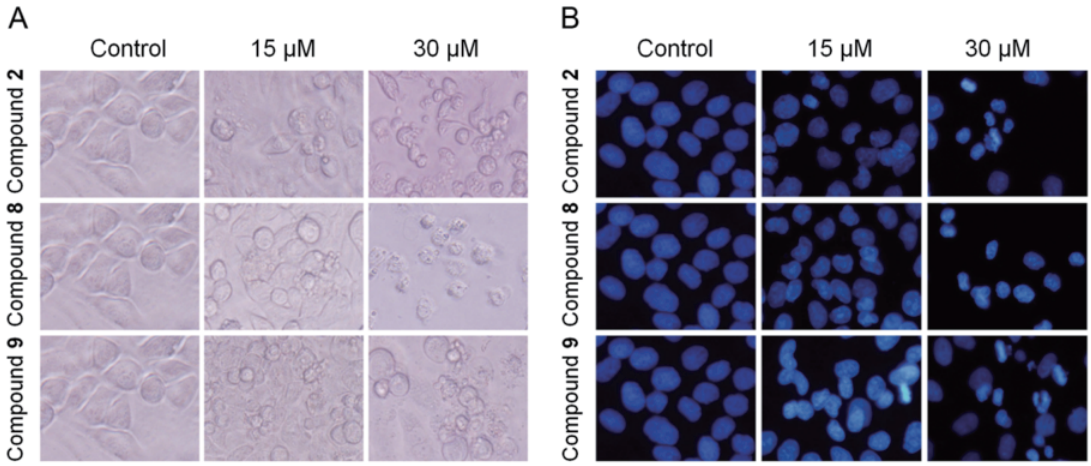

Figure 1. Morphological changes of MCF-7 cells after treatment with compounds 2, 8, and 9, respectively, for 24 h. Cell morphology was examined directly under light microscopy **(A)** or detected *via* fluorescence microscopy after the cells were stained with DAPI **(B)**.

stained with condensed chromatin forming crescent-shaped profiles around the periphery of the nucleus or separate globular structures (apoptotic bodies). The result implied that compounds **2**, **8**, and **9** induced cell apoptosis in MCF-7 cells.

3.3. *Quantification of apoptotic cells solicited by compounds **2**, **8**, and **9** in MCF-7 cells*

To further quantify the extent of compounds **2**, **8**, **9**-induced apoptosis, MCF-7 cells double stained with annexin V and PI were analyzed by flow cytometry. The analysis results revealed that the proportion of cells stained with annexin V increased with compounds **2**, **8**, and **9** treatment (Figure 2). The percentages of apoptotic cells increased from 0.88%, 0.07%, and 0.07% to 8.58%, 9.16%, and 10.56% when cells were exposed to 15 μM compounds **2**, **8**, and **9**, respectively, for 24 h. The proportion of apoptotic cells went up to 30.36%, 36.71%, and 34.18% when cells were treated with 30 μM of the above agents.

3.4. *Compounds **2**, **8**, and **9** induced cell cycle arrest at G_2/M phase in MCF-7 cells*

To determine whether compounds **2**, **8**, and **9** exerted cell growth inhibition activity *via* the induction of cell cycle arrest in addition to apoptosis, we next focused on the effect of compounds **2**, **8**, and **9** on the cell cycle of MCF-7 cells. We observed that compounds **2**, **8**, and **9** treatment led to cells accumulating in the G_2/M phase compared with non-treated cells (Figure 3). The ratio of cells in the G_2/M phase following the treatment with 15 μM compounds **2**, **8**, and **9** for 24 h increased from 6.60%, 5.79%, and 4.35% to 11.18%, 11.41%, and 7.71%, respectively. The values rose to 14.33%, 17.26%, and 17.84%, respectively, when cells were incubated with 30 μM of the above compounds for 24 h.

In summary, solasodine **1** together with its eight glycoside derivatives **2-9** were synthesized *via* a Koenigs-Knorr strategy. The preliminary structure-activity relationship (SAR) analysis indicated that

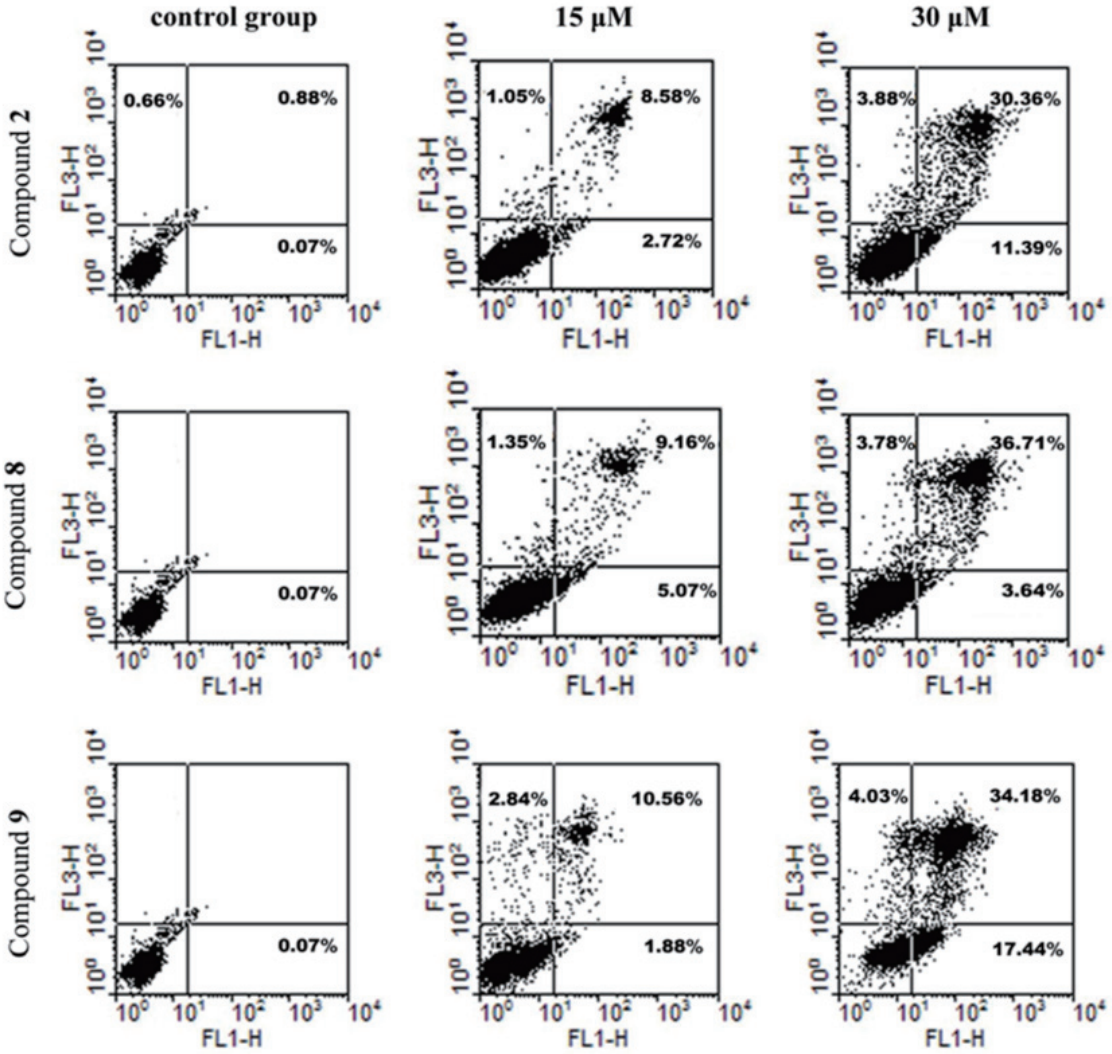

Figure 2. Flow cytometry analysis of cell apoptosis. MCF-7 cells were treated with compounds **2**, **8**, and **9**, respectively, for 24 h and then stained with Annexin-V/PI.

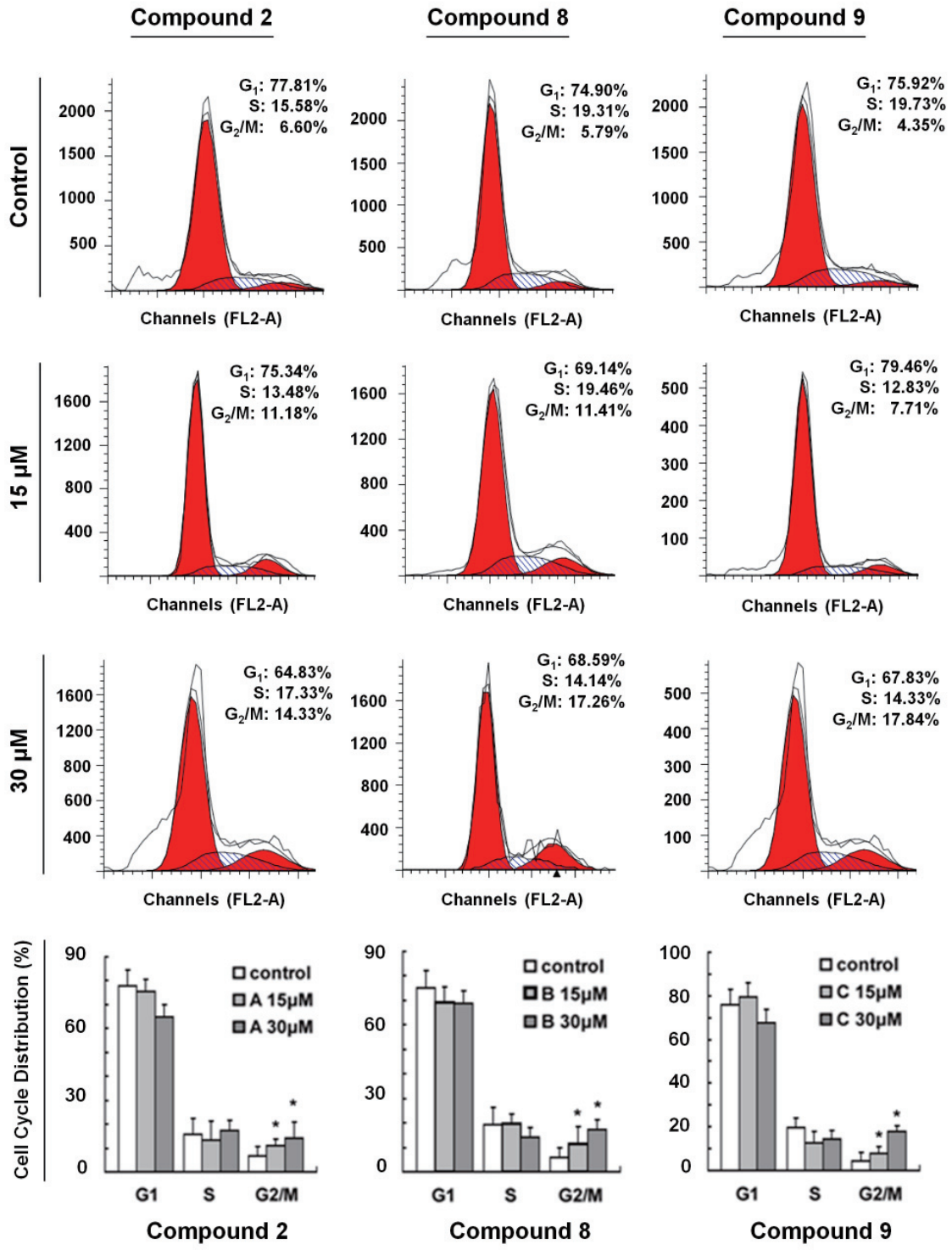

Figure 3. DNA content analysis. MCF-7 cells were treated with compounds **2**, **8**, and **9**, respectively, for 24 h and then stained with PI. The fluorescence of PI-stained cells was analyzed using flow cytometry. Cell cycle distribution was analyzed based on the DNA content. * $p < 0.05$ *vs*. control.

the rhamnose substituent was essential and the chain substituents in compounds **8** and **9** were also very important for its anticancer activity. The other sugar substituted derivatives exhibited less anticancer activity. These results were consistent with the previous report (*21*). Furthermore, it was demonstrated that the chain and rhamnose substituents exhibited similar cytotoxic potency. Our underlying work suggested that compounds **2**, **8**, and **9** have the ability to kill cancer cells *via* a form of apoptosis-like cell death. Moreover, compounds **2**, **8**, and **9**-treated cells were arrested predominantly at the G_2/M phase. This study demonstrated that compounds **2**, **8**, and **9** may merit further investigation as potential therapeutic leads for the development of novel anticancer drugs. Much more work concerning the biochemical mechanism is ongoing.

Acknowledgements

This work was supported by grants from National Natural Science Foundation of China (No. 30925038 and 81172956) and Shandong Provincial Foundation (No. 06GG1102023).

References

1. Sparg SG, Light ME, van Staden J. Biological activities and distribution of plant saponins. J Ethnopharmacol. 2004; 94:219-243.
2. Kwak WJ, Han CK, Chang HW, Kim HP, Kang SS, Son KH. Loniceroside C, an antiinflammatory saponin from Lonicera japonica. Chem Pharm Bull (Tokyo). 2003; 51:333-335.
3. Iorizzi M, Lanzotti V, Ranalli G, De Marino S, Zollo F. Antimicrobial furostanol saponins from the seeds of *Capsicum annuum* L. var. *acuminatum*. J Agric Food Chem. 2002; 50:4310-4316.
4. De Lucca AJ, Bland JM, Vigo CB, Cushion M, Selitrennikoff CP, Peter J, Walsh TJ. CAY-I, a fungicidal saponin from Capsicum sp. fruit. Med Mycol. 2002; 40:131-137.
5. Tran QL, Tezuka Y, Banskota AH, Tran QK, Saiki I, Kadota S. New spirostanol steroids and steroidal saponins from roots and rhizomes of *Dracaena angustifolia* and their antiproliferative activity. J Nat Prod. 2001; 64:1127-1132.
6. Wang Y, Zhang Y, Zhu Z, Zhu S, Li Y, Li M, Yu B. Exploration of the correlation between the structure, hemolytic activity, and cytotoxicity of steroid saponins. Bioorg Med Chem. 2007; 15:2528-2532.
7. Man S, Gao W, Zhang Y, Huang L, Liu C. Chemical study and medical application of saponins as anti-cancer agents. Fitoterapia. 2010; 81:703-714.
8. Gao J, Li X, Gu G, Sun B, Cui M, Ji M, Lou HX. Efficient synthesis of trisaccharide saponins and their tumor cell killing effects through oncotic necrosis. Bioorg Med Chem Lett. 2011; 21:622-627.
9. Cham BE, Gilliver M, Wilson L. Antitumour effects of glycoalkaloids isolated from *Solanum sodomaeum*. Planta Med. 1987; 53:34-36.
10. Daunter B, Cham BE. Solasodine glycosides. *In vitro* preferential cytotoxicity for human cancer cells. Cancer Lett. 1990; 55:209-220.
11. Cham B, Daunter B, Evans R. Curaderm – or is it? Med J Aust. 1990; 152:329-330.
12. Cham BE, Daunter B. Topical treatment of pre-malignant and malignant skin cancers with Curaderm. Drugs of Today. 1990; 26:55-58.
13. Cham BE. Solasodine glycosides: A new modality for cancer. In Proc. 2nd Oceania Symposium. 1991; 30-36.
14. Cham BE. Efficacy and mode of action of solasodine glycosides (BEC) on cancer cells. In Proc. 4th Oceania Symposium. 1993; 41-51.
15. Cham BE. Solasodine glycosides as anti-cancer agents: Pre-clinical and clinical studies. Asia Pacif J Pharmacol. 1994; 9:113-118.
16. Lee KR, Kozukue N, Han JS, Park JH, Chang EY, Baek EJ, Chang JS, Friedman M. Glycoalkaloids and metabolites inhibit the growth of human colon (HT29) and liver (HepG2) cancer cells. J Agric Food Chem. 2004; 52:2832-2839.
17. Esteves-Souza A, da Silva TMS, Alves CCF, de Carvalho MG, Braz R, Echevarria A. Cytotoxic activities against Ehrlich carcinoma and human K562 leukaemia of alkaloids and flavonoid from two Solanum species. J Brazil Chem Soc. 2002; 13:838-842.
18. Ghazi M, Matthees DP. Quantitative inhibitory effects of steroidal alkaloids: Relative involvement of aglycones and sugar moieties on lettuce seed radicle elongation. Botanical Gazette. 1990; 151:38-40.
19. Chataing B, Concepcion JL, Lobaton R, Usubillaga A. Inhibition of *Trypanosoma cruzi* growth *in vitro* by solanum alkaloids: A comparison with ketoconazole. Planta Med. 1998; 64:31-36.
20. Yoshikawa M, Nakamura S, Ozaki K, Kumahara A, Morikawa T, Matsuda H. Structures of steroidal alkaloid oligoglycosides, robeneosides A and B, and antidiabetogenic constituents from the Brazilian medicinal plant *Solanum lycocarpum*. J Nat Prod. 2007; 70:210-214.
21. B.E.C. Solasodine rhamnosyl glycosides specifically bind cancer cell receptors and induce apoptosis and necrosis. Treatment for skin cancer and hope for internal canners. Research Journal of Biological Sciences. 2007; 2:503-514.
22. Zha X, Sun H, Hao J, Zhang Y. Efficient synthesis of solasodine, *O*-acetylsolasodine, and soladulcidine as anticancer steroidal alkaloids. Chem Biodivers. 2007; 4:25-31.
23. Bianchi A, Bernardi A. Traceless Staudinger ligation of glycosyl azides with triaryl phosphines: Stereoselective synthesis of glycosyl amides. J Org Chem. 2006; 71:4565-4577.
24. Radi S, Lazrek HB. Synthesis of certain new 1,2,3-triazole acyclonucleosides *via* 1,3-dipolar cycloaddition. B Kor Chem Soc. 2002; 23:437-440.
25. Sheng R, Xu Y, Weng Q, Xia Q, He Q, Yang B, Hu Y. Synthesis and cytotoxic activity of 3-phenyl-2-thio-quinoxaline 1,4-dioxide derivatives in hypoxia and in normoxia. Drug Discov Ther. 2007; 1:119-123.
26. Carson DA, Ribeiro JM. Apoptosis and disease. Lancet. 1993; 341:1251-1254.
27. Sarraf CE, Bowen ID. Proportions of mitotic and apoptotic cells in a range of untreated experimental tumours. Cell Tissue Kinet. 1988; 21:45-49.
28. Rechsteiner M, Rogers SW. PEST sequences and regulation by proteolysis. Trends Biochem Sci. 1996; 21:267-271.
29. Wyllie AH, Kerr JF, Currie AR. Cell death: The significance of apoptosis. Int Rev Cytol. 1980; 68:251-306.
30. Sun L, Zhao Y, Yuan H, Li X, Cheng A, Lou H. Solamargine, a steroidal alkaloid glycoside, induces oncosis in human K562 leukemia and squamous cell carcinoma KB cells. Cancer Chemother Pharmacol. 2011; 67:813-821.

(Received January 26, 2012; Revised February 3, 2012; Accepted February 4, 2012)

Appendix

Flash column chromatography was performed on silica gel (200-300 mesh, Qindao Ocean Chemical Co., Qingdao, Shandong, China). Analytical thin-layer chromatography (TLC) was carried out on precoated

Silica Gel 60 F_{254} plates (E. Merck, Darmstadt, Germany) with detection by fluorescence and/or by charring with 30% (v/v) H_2SO_4 in EtOH. Dichloromethane was distilled from CaH_2. The chemicals and materials were purchased from Alfa-Aesar (Ward Hill, MA, USA) and were used as received. NMR spectra were recorded on a Bruker Avance DRX 600 spectrometer (Bruker BioSpin, Rheinstetten, Germany) at 600 (^{1}H) and 150 (^{13}C) MHz, respectively. Elucidations of chemical structures were based on ^{1}H, ^{13}C, ^{1}H-^{1}H COSY, HMBC, and HMQC NMR experiments. Signals are reported as follows: s (singlet), d (doublet), t (triplet), q (quintet), m (multiplet), and coupling constants are reported in Hz (hertz). Melting points were determined in an X-6 melting-point apparatus and are uncorrected. Optical rotations were measured on a Perkin-Elmer 241 MC polarimeter (Waltham, MA, USA). Mass spectral data (HR-ESI-MS and HR-FAB-MS) were obtained on LTQ-Orbitrap XL (Thermo Fisher Scientific Inc.) and JEOL JMS-DX-303HF (JEOL, Tokyo, Japan) in the positive ion mode, respectively.

*Synthesis of compound **1** (Ref. 28)*

Yield 18%, white solid; ^{1}H-NMR (600 MHz, $CDCl_3$): 5.37 (br. s, H-C(6)); 4.31 (m, Ha-C(16)); 3.54 (m, Ha-C(3)); 2.68 (m, CH_2-(26)); 1.19 (s, Me-(19)); 1.10 (s, Me-(21)); 0.97 (s, Me-(27)); 0.84 (s, Me-(18)). ESI-MS: 414.3 ($[M + H]^+$).

*Synthesis of compounds **10-14***

HBr/HOAc (1.0 mmol) was added to a solution of each of the protected sugars (0.5 mmol) in 4 mL CH_2Cl_2 at 0°C. The reaction mixture was stirred at 0°C for 12 h, the progress of the reaction was monitored by TLC. The solvent was removed under reduced pressure to afford a residue. Purification of the residue on a silica gel column with a 6:1 solution of petroleum ether-EtOAc gave **10-14** (yield 40-50%, oil).

*Synthesis of compound D-glucopyranosyl bromide **(15)***

Triethylamine (1.7 mL, 11.6 mmol) was added to the suspension of D-galactosamine hydrochloride (1 g, 4.65 mmol) in DMF (30 mL). After 20 min stirring at room temperature, phtalic anhydride (688 mg, 4.65 mmol) was added to this solution, and the mixture was stirred for 2 h at 50°C under N_2 atmosphere. The reaction mixture was allowed to stand until its temperature dropped to room temperature, excess amounts of triethylamine (5 mL) and acetic anhydride (5 mL) were added. After a 2-day stirring at room temperature under a N_2 atmosphere, the reaction mixture was concentrated in vacuo, mixed with water (150 mL), extracted three times with petroleum ether-EtOAc 1:1, and dried over Na_2SO_4. The organic layer was concentrated and separated by silicagel column chromatography (petroleum ether-EtOAc 1:1) to give the protected D-galactosamine (1.82 g, 82%). The resulting protected D-galactosamine (1.395 g, 2.92 mmol) was mixed with acetic anhydride (0.69 mL, 7.31 mmol), and treated with HBr-AcOH (30%, 16 mL, excess) with ice-cooling. After stirring for an hour at room temperature under a N_2 atmosphere, the mixture was concentrated in vacuo. The reaction mixture was mixed with saturated $NaHCO_3$, extracted three times with CH_2Cl_2, dried over Na_2SO_4, and concentrated to give **15** (1.41 g, 97%, Crude).

*Synthesis of compounds **16** and **17***

AcBr (5.05 mmol) was added to a solution of each of the acetyl protected rings (5 mmol) in 6 mL anhydrous CH_2Cl_2 at room temperature. The mixture was stirred at the same temperature for 12 h. The solvent was removed under reduced pressure to afford **16** and **17** (yield 70-80%, oil).

*Synthesis of compounds **18-23***

AgOTf (33 mg, 0.13 mmol) was added to a stirred mixture of brominated sugar (1.01 mmol) and solasodine (0.414 g, 1.0 mmol) in anhydrous CH_2Cl_2 (8 mL) with a 4 Å molecular sieve at −20°C under a N_2 atmosphere. The reaction mixture was stirred under this condition for 90 min. The solution was filtered and the solvent was evaporated under reduced pressure. The residue was subjected to silica column chromatography with a 40:1 solution of CH_2Cl_2-MeOH to afford **18-23** as white solids (yield 20-70%).

*Synthesis of compounds **24** and **25***

Ethyldiisopropylamine (DIEA) (3 mL) was added to a solution of solasodine (0.414 g, 1 mmol) in 5 mL CH_2Cl_2 at room temperature. After stirring for 15 min, compounds **16** and **17** (1.01 mmol) were added to the mixture and stirred for 12 h. The mixture was concentrated and purified by silica column chromatography with a 40:1 solution of CH_2Cl_2-MeOH to afford **24** and **25** (yield 70-80%).

*Synthesis of compounds **2-6**, **7a**, **8**, and **9***

Compounds **18-25** were dissolved in a solution of MeOH-CH_2Cl_2 (2:1, 10 mL). To the solution was added 2 g/100 mL MeONa/MeOH until a pH 9-10 was attained. The mixture was stirred at room temperature for 4 h, neutralized with Amberlite IR-120 (H^+), filtered and concentrated. The residue was added to a silica gel column with a 45:1 solution of CH_2Cl_2-MeOH to afford compounds **2-6**, **7a**, **8**, and **9** (yield 95-100%).

Solasodine 3-O-L-rhamnoside (**2**). ^{1}H-NMR (DMSO, 600 MHz) δ: 0.76 (3H, s, Me-18), 0.89 (3H, s, Me-27), 0.97 (3H, s, Me-21), 1.10 (3H, s, Me-19),

2.64 (2H, m, H-26), 3.54 (1H, s, H-3), 4.54 (1H, s, H-16), 4.71 (1H, d, J = 19.2 Hz, H-1′), 5.33 (1H, s, H-6); ^{13}C-NMR (DMSO, 600 MHz) δ: 140.7; 121.6; 98.6; 75.8; 71.4; 71.1; 69.0; 56.1; 49.8; 41.9; 40.5; 39.4; 38.5; 36.9; 32.2; 32.0; 31.2; 29.7; 20.7; 19.5; 18.6; 18.4. ESI-MS: 559.8 ([M + H]$^+$).

Solasodine 3-O-D-xylosidase (**3**). ^{1}H-NMR (DMSO, 600 MHz) δ: 0.76 (3H, s, Me-18), 0.89 (3H, s, Me-27), 0.97 (3H, s, Me-21), 1.10 (3H, s, Me-19), 2.67 (2H, m, H-26), 3.63 (1H, s, H-3), 4.54 (1H, s, H-16), 4.94 (1H, d, J = 17.4 Hz, H-1′), 5.33 (1H, s, H-6); ^{13}C-NMR (DMSO, 600 MHz) δ: 140.93; 121.4; 105.2; 102.2; 97.3; 83.2; 77.7; 73.7; 70.0; 61.6; 56.4; 49.8; 46.2; 41.5; 40.5; 38.7; 37.2; 36.8; 32.2; 31.9; 31.4; 29.8; 28.0; 20.7; 19.5; 18.7; 16.2; 15.0. ESI-MS: 545.7 ([M + H]$^+$).

Solasodine 3-O-D-galactosidase (**4**). ^{1}H-NMR (DMSO, 600 MHz) δ: 0.74 (3H, s, Me-18), 0.86 (3H, d, J = 7.2 Hz, Me-27), 0.97 (3H, s, Me-21), 1.05 (3H, t, J = 7.2 Hz, Me-19), 2.37 (2H, m, H-26), 3.61 (1H, s, H-3), 4.17 (1H, s, H-16), 4.18 (1H, d, J = 17.4 Hz, H-1′), 5.32 (1H, m, H-6); ^{13}C-NMR (DMSO, 600 MHz) δ: 141.0; 121.6; 101.8; 78.3; 77.2; 75.5; 74.0; 71.0; 68.6; 62.8; 60.9; 56.5; 47.6; 41.3; 38.8; 36.8; 29.8; 19.9; 19.6; 16.6; 15.8. ESI-MS: 575.7 ([M + H]$^+$).

Solasodine 3-O-L-arabinoside (**5**). ^{1}H-NMR (CD_3OD, 600 MHz) δ: 0.83 (3H, s, Me-18), 0.87 (3H, d, J = 6.0 Hz, Me-27), 0.99 (3H, d, J = 7.2 Hz, Me-21), 1.04 (3H, s, Me-19), 2.64 (2H, m, H-26), 3.58 (1H, m, H-3), 3.70 (2H, m, H-2′), 3.96 (2H, m, H-1′), 4.32 (1H, s, H-16), 5.37 (1H, s, H-6); ^{13}C-NMR (CD_3OD, 600 MHz) δ: 140.0; 122.0; 100.7; 98.5; 78.5; 72.7; 71.6; 67.6; 65.2; 62.7; 56.5; 50.1; 47.5; 41.3; 40.5; 39.8; 38.7; 37.2; 36.9; 34.0; 32.1; 31.4; 30.1; 29.6; 20.9; 19.4; 16.4; 15.2. ESI-MS: 545.7 ([M + H]$^+$).

Solasodine 3-O-D-riboside (**6**). ^{1}H-NMR (DMSO, 600 MHz) δ: 0.75 (3H, s, Me-18), 0.88 (3H, d, J = 6.6 Hz, Me-27), 0.96 (3H, s, Me-21), 1.07 (3H, d, J = 6.0 Hz, Me-19), 2.69 (2H, s, H-26), 3.67 (1H, s, H-3), 4.53 (1H, m, H-16), 4.85 (1H, t, J = 6.0 Hz, H-1′), 5.33 (1H, d, J = 4.8 Hz, H-6); ^{13}C-NMR (DMSO, 600 MHz) δ: 140.4; 121.7; 98.7; 97.9; 76.3; 70.9; 68.5; 63.7; 61.4; 55.8; 54.9; 49.3; 48.5; 45.2; 41.0; 40.3; 38.7; 38.2; 36.8; 31.7; 31.4; 31.0; 30.1; 20.3; 19.1; 18.3; 17.3; 15.8. ESI-MS: 545.7 ([M + H]$^+$).

Solasodine 3-O-(2′-hydroxyethoxy)methyl ether (**8**). ^{1}H-NMR (CD_3OD, 600 MHz) δ: 0.84 (3H, s, Me-18), 0.87 (3H, d, J = 6.0 Hz, Me-27), 0.98 (3H, d, J = 4.8 Hz, Me-21), 1.05 (3H, s, Me-19), 2.66 (2H, m, H-26), 3.50 (1H, m, H-3), 3.75 (4H, m, H-2',3'), 4.32 (1H, s, H-16), 4.81 (2H, m, H-1′), 5.38 (1H, s, H-6); ^{13}C-NMR (CD_3OD, 600 MHz) δ: 140.5; 121.7; 98.3; 94.2; 71.0; 62.3; 56.5; 50.1; 41.2; 40.5; 40.0; 39.4; 37.1; 36.9; 32.2; 31.4; 28.8; 20.8; 19.4; 16.5; 15.4. ESI-MS: 487.7 ([M + H]$^+$).

Solasodine 3-O-(1′,3′-dihydroxypropan-2′-yloxy)methyl ether (**9**). ^{1}H-NMR (DMSO, 600 MHz) δ: 0.75 (3H, s, Me-18), 0.85 (3H, m, Me-27), 0.97 (3H, s, Me-21), 1.05 (3H, t, J = 7.2 Hz, Me-19), 3.09 (1H, m, H-2′), 3.24 (2H, m, H-26), 3.61 (1H, m, H-3), 4.38 (1H, t, J = 4.8 Hz, H-16), 5.32 (1H, d, J = 4.8 Hz, H-6); ^{13}C-NMR (DMSO, 600 MHz) δ: 140.9; 120.6; 95.8; 94.5; 79.4; 76.7; 61.6; 60.7; 59.1; 58.7; 56.4; 55.5; 54.9; 41.4; 40.9; 37.2; 36.7; 32.2; 31.4; 29.2; 20.7; 19.5; 16.4; 15.2. ESI-MS: 487.7 ([M + H]$^+$).

Synthesis of compound 7

$CH_3NH_2 \cdot H_2O$ (1 mL) was added to a solution of compound **7a** (1 mmol) in 3 mL anhydrous MeOH at room temperature. The mixture was stirred at this temperature for 4 h. The mixture was concentrated and purified by silica column chromatography with a 40:1 solution of CH_2Cl_2-MeOH to afford **7** (yield: 90%).

Solasodine 3-O-glucosaminidase (**7**). ^{1}H-NMR (DMSO, 600 MHz) δ: 0.75 (3H, s, Me-18), 0.78 (3H, d, J = 6.6 Hz, Me-27), 0.88 (3H, d, J = 6.6 Hz, Me-21), 0.98 (3H, s, Me-19), 2.67 (2H, m, H-26), 3.66 (1H, d, J = 10.8 Hz, H-3), 4.56 (1H, s, H-16), 5.21 (1H, s, H-1′), 5.34 (1H, d, J = 4.2 Hz, H-6); ^{13}C-NMR (DMSO, 600 MHz) δ: 140.7; 121.7; 98.0; 77.7; 73.9; 70.5; 65.5; 62.7; 61.2; 59.0; 56.8; 50.0; 41.4; 38.3; 37.2; 36.8; 34.2; 32.2; 31.5; 29.5; 20.8; 19.9; 19.6; 16.6; 15.7. ESI-MS: 574.8 ([M + H]$^+$).

Brief Report

DOI: 10.5582/ddt.2012.v6.1.18

Identification and evaluation of agents isolated from traditionally used herbs against *Ophiophagus hannah* venom

Rima Salama[1], Jintana Sattayasai[2], Arun Kumar Gande[1], Nison Sattayasai[3], Mike Davis[1], Eric Lattmann[1,*]

[1] *Division of Pharmacy, School of Life and Health Sciences, Aston University, Birmingham, England;*
[2] *Department of Pharmacology, Faculty of Medicine, Khon Kaen University, Khon Kaen, Thailand;*
[3] *Department of Biochemistry, Faculty of Science, Khon Kaen University, Khon Kaen, Thailand.*

ABSTRACT: The aim of this study was firstly to identify active molecules in herbs, that are traditionally used for the treatment of snake bite, such as *Curcuma antinaia*, *Curcuma contravenenum*, *Andrographis paniculata*, and *Tanacetum parthenium*; secondly to test similar structurally related molecules and finally to prepare and evaluate an efficient formulation against *Ophiophagus hannah* venom intoxification. Three labdane based compounds, including labdane dialdehyde, labdane lactone, and labdane trialdehyde and two lactones including 14-deoxy-11,12-didehydro-andrographolide and parthenolide were isolated by column chromatography and characterised. Using the isolated rat phrenic nerve-hemidiaphragm preparation, the antagonistic effect of crude extracts, isolated compounds and prepared formulations were measured *in vitro* on the inhibition of the neuromuscular transmission. Inhibition on muscle contraction, produced by the 5 µg/mL venom, was reversed by test agents in organ bath preparations. A labdane trialdehyde, isolated from *C. contravenenum*, was identified as the best antagonising agent in the low micromolar range. Tests on formulations of the most potent *C. contravenenum* extract showed, that the suppository with witepsol H15 was an effective medicine against *O. hannah* venom. This study elucidated the active compounds, accounting for the antivenin activity of traditionally used herbs and suggested the most suitable formulation, which may help to develop potent medicines for the treatment of snake bite in the future.

Keywords: Antivenin activity, rat nerve-hemidiapragm, labdane dialdehyde, labdane trialdehyde, parthenolide, desoxy-andrographolide

**Address correspondence to:*
Dr. Eric Lattmann, Division of Pharmacy, School of Life and Health Sciences, Aston University, Aston Triangle, Birmingham B4 7ET, England.
E-mail: e.lattmann@aston.ac.uk

1. Introduction

The actual incidence and the severity of snake poisoning are currently highly undervalued (*1*). The importance of snake bites is considered a major occupational disease causing both disabilities and mortalities. This disease is causing devastation to individuals, who are involved in agricultural work in the tropical regions worldwide. Inaccurate epidemiological data resulted in the underestimation of this international problem, which requires both high attention and sincere efforts to alleviate its burden (*2*). Based on these facts, the World Health Organization (WHO) is calling for new, proven and affordable treatments. Traditional medicine or herbal medicine has long been used for the treatment of snake bite worldwide for its affirmed effectiveness, easy availability, and fine economic affordability. However, the active ingredients contained in these herbs and most effective formulations are still needed to be elucidated.

We have previously reported a labdane dialdehyde structure (Figure 1), which was isolated from a novel *Curcuma zedoaroides* species and exhibited well antivenin activity (*3*). Species in the genus *Curcuma* including *Curcuma antinaia* and *Curcuma contravenenum* were in regular use in Thailand against cobra intoxication, but they are very hard to find on local markets in Isarn today. Besides of those herbs, another two medical plants including *Andrographis paniculata* and *Tanacetum parthenium* are widely applied for the treatment of snake bite in India and China. *Andrographis paniculata* is in use in India as a snake venom antidote.

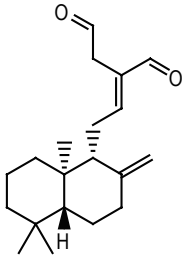

Figure 1. Chemical structure of labdane dialdehyde.

The leaves of *A. paniculata*, locally known as Nilavembu, were grinded into a paste and applied topically at the site of the snake's bite (*4*). *Tanacetum parthenium*, a member of the Asteraceae family, which is also known as the Compositae family, represents a herb well known for its medicinal properties. Since ancient times this herb was used by the Greeks and the Egyptians as well as the early Europeans for the treatment of a number of illnesses, such as headaches, stomach ache, menstrual pain, joint pain, fever. The Chinese used this herb due to its healing properties against insects and snake bites (*5*). In order to further elucidate the ingredients, that account for antivenin activity of these herbs and develop formulations, that are effective against snake venom, we prepared and tested the *in vitro* antivenin activity of the crude extracts, purified compounds and certain formulations against *Ophiophagus hannah* venom in the present study.

2. Materials and Methods

2.1. *Materials*

Lyophilized *O. hannah* venom was obtained from the Queen Suavabha Memorial Institute, Bangkok, Thailand. The venom was dissolved in normal saline, aliquoted and kept at –20°C as stock solution. Herbs including *C. zedoaroides*, *C. antinaia*, *C. contravenenum*, *A. paniculata*, and *T. parthenium* were purchased from the King Cobra Village, Khon Kaen Province, Thailand. The chemicals and solvents were purchased from Aldrich (Gillingham, UK) and Lancaster Synthesis (Lancaster, UK). Mass spectra were obtained by Atmospheric Pressure Chemical Ionisation (APCI), using a Hewlett-Packard 5989b quadrupole instrument (Vienna, Austria). Both proton and carbon NMR spectra were obtained on a Brucker AC 250 instrument (Follanden, Switzerland), calibrated with the solvent reference peak. Infra-red spectra were plotted from KBr discs on a Mattson 300 FTIR spectrophotometer (Coventry, UK).

Laboratory and HPLC grade dichloromethane, petroleum ether 60-80ºC, ethyl acetate, chloroform-d and methanol were purchased from Fisher-Scientific (Waltham, MA, USA). The Soxhlet extraction system was the Quickfit (C5/23) model with (24/29) joint from BÜCHI, Switzerland. The heating mantle used was the Heidolph EKT 3001 from Sigma-Aldrich, UK. The rotary evaporator used was the BÜCHI Rotavapor Model R-144, Switzerland. ^{1}H-NMR and ^{13}C-NMR were recorded in Bruker advance 400 in chloroform-d. Column chromatography was carried out on silica gel and thin-layer chromatography (TLC) on TLC-silica gel 60 F_{254}.

2.2. *Preparation of crude extracts and isolation of the tested compounds*

The rhizomes of *C. zedoaroides*, *C. antinaia*, and *C. contravenenum* (30 g of the dried, powdered rhizomes) were extracted with dichloromethane using a Soxhlet extraction apparatus, respectively. Once the Soxhlet extractions were completed the solvent was removed under reduced pressure from the round bottom flasks using a rotary evaporator. The extract content of *C. zedoaroides*, *C. antinaia*, and *C. contravenenum* were gathered and the entry code **Kae1**, **Mia3**, and **Rat7** was assigned. Column chromoatography of the crude extract was performed using petroleum ether:ethyl acetate (60:40) as solvent system and the compounds were detected with UV light, permanganate, and 2,4-dinitrophenylhydrazine (DNPH). The **Kae1** extract finally provided labdane dialdehyde; **Mia3** extract finally provided labdane dialdehyde and labdane lactone; **Rat7** extract finally provided labdane dialdehyde, labdane lactone, and labdane trialdehyde. The spectra data of these three compounds are shown in the Appendix.

Fifty grams of dried and ground leaves of *A. paniculata* were extracted with 500 mL of methanol using to a Soxhlet extractor. The solvent was evaporated off solvent using rotary evaporation. TLC analysis was performed with a dichloromethane:methanol (95:5) solvent mixture, and both andrographolide and 14-deoxy-11,12-didehydroandrographolide, were purified by column chromatography. The spectra data of 14-deoxy-11,12-didehydroandrographolide are shown in the Appendix.

Fifty grams of grinded plant material *T. parthenium* was extracted with 500 mL of chloroform using a Soxhlet extractor. The extraction was monitored by TLC with ethyl acetate:petroleum ether 60-80°C (70:30) and the TLC plate was developed with vanillin reagent and heated at 400°C for 1 min. Two point five gram of crude extract was dissolved in a minimum volume of ethyl acetate in the heat and 1/3 of the volume of petrol ether was added and cooled on ice. The yellowish sample was recrystallised from ethyl acetate:petroleum ether (70:30) to give parthenolide, 130 mg, as an off white powder. The spectra data of this compound are shown in the Appendix.

2.3. *Preparation of C. contravenemum formulations*

*Ethanolic solution (entry code: **OHRat7**):* For the preparation of the ethanolic solution, 0.5 g of the concentrated extract of *C. contravenemum* was dissolved in 5 mL of ethanol and divided into two portions of 2.5 mL each. To one of the samples **OHRat7** 3 drops of trifluoroacetic acid were added. Both samples were incubated at 36°C for a period of 1 week, then tested.

*Water for injection (entry code: **AqRat7**):* For the preparation of a solution for the injection, 2.5 equivalents of an aqueous solution of 10% $Na_2S_2O_5$ to 0.2 g of the extract in 0.1 mL DMSO were mixed until homogenous and water was added until a final volume of 4 mL.

*Suppositories (entry code: **Rat7S**):* Suppositories (3 g) containing 30% active ingredients were prepared by the fusion method as previously described (*6*). Sixty six grams of *C. contravenemum* rhizomes, giving 1.98 g crude extract, were extracted with 300 mL of acetone as described. The

Table 1. Antivenin activity of crude extracts from *Curcuma* species

Entry Code	Source	Yield	Composition	Muscle contraction response
Kae1	*C. zedoaroides*	7.0%	Labdane dialdehyde, 79%	32.1% (50 µg/mL); 63.1% (100 µg/mL)
Mia3	*C. antinaia*	2.6%	Labdane dialdehyde, 45% Labdane lactone, 39%	26.4% (50 µg/mL); 56.5% (100 µg/mL)
Rat7	*C. contravenenum*	3.0%	Labdane dialdehyde, 32% Labdane lactone, 37% Labdane trialdehyde, 8%	53.5% (50 µg/mL); 82.6% (100 µg/mL)

Measurement time is 30 min; full contraction 100%, venom 0% at 5 µg/mL.

solvent was evaporated off to about a third of the volume and 6 g witepsol H15, a synthetic fat was added and the complete solvent was then evaporated off in vacuum. The homogeneous melt was poured into the suppository moulds and after cooling the suppositories were obtained. The melting point of the prepared suppositories was detected at 32ºC.

2.4. *In vitro antivenin activity assay*

Spraque Dawley rats (200-250 g) were obtained from the Animal House, Faculty of Medicine, Khon Kaen University. The treatment procedures, according to current UK legislation, were approved by the bioethics committee, Faculty of Medicine, Khon Kaen University (HO 2434-76). Animals had free access to fresh water and food pellets. They were exposed to automated 12 h light cycles.

Rat phrenic nerve-hemidiaphragms were prepared according to the staff of the Department of Pharmacology, University of Edinburgh (1970) and the contractile responses were studied. The entire nerve-muscle preparation was submerged in 50 mL Kreb's solution with carbogen and the temperature was maintained at 37°C. The phrenic nerve was stimulated with a rectangular-wave pulse of 0.5 msec/0.5 Hz through a bipolar platinum electrode, using a Grass Model S-48 stimulator. Muscle contraction was recorded with a force transducer and Grass Polygraph recorder. The indicated doses of crude extract (**Kae1**, **Mia3**, and **Rat7**), test solutions of the isolated compounds in DMSO, and prepared formulations (**OHRat7**, **AqRat7**, and **Rat7S**) were added, respectively, to a circulating water bath at 37°C for 30 min and then venom was added and 30 min later the muscle contraction was accessed. Two phrenic nerve-hemidiaphragm preparations were obtained from one animal. Control, DMSO, was set to 100%, 5 µg/mL venom to 0%. The % test response (muscle contraction) was measured at 30 min in presence of the test compounds and the venom. In the control group, 5 µg/mL venom alone gradually and completely inhibited the indirectly-evoked twitches within 30 min (0% response). In presence of the antidote the contraction remained at a certain percentage of the full contraction. This effect was used here to screen the 3 *Curcuma* plant extracts, the isolated compounds and the formulations of the best plant.

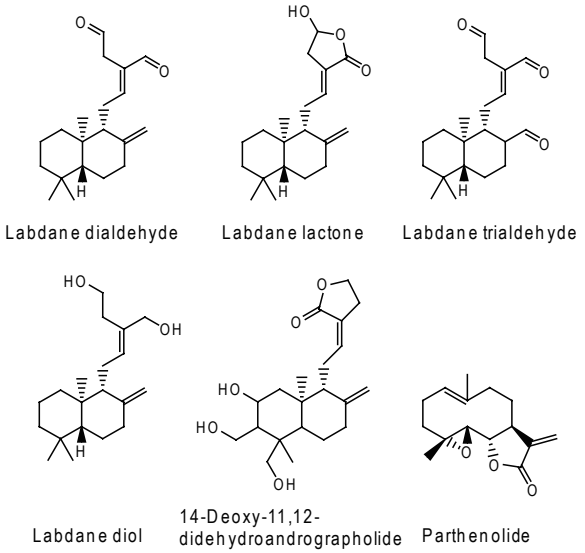

Figure 2. Chemical structures of the isolated compounds.

3. Results and Discussion

3.1. *In vitro antivenin activity of crude extracts from the genus Curcuma*

The protecting effects of crude extracts **Kae1**, **Mia3**, and **Rat7** from *C. zedoaroides*, *C. antinaia*, and *C. contravenenum* against *O. hannah* venom on the neuromuscular transmission of the rat phrenic nerve-hemidiaphragm are shown in Table 1. The **Kae1** extract was obtained in the highest yield (7%) and at a 100 µg/mL dose the response was still above 60%. The best protection was determined for **Rat7** extract (yield 3.0%), giving for the 100 µg/mL organ bath concentration a more than 80% of the original contraction of the diaphragm. **Mia3** extract was obtained in the lowest yield (2.6%) and demonstrated the lowest antivenom activity. The muscle contract response was determined as 56.5% when expososed to 100 µg/mL of this extract.

3.2. *Analysis of the ingredients in the crude extracts and evaluation of their antivenin activity*

The crude extracts from the five medicinal herbs, used in the present study, were further purified and generated the test compounds (Figure 2). The antivenin activities of

these agents were examined and the results are shown in Table 2. The crude extract **Kae1** from *C. zedoaroides* is a very good source of the labdane dialdehyde, which was obtained from this species in 79% yield and excellent purity, by simple column chromatography. A 10 µg/mL concentration of this compound showed 83% protection against the snake venom.

The crude extract **Mia3** from *C. antinaia* provided in addition to labdane dialdehyde, a second labdane derivative, identified as labdane lactone (Figure 2), which showed a bioactivity about 60%. Its formation can be understand if we assume that the labdane dialdehyde is oxidised to the corresponding carboxylic acid and the second aldehyde is able to form the hydroxyl-lactone structure of labdane lactone. The proportions of labdane dialdehyde and labdane lactone in **Mia3** were detected as 45% and 39%, respectively. Labdane lactone was previously isolated from members of the Zingiberaceae family, which are traditionally used as a medicine against inflammatory diseases. This antiinflammatory agent regulates NF-κB-regulated cellular responses in particular it inhibited NF-κB activation, suppressed phosphorylation, p65 nuclear translocation and reporter gene transcription (*11*).

From *C. contravenenum* extract **Rat7**, in addition to labdane dialdehyde and labdane lactone, a third molecule labdane trialdehyde (Figure 2) was finally isolated. The percentages of labdane dialdehyde, labdane lactone, and labdane trialdehyde in this extract were determined as 32%, 37%, and 8%, respectively. Labdane trialdehyde maintained nearly a full diaphragm contraction and with 99.5% protection it is considered the best venom antidote, reported to date. Comparing the activities of these three molecules, the labdane trialdehyde is the most potent antivenin agent, followed by labdane dialdehyde and labdane lactone. Through analyzing the relationship between activities and structures of the above isolated compounds, the succindialdehyde structure may be essential and if the dialdehyde moiety was reduced to a diol the activity was lost (labdane diol, Figure 2). The labdane trialdehyde was previously isolated from myoga extracts on the search for inhibitors of human platelet aggregation and human 5-lipoxygenase. This compound was found to be a potent inhibitor of human platelet aggregation and human 5-lipoxygenase (*7*). The percentage, in which it is present in this curcuma species, is with 8% a good new source of this agent and therefore, it can be evaluated for further therapeutic applications.

Guided by previous enzyme-linked immunosorbent assay (ELISA) study (*8*) *T. parthenium* (Feverfew) and *A. paniculata* were also investigated in addition to the *Curcuma* plant. From *A. paniculata*, andrographolide and 14-deoxy-11,12-didehydroandrographolide were isolated and tested. The desoxy-derivative displayed a weak inhibition of 32% at the 10 µM test concentration while andrographolide was found inactive as antidote. As 14-deoxy-11,12-didehydroandrographolide is only present in less than 0.01% in the traditional formulation, known as Nilavembu, it cannot be recommended. The concentration and resulting of this the active amount of 14-deoxy-11,12-didehydroandrographolide is simply too low to have any medicinal effect. *T. parthenium* is a herb well known for its medicinal properties. The Chinese used this herb due to its healing properties against insects and snake bites. Overall parthenolide isolated from this herb had reasonable antivenom activity of about 54% and it can easily be isolated in good quantities by crystallisation. It is the only European herb, which is readily available in a commercial formulation as a tablet from *e.g.* simply supplements (*9*).

Table 2. Antivenin activity of isolated compounds

Compound	Muscle contraction response
Labdane dialdehyde	
1 µM	66.1%
10 µM	82.6%
Labdane diol	
1 µM	0
10 µM	2.1%
Labdane lactone	
1 µM	45.6%
10 µM	61.9%
Labdane trialdehyde	
1 µM	83.5%
10 µM	99.5%
14-Deoxy-11,12-di-dehydroandrographolide	
1 µM	12.2%
10 µM	32.4%
Parthenolide	
1 µM	29.4%
10 µM	54.0%

Measurement time is 30 min; full contraction 100%, venom 0% at 5 µg/mL.

3.3. *In vitro antivenin activity of C. contravenenum formulations*

C. contravenenum is the easiest plant in terms of plant production and has the biggest rhizome based on the total weight of the entire plant. It gave a 3.0% yield of the crude extract (**Rat7**) which exhibited most potent antivenin activity. For these reasons, three formulations of **Rat7** extract were prepared and tested on their antivenin activity (Table 3). The ethanolic extract of **Rat7** was

Table 3. Antivenin activity of crude extracts from *Curcuma* species

Entry Code	Formulation	Muscle contraction response
OHRat7	10% in ethanol	1.1% (500 µg/mL); 0.2% (1,000 µg/mL)
AqRat7	Hydrogensulfite adduct; 5% in water	5.1% (1,000 µg/mL); 6.3% (5,000 µg/mL)
Rat7S	Suppository 30%	46.1% (200 µg/mL); 77.4% (400 µg/mL)

Measurement time is 30 min; full contraction 100%, venom 0% at 5 µg/mL.

found inactive, and therefore formulations in Thai whisky cannot be recommended. Chemically, the aldehyde functionality has been converted into an ethoxy semi-acetale. Thus, a protected, chemically unreactive structure was formed without any bioactivity. The formulation as hydrogen sulfite adduct was supposed to work as an injection in water, but again with the loss of the chemical reactivity the bioactivity was also lost, at least in the *in vitro* (*ex vivo*) experiment. The formulation of the extract **Rat7** as a suppository worked well; *in vitro* 77% response remained for the 400 µg/mL dose, compared with the original extract of **Rat7** at a 100 µg/mL dose, which gave 83% venom protection. Based on a good *in vitro-in vivo* correlation, we obtained from a previous study, 1-2 suppositories (3 g) should translate into a working anti-venom medication.

Three curcuma species, *i.e. C. zedoaroides*, *C. antinaia*, and *C. contravenenum*, and two other traditional medicines *A. paniculata*, and *T. parthenium* were confirmed active against *O. hannah* venom in our *ex-vivo* assay. In addition to the labdane dialdehyde, which was discovered in *C. zedoaroides* in our previous study, labdane lactone and labdane trialdehyde, isolated from curcuma species *C. antinaia* and *C. contravenenum* were found effective now against the venom. Labdane trialdehyde is the best anti-neurotoxic agent known to date. However, the isolated labdane trialdehyde is unstable. It is supposed, that the natural plant formulation is stabilising labdane trialdehyde with the labdane dialdehyde. Feverfew extract at high doses may be used for snake venom intoxication as a common European alternative. It should be noted, that the only efficient formulation is a suppository, in addition to the preparation of the freshly grinded root of the fresh rhizome. These results provided evidences about the usefulness of some traditional medicines as antidotes and gave clues on the drug development in the future. Further studies are ongoing to replace the *in vitro* antivenin assay, used in this study, by an *in vitro* method, in which chicken intestine is used and not laboratory animal tissue.

Acknowledgements

This study was partly supported by the Khon Kaen University Research Fund. We are grateful for the technical assistance of Wanchai Airarat.

References

1. Warrell DA. Snake bite. Lancet. 2010; 375:77-88.
2. Cruz LS, Vargas R, Lopes AA. Snakebite envenomation and death in the developing world. Ethn Dis. 2009; 19(1 Suppl 1):S1-42-46.
3. Chavaeerach A, Sudmoon R, Tanee T, Mokkamul P, Sattayasai N, Sattayasai J. Two new species of *Curcuma* (Zingiberaceae) used as cobra-bite antidotes. J Syst Evolut. 2008; 46:80-88.
4. Rajadurai M, Vidhya VG, Ramya M, Bhaskar A. Ethno-medicinal plants used by the traditional healers of pachamalai hills, Tamilnadu, India. Ethno-Med. 2009; 3:39-41.
5. Lee KH, Wang HK, Itokawa H, Morris-Natschke SL. Current perspectives on Chinese medicines and dietary supplements in China, Japan and United States. Yao Wu Shi Pin Fen Xi. 2000; 8:219-228.
6. Adegboye TA, Itiola OA. Physical and release properties of metronidazole suppositories. Trop J Pharm Res. 2008; 7:887-896.
7. Suebsasana S, Pongnaratorn P, Sattayasai J, Arkaravichien T, Tiamkao S, Aromdee C. Analgesic, antipyretic, anti-inflammatory and toxic effects of andrographolide derivatives in experimental animals. Arch Pharm Res. 2009; 32:1191-1200.
8. Daduang S, Sattayasai N, Sattayasai J, Tophrom P, Thammathaworn A, Chaveerach A, Konkchaiyaphum M. Screening of plants containing Naja naja siamensis cobra venom inhibitory activity using modified ELISA technique. Anal Biochem. 2005; 341:316-325.
9. Kemper K. Seven herbs every paediatrician should know. Contemporary Paediatrics. 1996; 13:79-90.
10. Lattmann E, Sattayasai J, Sattayasai N, Staaf A, Phimmasone S, Schwalbe CH, Chaveerach A. *In-vitro* and *in-vivo* antivenin activity of 2-[2-(5,5,8a-trimethyl-2-methylene-decahydro-naphthalen-1-yl)-ethylidene]-succinaldehyde against *Ophiophagus hannah* venom. J Pharm Pharmacol. 2010; 62:257-262.
11. Kunnumakkara AB, Ichikawa H, Anand P, Mohankumar CJ, Hema PS, Nair MS, Aggarwal BB. Coronarin D, a labdane diterpene, inhibits both constitutive and inducible nuclear factor-κB pathway activation, leading to potentiation of apoptosis, inhibition of invasion, and suppression of osteoclastogenesis. Mol Cancer Ther. 2008; 7:3306-3317.
12. Tiuman TS, Ueda-Nakamura T, Garcia Cortez DA, Dias Filho BP, Morgado-Diaz JA, de Souza W, Nakamura CV. Antileishmanial activity of parthenolide, a sesquiterpene lactone isolated from *Tanacetum parthenium*. Antimicrob Agents Chemother. 2005; 49:176-182.

(Received January 23, 2012; Revised February 1, 2012; Accepted February 3, 2012)

Appendix

Labdane dialdehyde. 2-[2-(5,5,8a-Trimethyl-2-methylene-decahydro-naphthalen-1-yl)-ethylidene]-succinaldehyde. The ^{1}H-NMR and ^{13}C-NMR data are identical with Lattmann *et al.* (*10*).

^{1}H-NMR ($CDCl_3$, 300 MHz): δ: 9.7 + 9.5 (1H, 1H, CHO), 6.75 (1H, t, C12H), 4.90 + 4.40 (1H, 1H, s, C17H), 3.40 (2H, d, C14H), 2.40 (3H, m, C11H, C6H), 2.0-1.0 (10H, m), 0.9 + 0.8 + 0.7 (9H, s, 3×Me); ^{13}C-NMR: δ: 196.38, 192.60 CHO, C15 + C16; 146.96, 133.78 C8, C13, 159.05 C12, 106.33 C17, 55.20, 54.18 C6, C7, 32.22, 39.34 C1, C5, 34.15, 23.83,14.23 Me, 40.54, 38.30, 38.15, 36.78, 23.55, 23.52, 18.23 C14, C11, C9, C10, C2, C3, C4.

Labdane lactone. 5-Hydroxy-3-[2-(5,5,8a-trimethyl-2-methylene-decahydro-naphthalen-1-yl)-ethylidene]-dihydro-furan-2-one. The ^{1}H-NMR and ^{13}C-NMR data are identical with Kunnumakkara *et al*. (*11*).

^{1}H-NMR ($CDCl_3$, 300 MHz): δ: 6.69 (br s, 1H), 5.94 (br s, 1H), 4.81 (s, 1H), 4.36 (br s, 1H), 2.99 (m, 1H), 2.71 (m, 1H), 2.40-2.36 (m, 2H), 2.20 (m, 1H), 2.05-1.08 (m, 12H), 0.89 (s, 3H), 0.82 (s, 3H), 0.71 (s, 3H); ^{13}C-NMR (75 MHz): δ: 170.65, 148.01, 143.45, 124.48, 107.52, 96.46, 56.02, 55.21, 41.90, 39.94, 39.12, 37.68, 33.57, 33.45, 25.58, 23.99, 21.62, 19.21, 14.23.

Labdane trialdehyde. 2-[2-(2-Formyl-5,5,8a-trimethyl-decahydro-naphthalen-1-yl)-ethylidene]-succinaldehyde. The ^{1}H-NMR and ^{13}C-NMR data are identical with Suebsasana *et al*. (*7*).

^{1}H-NMR ($CDCl_3$, 300 MHz): δ: 9.96 (s, 1H, H-17), 9.62 (s, 1H, H-15), 9.50 (s, 1H, H-16), 7.10 (dd, 1H, *J* = 6.0, 8.8, H-12), 3.54 (d, 1H, *J* = 17, H-14a), 3.48 (d, 1H, *J* = 17, H-14b), 2.85 (m, 1H, *J* = 8.8,12, 15.2, H-11a), 2.65 (m, 1H, *J* = 4, 6, 15.2, H-11b), 2.50 (m, 1H, H-8), 2.35 (m, 1H, H-7b), 1.92 (m, 1H, H-5), 1.75 (m, 1H, H-1b), 1.60 (m, 2H, H-6), 1.42 (m, 1H, H-3b), 1.40 (m, 2H, H-2), 1.40 (m, 1H, H-7a), 1.22 (m, 1H, H-3a), 1.15 (m, 1H, H-1a), 1.05 (m, 1H, H-9), 0.88 (s, 2H, H-18), 0.82 (s, 3H, H-19), 0.80 (s, 3H, H-20); ^{13}C-NMR (75 MHz): δ: 205.37 (C-17), 198.84 (C-15), 194.80 (C-16), 158.72 (C-12), 138.35 (C-13), 56.87 (C-9), 55.03 (C-5), 49.23 (C-8), 43.16 (C-3), 40.29 (C-14), 39.88 (C-10), 39.88 (C-1), 34.25 (C-4), 34.25 (C-18), 25.65 (C-7), 27.14 (C-11), 22.31 (C-19), 20.11 (C-6), 19.82 (C-2), 16.16 (C-20).

14-Deoxy-11,12-didehydro-andrographolide. The ^{1}H-NMR and ^{13}C-NMR data are identical with Suebsasana *et al.* (*7*).

^{1}H-NMR ($CDCl_3$, 300 MHz): δ: 7.43 (1H, t, *J* = 1.76 Hz, H-14), 6.85 (1H, dd, *J* = 10.1 and 15.8 Hz, H-12), 6.15 (1H, d, *J* = 15.8 Hz, H-11), 4.86 (2H, d, *J* = 1.3 Hz, H-15), 4.75 (1H, d, *J* = 1.8 Hz, 17a), 4.49 (1H, d, *J* = 1.8 Hz, 17b), 4.12 (1H, d, *J* = 11.0 Hz, H-19a), 3.39 (1H, t, *J* = 5.3 Hz, H-3), 3.38 (1H, d, *J* = 11.4 Hz, H-19b), 1.22 (3H, s, H-18), 0.83 (3H, s, H-20); ^{13}C-NMR: δ: 172.2 (C=O, C-16), 148.0 (C, C-8), 142.8 (CH, C-12), 136.0 (CH, C-11), 129.2 (C, C-13), 121.1 (CH, C-14), 109.2 (CH2, C-17), 80.8 (CH, C-3), 69.5 (CH2, C-15), 64.2 (CH2, C-19), 61.7 (CH, C-9), 54.7 (CH, C-5), 43.0 (C, C-4), 38.5 (C, C-10), 38.2 (CH2, C-1), 36.6 (CH2, C-7), 28.1 (CH2, C-2), 22.9 (CH2, C-6), 22.6 (CH3, C-18), 15.9 (CH3, C-20).

Parthenolide. The ^{1}H-NMR and ^{13}C-NMR data are identical with Tiuman *et al*. (*12*).

^{1}H-NMR ($CDCl_3$, 300 MHz): δ: 6.34 (d, *J* = 3.6 Hz, H-13α), 5.62 (d, *J* = 3.0 Hz, H-13β), 5.21 (dd, *J* = 2.7, 12.0 Hz, H-1), 3.86 (t, *J* = 8.4 Hz, H-6), 2.79 (d, *J* = 9.0 Hz, H-5), 2.74 to 2.82 (m, H-7), 2.32 to 2.44 (m, H-9β), 2.32 to 2.49 (m, H-2β), 2.11 to 2.21 (m, H-2α, H-3β, H-8α, H-9α), 1.72 (s, H-14), 1.70 to 1.77 (m, H-8β), 1.31 (s, H-15), 1.20 to 1.28 (m, H-3α). ^{13}C-NMR ($CDCl_3$, 75.5 MHz): δ: 169.3 (C-12), 139.2 (C-11), 134.6 (C-10); 125.3 (C-1), 121.3 (C-13), 82.4 (C-6), 66.4 (C-5), 61.5 (C-4), 47.7 (C-7), 41.2 (C-9), 36.3 (C-3), 30.6 (C-8), 24.1 (C-2), 17.3 (C-15), 16.9 (C-14).

Original Article

DOI: 10.5582/ddt.2012.v6.1.24

LKB1, *TP16*, *EGFR*, and *KRAS* somatic mutations in lung adenocarcinomas from a Chiba Prefecture, Japan cohort

Yoshio Suzuki[1], Tadahiro Oonishi[2], Takashi Kudo[3], Hirofumi Doi[3,*]

[1] *Department of Pathology, Asahi General Hospital, Asahi-Shi, Chiba, Japan;*
[2] *MCO, Inc., Yokohama, Kanagawa, Japan;*
[3] *Celish FD, Inc., Chiba-Shi, Chiba, Japan.*

ABSTRACT: The discovery of somatic mutations in cancer-related genes has been applied to understand the genetic basis of cancer. Here we report somatic mutations of two tumor suppressor genes: *LKB1* (exons 1, 4, and 8) and *TP16* (*CDKN2A*) (exons 1 and 2); and two oncogenes: epidermal growth factor receptor *EGFR* (exons 18-21) and *KRAS* (exon 2) in 97 lung adenocarcinoma tissues in a cohort from the Kujukuri coast area of Chiba, Japan. In the *LKB1* gene, only F354L substitutions were observed in 14 of the 97 tissue samples (14.4%). In the *TP16* gene, only two deletions were observed in contrast to previous reports. On the other hand, the *EGFR* gene was highly mutated (38.1%) and mainly L858R substitutions occurred (23.7%) as well as insertions and deletions. In the *KRAS* gene, 10 substitutions at codon 12 were observed (10.3%). Co-occurrence of *EGFR* and *KRAS* somatic mutations was identified in one patient, those of *EGFR* and *LKB1* were in three patients, and those of *KRAS* and *LKB1* were in four patients. The lower rates of *LKB1*, *TP16*, and *KRAS* somatic mutations in lung adenocarcinomas are characteristic of the Kujukuri cohort as compared to Caucasians.

Keywords: Chromatograms, tumor suppressor genes, oncogenes, mTOR pathway, RAS pathway, co-occurrence of mutations

1. Introduction

The *LKB1* tumor suppressor gene, which encodes serine-threonine kinase 11 (STK11), has been shown to regulate cell cycle progression, apoptosis, and cell polarity (*1*). Previous reports have suggested a *LKB1* somatic mutation rate as high as 30% in non-small cell lung carcinoma (NSCLC) tumors derived from Caucasian patients (*2,3*), while being infrequent in NSCLC Asian patients (3%) (*4*). Another review (*5*) reported that *LKB1* somatic mutations were observed in 20.18% of lung adenocarcinoma by analyzing the Catalog of Somatic Mutations in Cancer (COSMIC) (*6*), a large-scale database curated by the Wellcome Trust Sanger Institute. The *TP16* gene (*CDKN2A*, cyclin-dependent kinase inhibitor 2A) is also a tumor suppressor gene and has been reported to show a high rate of deletions as a major type of somatic mutation in cancer, consisting of 24.57% of lung adenocarcinomas in the COSMIC database (*5*). In contrast to these tumor suppressor genes, *EGFR* and *KRAS* oncogenes play a central role in tumorigenesis. The tyrosine kinase activity of EGFR phosphorylates tyrosine residues of target proteins, including KRAS, to initiate multiple signaling pathways resulting in cell proliferation, migration, metastasis, resistance to apoptosis, and angiogenesis (*7,8*). Small-molecule inhibitors of EGFR tyrosine kinase activity (TKIs) such as gefitinib and erlotinib provide a good concept for anticancer drugs. However, clinical trials have revealed significant variability in the TKI response depending on *EGFR* and *KRAS* gene mutations (*9*). Interestingly, somatic *EGFR* and *KRAS* gene mutations, which are upstream and downstream of the RAS pathway, respectively, have been reported to be mutually exclusive. Thus, concurrent *EGFR* and *KRAS* mutations have been very rare (*5*).

Lung adenocarcinoma is the most common form of lung cancer, which has an average 5-year survival rate of 15%, mainly because of late-stage detection and paucity of late-stage treatment options (*10,11*). To determine the genetic basis of lung adenocarcinoma in a cohort from the Kujukuri coast area in Chiba prefecture, Japan, we analyzed exons 1, 4, and 8 of *LKB1*, exons 1 and 2 of *TP16* which includes almost the entire sequence of the protein coding region, exons 18-21 of *EGFR*, and exon 1 of *KRAS*, according to the histogram of somatic mutations in *LKB1*, *TP16*, *EGFR* and *KRAS* from the COSMIC database (*6*).

2. Materials and Methods

2.1. *Patients*

Primary tumor samples from patients with lung adeno-

**Address correspondence to:*
Dr. Hirofumi Doi, Celish FD, Inc., Chibadai Inohana Innovation Plaza, 1-8-15, Inohana, Chuo-Ku, Chiba-Shi, Chiba, 260-0856, Japan.
E-mail: uii58654@nifty.com

carcinoma were obtained from 97 randomly selected patients (54 males and 43 females) with lung cancer who were diagnosed and had undergone surgical resection at Asahi General Hospital, Asahi-Shi, located in the Kujukuri coast area, Chiba prefecture, Japan from September 2004 to March 2009. This study was conducted according to the principles expressed in the Declaration of Helsinki. Asahi General Hospital obtained written informed consent from all subjects. The Asahi General Hospital Institutional Review Board approved use of human tissue in this study according to the Ethical Guidelines of the Ministry of Health, Labour, and Welfare of Japan. The data were analyzed anonymously. All patients were pathologically diagnosed as having primary lung adenocarcinoma and subclassified into histological subtypes by examining more than 10 histological slides. The age distribution was: 5 patients under 50-years old; 12 patients 50- to 59-years-old; 28 patients 60- to 69-years-old; 39 patients 70- to 79-years-old; and 13 patients 80 or over (average = 69.11, S.D. = 9.94).

2.2. *DNA extraction and sequencing analysis*

Genomic DNA extraction was performed using a simple 96-well plate based DNA extraction. A few milligrams of the frozen specimen was digested with Proteinase K at 55°C for 2 h in 100 μL of extraction buffer (10 mM Tris-HCl pH 7.5, 5 mM EDTA, 0.5% Tween 20) followed by heat inactivation at 95°C for 10 min. The preparation was centrifuged at 3000 × g for 15 min, and 2-5 μL of the supernatant was used as a PCR template.

Mutations were detected using PCR-based direct sequencing of three *LKB1* exons (exons 1, 4, 8), two *TP16* exons (exons 1, 2), four *EGFR* exons (exons 18-21), and exon 1 of the *KRAS* gene. The primers for PCR amplification and sequencing analysis are shown in Table 1. PCR amplification was done in 50 μL reactions containing 0.2 μM of each primer pair and 0.25 units of Pfu DNA polymerase (Celestar-Lexico Sciences, Chiba, Japan).

LKB1 exons were amplified by initial denaturation at 94°C for 5 min followed by 40 cycles of 10 sec at 98°C, 30 sec at 68°C, and a 1 min final extension at 72°C. *TP16* exons were amplified by initial denaturation at 94°C for 5 min followed by 40 cycles of 10 sec at 98°C, 30 sec at 65°C, 30 sec at 72°C, and a 1 min final extension at 72°C. *TP16* exon 2 amplification was performed with 5% of DMSO. *EGFR* exons were amplified by initial denaturation at 94°C for 1 min followed by 35 cycles of 5 sec at 98°C, 30 sec at 65°C, 1 min at 72°C, and a final extension at 72°C for 1 min. The exon 1 region of *KRAS* was amplified by initial denaturation at 94°C for 1 min followed by 40 cycles at 98°C for 5 sec, 50°C for 30 sec, and 72°C for 30 sec, and a final extension at 72°C for 5 min.

The PCR products were purified using a GFX96 PCR purification kit (GE Healthcare Life Sciences, Little Chalfont, UK) and sequenced directly using a 3730xl DNA Analyzer (Applied Biosystems, Foster City, CA, USA) with 1 μM of each sequencing primer.

Several samples that were difficult to determine the mutation status by the direct sequencing method were cloned into pUC118 before sequencing.

3. Results

Somatic mutations in *LKB1*, *TP16*, *EGFR*, and *KRAS* genes observed in the cohort from the Kujukuri coast area of Chiba prefecture are summarized in Table 2. The sequence chromatograms are shown in Figures 1, 2, and 3 for single nucleotide substitutions in *LKB1*, *EGFR*, and *KRAS*; two *TP16* deletions; and *EGFR* deletions and insertions, respectively.

Table 1. PCR primer sequences and sequencing primer sequences for exons 1, 4 and 8 of *LKB1*, exons 1 and 2 of *TP16*, exons 18-21 of *EGFR*, and exon 1 of *KRAS*

Gene	Exon	PCR primer sequences	Sequencing primer sequences
LKB1	exon 1	F 5'-TGGAGAAGGGAAGTCGGAACACAAGG-3'	F 5'-GGGAAGTCGGAACACAAGGAAGGAC-3'
		R 5'-GCCAGACGGGTCCAGCTCAG-3'	R 5'-GAACCATCAGCACCGTGACTGGC-3'
	exon 4	F 5'-CCAGCTGGGCCTGTGGTGTTTG-3'	F 5'-CCCCTGTGAGGGGCAGGGAG-3'
		R 5'-CTGGTCCGGCAGGTGTCGTC-3'	R 5'-AACGGGTGCAGTGCCTGTGG-3'
	exon 8	F 5'-AGAGGACATGGCTGAGCTTCTGTGG-3'	F 5'-CAGAGGAGCTGGGTCGGAAAACTGG-3'
		R 5'-GGGACGTGGGATTGGCCACC-3'	R 5'-TGCAGACAGGCAGGCACCCTG-3'
TP16	exon 1	F 5'-AGGGTCGGAGGGGGCTCTTC-3'	F 5'-AAGAGGAGGGGCTGGCTGGTC-3'
		R 5'-CTGATTCCAATTCCCCTGCAAACTTCG-3'	R 5'-CTCCAGAGTCGCCCGCCATC-3'
	exon 2	F 5'-GGGCTTGTGTGGGGGTCTGC-3'	F 5'-TGGCGGTGAGGGGGCTCTAC-3'
		R 5'-GGCGCGTGAGCTGAGGCAAG-3'	R 5'-TCCCGGGCTGAACTTTCTGTGC-3'
EGFR	exon 18	F 5'-TGTCCTTCCAAATGAGCTGGCAAGTG-3'	F 5'-GTGTCCTGGCACCCAAGC-3'
		R 5'-GGAGTTTCCCAAACACTCAGTGAAACAAAG-3'	R 5'-CCCCACCAGACCATGAGAG-3'
	exon 19	F 5'-GGGTGCATCGCTGGTAACATCC-3'	F 5'-GCAGCATGTGGCACCATCTC-3'
		R 5'-GATGTGGAGATGAGCAGGGTCTAG-3'	R 5'-CAGAGCAGCTGCCAGACATG-3'
	exon 20	F 5'-CTCAAGATCGCATTCATGCGTCTTCAC-3'	F 5'-GCATTCATGCGTCTTCACCTG-3'
		R 5'-CACACACATATCCCCATGGCAAACTC-3'	R 5'-CATATCCCCATGGCAAACTCTTG-3'
	exon 21	F 5'-GTCAGCAGCGGGTTACATCTTCTTTC-3'	F 5'-CAGCCATAAGTCCTCGACGTG-3'
		R 5'-CTCACCCAGAATGTCTGGAGAGC-3'	R 5'-TCCTCCCCTGCATGTGTTAAAC-3'
KRAS	exon 1	F 5'-AGGTACTGGTGGAGTATTTGATAGTG-3'	F 5'-TTGATAGTGTATTAACCTTATG-3'
		R 5'-CATACTCCCAAGGAAAGTAAAGTTCC-3'	R 5'-TGGTCCTGCACCAGTAATATGC-3'

F, forward. R, reverse.

Table 2. Somatic mutations in exons 1, 4 and 8 of *LKB1*, exons 1 and 2 of *TP16*, exons 18-21 of *EGFR*, and exon 1 of *KRAS* observed in the Kujukuri cohort

Gene/exon	Somatic mutations	Number	Male	Female
LKB1 (exons 1, 4, 8)	ttc/ttg (F354L)	14	9	5
TP16 (exons 1, 2)	del549c	1	1	0
	del666-673	1	1	0
EGFR (exons 18-21)	ctg/cgg (L858R)	23	11	12
	D770-N771 ins SVD	1	0	1
	cgc/tgc (R776C), ctg/cgg (L858R)	1	0	1
	746ELREA deletion	7	6	1
	746ELREA deletion, ctg/cgg (L858R)	1	1	0
	ggc/gcc (G719A)	1	0	1
	747LRE deletion, A750P, ctg/cgg (L858R)	1	0	1
	P772-H773 ins YNP, H773Y	1	0	1
	gtg/ctg (V834L), ctg/cgg (L858R)	1	0	1
KRAS (codon 1)	ggt/gtt (G12V)	1	0	1
	ggt/tgt (G12C)	4	2	2
	ggt/gat (G12D)	3	2	1
	ggt/gat (G12A)	2	2	0

The two right columns show the numbers related to gender.

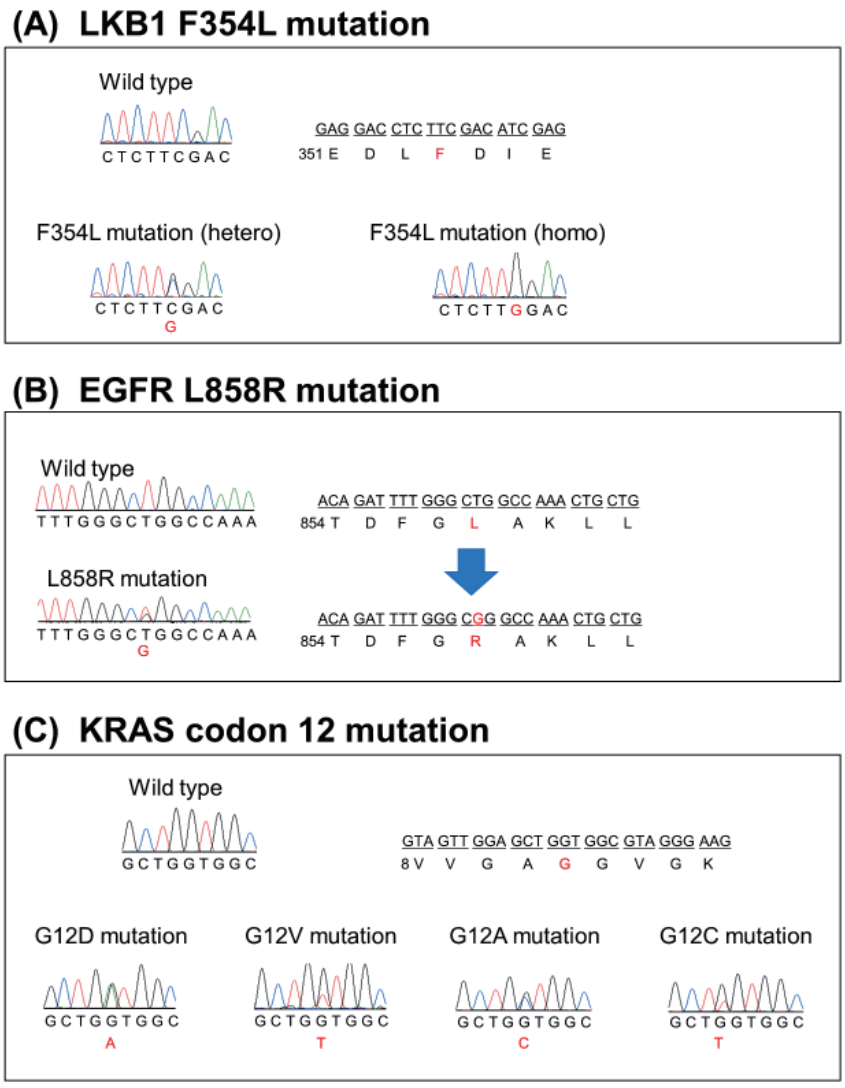

Figure 1. Wave charts of analyzed nucleotide sequences and corresponding amino acid sequences. (A) *LKB1* wild type nucleotide sequence and base substitutions (hetero and homo) at F354L. **(B)** *EGFR* wild type nucleotide sequence and base substitution at F858R. **(C)** *KRAS* wild type nucleotide sequence and base substitutions at codon 12.

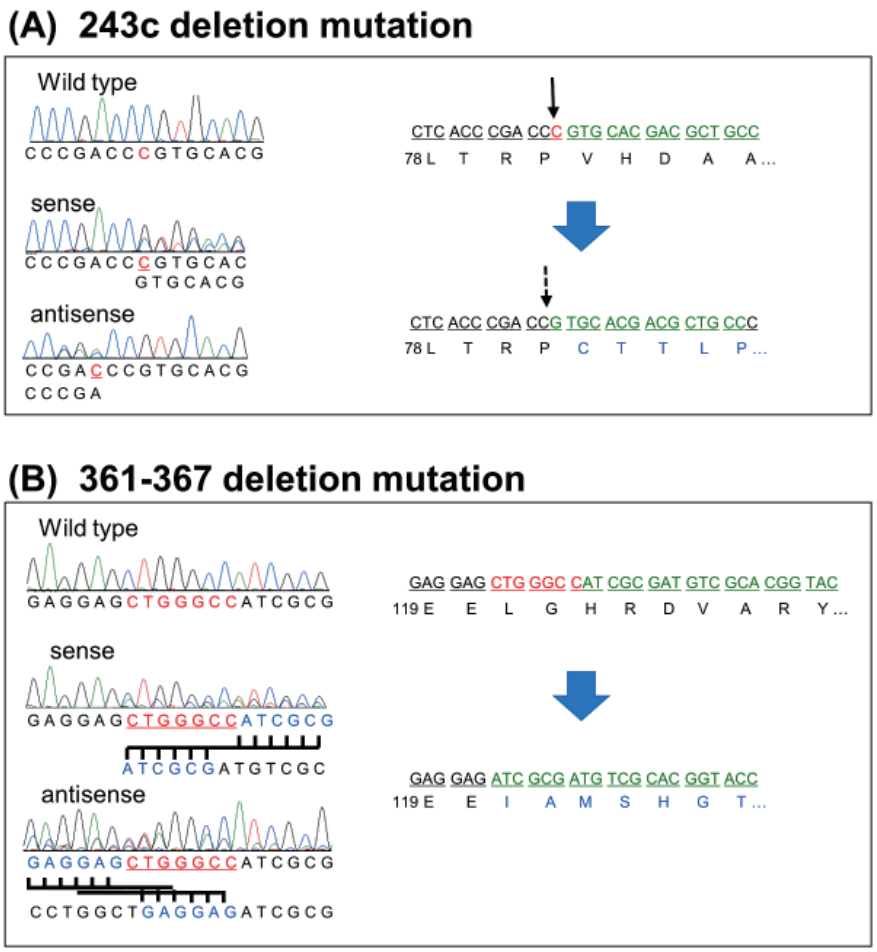

Figure 2. Wave charts of nucleotide sequences and corresponding amino acid sequences of wild type and two deletions observed in the *TP16* gene. (A) 549C deletion mutation. **(B)** 666-673 deletion mutation.

3.1. *LKB1 and TP16 mutations*

We analyzed the sequence of exons 1, 4, and 8 of the *LKB1* gene and the sequence of the *TP16* gene (exons 1 and 2). Of the 97 lung adenocarcinoma tissue samples, only 14 samples (14.4%) were observed to contain F354L substitutions in exon 8 of the *LKB1* gene, of which two samples showed biallelic mutations. Figure 1A shows the three types of *LKB1* sequences observed in chromatograms: wild type, hetero F354L mutation, and biallelic (homo) F354L mutation. On the other hand, only 2 of the 97 tissue samples (2.1%) showed deletions in exon 2 of the *TP16* gene (cytosine deletion at 549 changed the amino acid sequence after 82Val; and the deletion from 666 to 673 changed the amino acid sequence after 121Leu; the numbers of nucleotides and residues are from NM_000077.4 and NP_000068.1 in the NCBI database), as shown in Figures 2A and 2B.

3.2. *EGFR and KRAS mutations*

The major somatic mutations of the *EGFR* gene observed in the cohort were L858R substitutions at exon 21, as shown in the Figure 1B chromatogram. There were 23 samples of the 97 tissue samples (23.7%) that showed only this substitution and four samples that showed other types of mutations in addition to this substitution (Table 2). Another major mutation was the 746-ELREA-750 deletion at exon 19 that was observed in 7 samples (7.2%). The sequencing result chromatogram showed this deletion in Figure 3A. Figures 3B and 3C showed the sequencing results of insertion mutations. Figure 3B showed the insertion of three amino acids YNP between 772Pro and 773His in exon 20, and the histidine residue was substituted by Tyr. Figure 3C showed the insertion of three amino acids SVD between 770Asp and 771Asn in exon 20. The other mutations observed are summarized in Table 2. In total, 37 of 97 samples (38.1%) displayed somatic mutations in the *EGFR* gene.

The somatic mutations observed in the *KRAS* gene were only substitutions at codon 12 of amino acid residue Gly to Asp (3 samples), to Val (1 sample), to Ala (2 samples), and to Cys (4 samples). A total of 10 samples showed somatic mutations in *KRAS* (10.3%). Figure 1C shows the sequences of the somatic mutations at *KRAS* codon 12 on chromatograms.

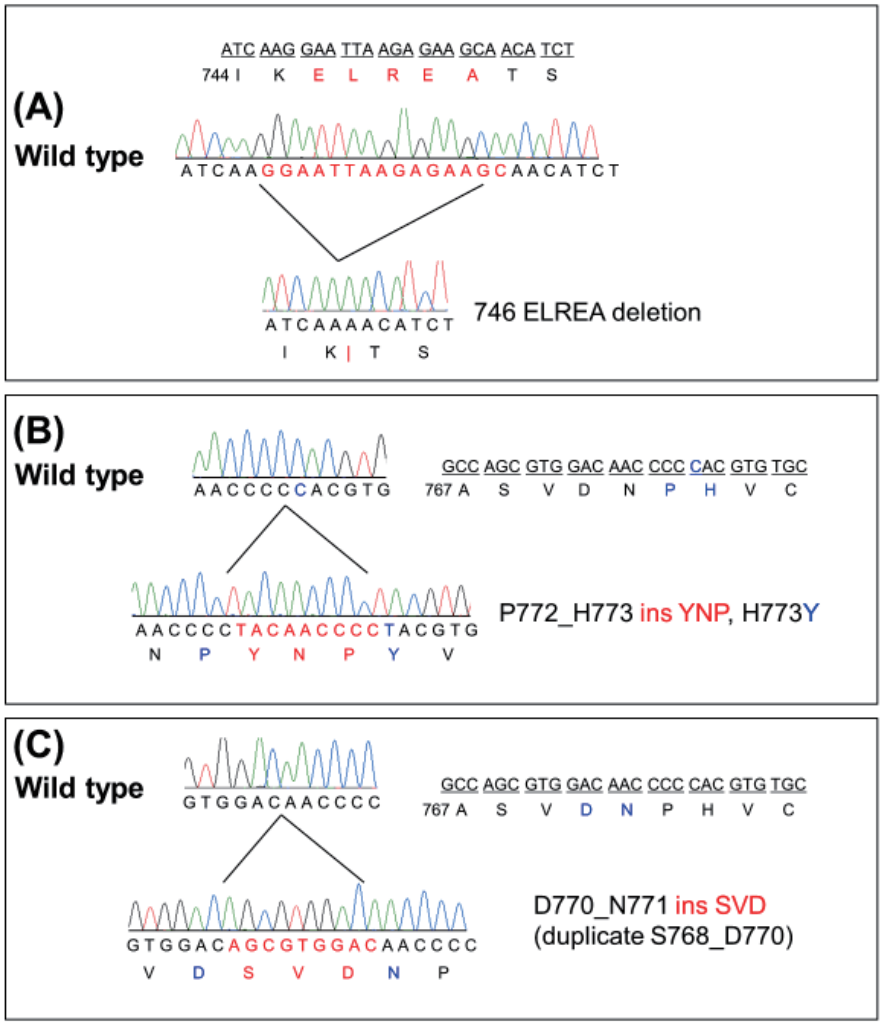

Figure 3. Wave charts of nucleotide sequences and corresponding amino acid sequences of wild type, deletions, and insertions observed in the *EGFR* gene. (A) 746ELREA deletion. **(B)** P772_H772 insertion YNP with H773Y. **(C)** D770_N771 insertion SVD (duplication S768_D770).

3.3. *Concurrency of mutations*

The concurrent *EGFR* and *KRAS* mutations have been reported to be very rare (*5*), meaning the occurrence of those mutations were mutually exclusive in lung adenocarcinoma. We observed that only one of the 97 tissue samples harbored the concurrent *EGFR* and *KRAS* mutations. In contrast, co-occurrence of *EGFR* and *LKB1* mutations were observed in three samples, while co-occurrence of *KRAS* and *LKB1* mutations were observed in four samples.

4. Discussion

We analyzed somatic mutations in tumor suppressor genes *LKB1* and *TP16*, and in oncogenes *EGFR* and *KRAS*, using 97 lung adenocarcinoma tissue samples in a cohort from the Kujukuri coast area of Chiba prefecture, Japan. Compared with the review paper that analyzed the COSMIC database (*5*), we showed the rate of *TP16* somatic mutations in the Kujukuri cohort to be very small (2.1%), while the COSMIC database showed a 24.57% mutation rate. The *LKB1* mutation rate was 14.4% from our observations, while that of the COSMIC database was 20.18%. In particular, only F354L substitutions in the *LKB1* gene were observed in the Kujukuri cohort.

As for *EGFR*, the somatic mutation rate was 38.1% from our observations, which is a little bit higher than the rate from the COSMIC database (35.85%). *KRAS* also showed a lower somatic mutation rate in the Kujukuri cohort (10.3%) than that from the COSMIC database (23.02%). The lower rates of somatic mutations for *LKB1*, *TP16*, and *KRAS* genes in lung adenocarcinomas are characteristic of the Kujukuri cohort.

EGFR mutations have been more commonly found in tumors from patients who never smoked cigarettes (*12*), while *KRAS* mutations have been present in those with significant tobacco exposure (*9,13*). Unfortunately, we could not follow the history of smoking or non-smoking patients from clinical records of the cohort,

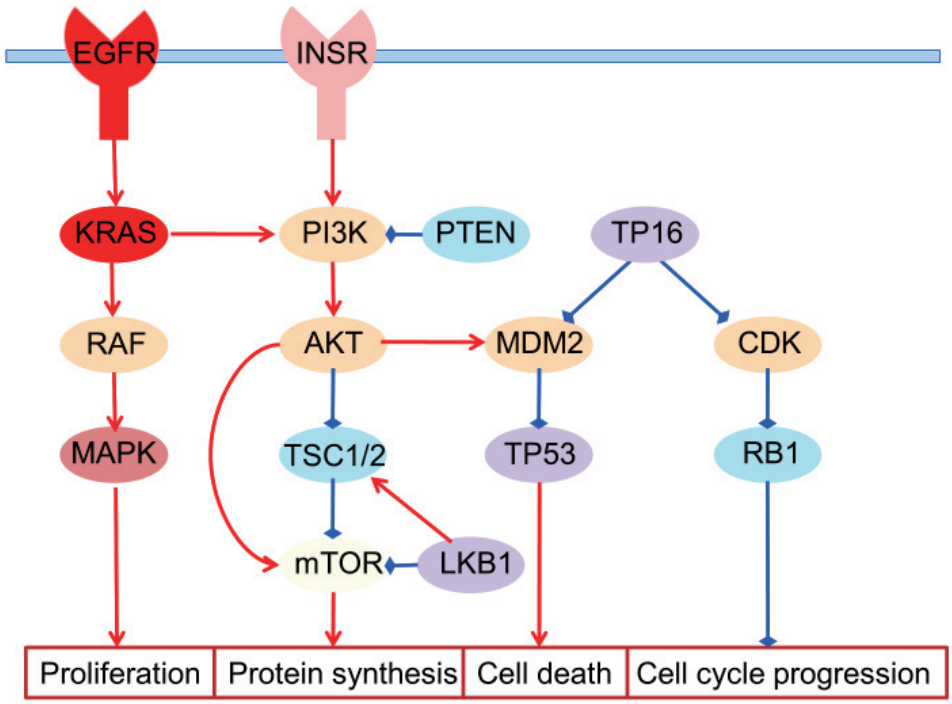

Figure 4. Pathways relating to *LKB1*, *TP16*, *EGFR*, and *KRAS*. The pathways were summarized from Kyoto Encyclopedia of Genes and Genomes (KEGG). Red lines represent activation and blue lines represent inhibition.

except for the 11 patients who were never-smokers. Among the 11 patients, we found four *EGFR* mutations (36.3% = 4/11) that included three L858R substitutions and one insertion, and a single *KRAS* mutation (9.1% = 1/11). The percentages of *EGFR* and *KRAS* mutations in the 11 never-smoking patients were not significantly different from those in the remaining 86 patients (*EGFR*: 38.3% = 33/86, and *KRAS*: 10.5% = 9/86), suggesting that *EGFR* and *KRAS* mutations in the cohort are not associated with tobacco use. Contrary to previous reports describing the association between *EGFR* mutations and non-smoking history (*12*), recent papers have reported no association with smoking or non-smoking history in Asian patients (*14-16*).

Gender also has been reported to be unconnected with *EGFR* mutations in Asian patients (*14,15*). We also found no association between gender and any type of *EGFR* mutations in the cohort. However, focusing on the 746ELREA deletions, 6 out of 7 patients with this type of deletion were male patients. Moreover, we investigated the distribution of mutations in the four genes across different clinicopathological subgroups based on tumor size, clinical stage, and histological subtypes including acinar, papillary, and bronchioloalveolar carcinoma patterns. However, no significant association with clinicopathological subgroups was found (data not shown), which is consistent with a previous report (*17*).

One interesting topic in analyzing genetic somatic mutations is the co-occurrence of mutations in two genes. Co-occurrence of *EGFR* and *KRAS* mutations, which lie upstream and downstream of the RAS pathway respectively, has been reported to be mutually exclusive (*5*). In the review paper that analyzed the COSMIC database (*5*), the co-occurrence of *TP16* and *KRAS* mutations was reported in pancreatic cancer, lung large cell cancer, colon cancer, kidney tumors, and lung adenocarcinoma. However, in the present study, co-occurrence of *TP16* and *KRAS* mutations was not observed because of the lower mutation rate of *TP16* in the Kujukuri cohort. On the other hand, as to *LKB1* we co-sequenced *LKB1* and *KRAS* in the 97 lung adenocarcinomas tissue samples, and found four co-occurring mutations in these genes. So, mutations in these genes may not be mutually exclusive and therefore these genes may not be located on the same pathway. Co-occurrence of *LKB1* and *EGFR* mutations was also observed in three samples. Taken together, *LKB1* might act separately from the RAS pathway to suppress tumorigenesis. According to the known pathways summarized from the Kyoto Encyclopedia of Genes and Genomes (KEGG) (Figure 4) related to the *LKB1*, *TP16*, *EFGR*, and *KRAS* genes pathways, *LKB1* attenuates protein synthesis by inhibiting the mTOR pathway (*18*), that is separated from the RAS pathway.

Acknowledgements

We acknowledge Hiroshi Yoshida for his assistance in preparing this manuscript.

References

1. Tiainen M, Ylikorkala A, Mäkelä TP. Growth suppression by Lkb1 is mediated by a G(1) cell cycle arrest. Proc Natl Acad Sci U S A. 1999; 96:9248-9251.
2. Carretero J, Medina PP, Pio R, Montuenga LM, Sanchez-Cespedes M. Novel and natural knockout lung cancer cell lines for the *LKB1/STK11* tumor suppressor gene. Oncogene. 2004; 23:4037-4040.
3. Matsumoto S, Iwakawa R, Takahashi K, Kohno T, Nakanishi Y, Matsuno Y, Suzuki K, Nakamoto M, Shimizu E, Minna JD, Yokota J. Prevalence and specificity of *LKB1* genetic alterations in lung cancers. Oncogene. 2007; 26:5911-5918.
4. Onozato R, Kosaka T, Achiwa H, Kuwano H, Takahashi T, Yatabe Y, Mitsudomi T. *LKB1* gene mutations in Japanese lung cancer patients. Cancer Sci. 2007; 98:1747-1751.
5. Yeang CH, McCormick F, Levine A. Combinatorial patterns of somatic gene mutations in cancer. FASEB J. 2008; 22:2605-2622.
6. Welcome Trust Sanger Institute. Catalogue of Somatic Mutations in Cancer. *http://www.sanger.ac.uk/genetics/CGP/cosmic/* (accessed November 15, 2010).
7. Takeuchi K, Ito F. EGF receptor in relation to tumor development: Molecular basis of responsiveness of cancer cells to EGFR-targeting tyrosine kinase inhibitors. FEBS J. 2010; 277:316-326.
8. Arteaga CL. Overview of epidermal growth factor receptor biology and its role as a therapeutic target in human neoplasia. Semin Oncol. 2002; 29(5 Suppl 14):3-9.
9. Riely GJ, Marks J, Pao W. *KRAS* mutations in non-small cell lung cancer. Proc Am Throc Soc. 2009; 6:201-205.
10. Prkin DM, Bray F, Ferlay J, Pisani P. Global cancer statistics, 2002. CA Cancer J Clin. 2005; 55:74-108.
11. Collins LG, Haines C, Perkel R, Enck RE. Lung cancer: Diagnosis and management. Am Fam Physician. 2007; 75:56-63.
12. Pao W, Miller V, Zakowski M, Doherty J, Politi K, Sarkaria I, Singh B, Heelan R, Rusch V, Fulton L, Mardis E, Kupfer D, Wilson R, Kris M, Varmus H. EGF receptor gene mutations are common in lung cancers from "never smokers" and are associated with sensitivity of tumors to gefitinib and erlotinib. Proc Natl Acad Sci U S A. 2004; 101:13306-13311.
13. Pao W, Wang TY, Riely GJ, Miller VA, Pan Q, Ladanyi M, Zakowski MF, Heelan RT, Kris MG, Varmus HE. *KRAS* mutations and primary resistance of lung adenocarcinomas to gefitinib or erlotinib. PLoS Med. 2005; 2:e17.
14. Shigematsu H, Lin L, Takahashi T, *et al*. Clinical and biological features associated with epidermal growth factor receptor mutations in lung cancers. J Natl Cancer Inst. 2005; 97:339-346.
15. Huang SF, Liu HP, Li LH, Ku YC, Fu YN, Tsai HY, Chen YT, Lin YF, Chang WC, Kuo HP, Wu YC, Chen YR, Tsai SF. High frequency of epidermal growth factor receptor mutations with complex patterns in non-small cell lung cancers related to gefitinib responsiveness in Taiwan. Clin Cancer Res. 2004; 10:8195-8203.
16. Jang TW, Oak CH, Chang HK, Suo SJ, Jung MH. *EGFR* and *KRAS* mutations I patients with adenocarcinoma of the lung. Korean J Intern Med. 2009; 24:48-54.
17. Ding L, Getz G, Wheeler DA, *et al*. Somatic mutations affect key pathways in lung adenocarcinoma. Nature. 2008; 455:1069-1075.
18. Shaw RJ. *LKB1* and AMP-activated protein kinase control of mTOR signaling and growth. Acta Physiol. 2009; 196:65-80.

(Received January 19, 2012; Revised February 5, 2012; Accepted February 6, 2012)

Original Article

DOI: 10.5582/ddt.2012.v6.1.31

Inhibition of morphine tolerance is mediated by painful stimuli *via* central mechanisms

Shigeki Iwai, Norikazu Kiguchi*, Yuka Kobayashi, Yohji Fukazawa, Fumihiro Saika, Keiko Ueno, Chizuko Yamamoto, Shiroh Kishioka

Department of Pharmacology, Wakayama Medical University, Wakayama, Japan.

ABSTRACT: Tolerance to morphine analgesia following repeated administration disturbs the continuation of opioid therapy for severe pain. Emerging evidence suggests that the development of morphine tolerance may be antagonized by painful stimuli. To clarify the detailed mechanisms of these phenomena, we examined the effects of several pain stimuli on morphine-induced tolerance. Subcutaneous (*s.c.*) injection of morphine (10 mg/kg) produced an analgesic effect, which was evaluated by tail-pinch test. Morphine-induced analgesia was diminished by repeated administration of morphine (10 mg/kg, *s.c.*) once a day for 5 days, demonstrating the development of tolerance. Morphine analgesic tolerance was suppressed by nerve injury-induced neuropathic pain and formalin- or carrageenan-induced inflammatory pain. Tolerance to serum corticosterone elevation by morphine (10 mg/kg), which was evaluated by fluorometric assay, was also suppressed by formalin-induced inflammatory pain. Moreover, morphine analgesia induced by intracerebroventricular (10 nmol) or intrathecal (5 nmol) injection was diminished by repeated administration of morphine *s.c.*, and this was also suppressed by carrageenan-induced inflammatory pain. These results suggest that morphine tolerance is inhibited by several pain stimuli, including neuropathic and inflammatory pain, through central mechanisms.

Keywords: Opioid, analgesia, neuropathic pain, inflammatory pain

**Address correspondence to:*
Dr. Norikazu Kiguchi, Department of Pharmacology, Wakayama Medical University, 811-1 Kimiidera, Wakayama 641-0012, Japan.
E-mail: kiguchi@wakayama-med.ac.jp

1. Introduction

Opioid ligands including morphine are potent analgesics that are widely used for the treatment of severe pain, *e.g.*, cancer progression (*1,2*). In addition to other serious adverse effects such as respiratory depression and constipation, tolerance and dependence may also disturb the continuation of opioid therapy (*3*). Therefore, an understanding of the molecular mechanisms underlying opioid tolerance and dependence is required. Several hypotheses concerning opioid tolerance have been published. For instance, alterations of neural networks and glial activities after chronic exposure to opioids were revealed (*4-6*). These phenomena might be responsible for the opioid tolerance and dependence.

In contrast, emerging evidence suggests that the development of opioid tolerance may be antagonized by painful stimuli (*7,8*). Experimental inflammatory pain or surgical pain suppressed the morphine tolerance (*9,10*). Despite several lines of evidence, the effects of different types of pain on opioid tolerance have not been yet clarified. Moreover, detailed mechanisms underlying the inhibition of opioid tolerance by painful stimuli are unclear. Therefore, we examined the effects of several pain stimuli (*i.e.*, neuropathic and inflammatory pain) on morphine-induced tolerance, and investigated whether the central nervous system (CNS) is a key region relating to these phenomena.

2. Materials and Methods

2.1. *Animals*

Male ICR mice (15-25 g) were obtained from Japan SLC, Inc. (Osaka, Japan), and they were housed in an air-conditioned (23-24°C, 60-70% relative humidity) vivarium with a 12 h dark/light cycle (light on from 8:00 to 20:00). Water and food were available *ad libitum*. All experimental procedures were approved by the Animal Research Committee of Wakayama Medical University and complied with the ethical guidelines of the International Association for the Study of Pain (*11*).

2.2. *Morphine administration*

Morphine hydrochloride (Takeda, Osaka, Japan) was dissolved in physiological saline, and administered to mice by subcutaneous (*s.c.*, 0.1 mL/10 g), intracerebroventricular (*i.c.v.*, 5 μL), or intrathecal (*i.t.*, 5 μL) injection. The *i.c.v.* injections were administered into the left lateral ventricle, and the *i.t.* injections were administered into the region between spinal L5 and L6 segments as described in a previous report (*12,13*). For the *i.c.v.* and *i.t.* injections, Hamilton microsyringes fitted with 32-gauge or 26-gauge needles were used, respectively.

2.3. *Tail-pinch test*

The analgesic effects of morphine were evaluated by the tail-pinch test as described in our previous report (*14*). Briefly, the mouse tail root was pressed with a 6-mm-wide flattened clip, which was adjusted to about 500 g pressure. Nociceptive responses were indicated by the latency required for response to the pressure by biting the clip. To avoid tissue damage, a cut-off time of 15 sec was set. The clip was applied every 15 min following morphine administration over a 120 min period. The percentage of maximum possible effect (%MPE) was calculated using the following formula: %MPE = 100 × (measured latency – baseline latency)/(15 – baseline latency). The magnitude of analgesia was evaluated by the area under the curve (AUC) calculated from the time course of %MPE.

2.4. *Estimation of serum corticosterone (SCS) level*

Because the level of SCS due to circadian rhythm was most stable before noon each day, the blood was collected for SCS determination at 10:00-11:30. Mice were killed by decapitation and trunk blood was collected 1 h after morphine injection. The serum was separated by centrifugation and SCS level was measured by fluorometric assay according to the method of Zenkar and Bernstein (*15*).

2.5. *Pain models*

Three pain models were used in this study. For the neuropathic pain model, mice were anesthetized with sodium pentobarbital (70 mg/kg, *i.p.*) and the sciatic nerves of both hind limbs were exposed through a small incision. Then, 1/3 of the nerve thickness was tightly ligated with a silk suture (*16,17*). As a sham control, the incision site was closed without ligation. To induce acute inflammatory pain, mice were given 2% formalin or 1% λ-carrageenan into the intraplantar (*i.pl.*, 20 μL) surface of both hind paws (*18,19*). Formalin and carrageenan were dissolved in phosphate buffered saline (PBS, vehicle control). The *i.pl.* injection was performed using a Hamilton microsyringe fitted with a 30-gauge needle.

2.6. *Statistical analysis*

Data are presented as the mean ± S.E.M. Statistical analysis was performed using a one-way analysis of variance (ANOVA) followed by Tukey multiple comparisons test, or two-way ANOVA followed by Bonferroni multiple comparisons test. Significance was established at $p < 0.05$.

3. Results

3.1. *Evaluation of morphine analgesia and its tolerance*

Subcutaneous injection of morphine (10 mg/kg) prolonged the withdrawal latency at 15 min after administration. The prolonged latency lasted for 75 min and was restored within 120 min, indicating the analgesic effect of morphine. Saline injected as a control had no effect on the pain threshold (Figure 1A). By repeated administration of morphine (10 mg/kg) once a day for 5 days, morphine-induced analgesia was gradually diminished, demonstrating the development of analgesic tolerance as shown in AUC (Figure 1B).

3.2. *Inhibition of morphine analgesic tolerance by nerve ligation-induced neuropathic pain*

To examine whether an analgesic tolerance to morphine is affected by neuropathic pain, mice were given partial sciatic nerve ligation (PSL) 1 day before the first morphine administration. Morphine (10 mg/kg) was administered once a day for 5 days, and morphine-induced analgesia was evaluated on days 1, 3 and 5. On day 1, the time-course of morphine analgesia in PSL-operated mice was similar to that in sham-operated mice (Figure 2A), indicating that morphine analgesia was not affected by neuropathic pain. In contrast, on day 5, the analgesic

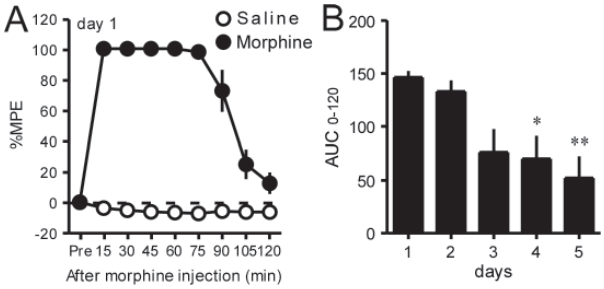

Figure 1. Evaluation of morphine analgesia and tolerance. **(A)** Time course of morphine analgesia on day 1. Morphine (10 mg/kg) or saline was subcutaneously (*s.c.*) administered, and the analgesic effects during a 120 min period after injection were evaluated by tail-pinch test. Analgesic effects are shown as time course of %MPE. **(B)** The development of tolerance to morphine analgesia, estimated by AUC. Morphine (10 mg/kg, *s.c.*) was repeatedly administered once a day for 5 days, and analgesic effect on each day is shown as AUC calculated from time course of %MPE. Data are presented as the mean ± S.E.M. of 6-8 mice. %MPE: the percentage of maximum possible effect; AUC: area under the curve. * $p < 0.05$, ** $p < 0.01$ *vs.* day 1.

effect in PSL-operated mice was greater than that in sham-operated mice (Figures 2B and 2C), indicating that the development of tolerance to morphine analgesia was significantly suppressed by PSL-induced neuropathic pain.

3.3. *Inhibition of morphine analgesic tolerance by formalin- or carrageenan-induced inflammatory pain*

We examined the effects of inflammatory pain on the development of analgesic tolerance to morphine. First, 2% formalin was *i.pl.* injected into mice 2 h before the first morphine administration. Repeated morphine administration and the evaluation of morphine tolerance were performed as shown in Figure 2. On day 1, there was no difference between morphine (10 mg/kg)-induced analgesia in formalin-treated mice and that in PBS-treated control mice, indicating that morphine analgesia was not affected by inflammatory pain (Figure 3A). In contrast, on day 5, the analgesic effect in FOR-treated mice was greater than that in PBS-treated mice (Figure 3B). As shown in AUC, the development of morphine tolerance was significantly suppressed by formalin-induced

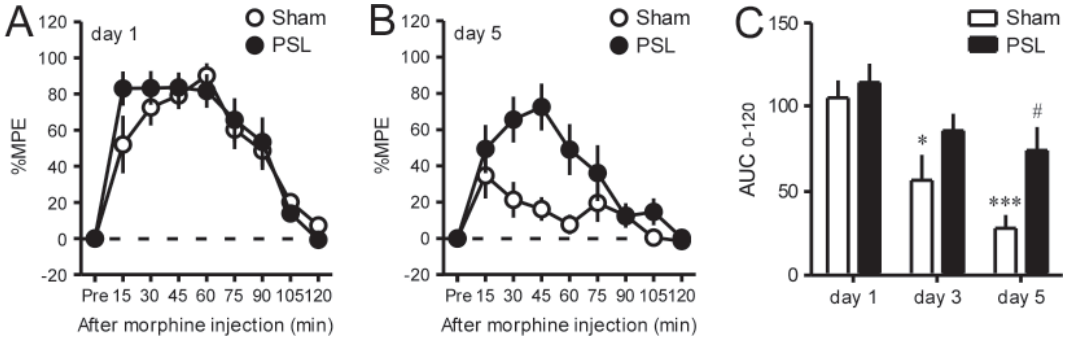

Figure 2. Inhibition of morphine analgesic tolerance by nerve ligation-induced neuropathic pain. Partial sciatic nerve ligation (PSL) was performed 1 day before morphine administration. As sham control, nerve was exposed. Morphine (10 mg/kg, *s.c.*) was administered once a day for 5 days, and morphine analgesia was evaluated for 120 min on days 1, 3, and 5. Analgesic effects of morphine on days 1 **(A)** and 5 **(B)** are shown as time course of %MPE and AUC **(C)**. Data are presented as the mean ± S.E.M. of 8-9 mice. %MPE: the percentage of maximum possible effect; AUC: area under the curve. * $p < 0.05$, *** $p < 0.001$ *vs.* day 1. # $p < 0.05$ *vs.* sham.

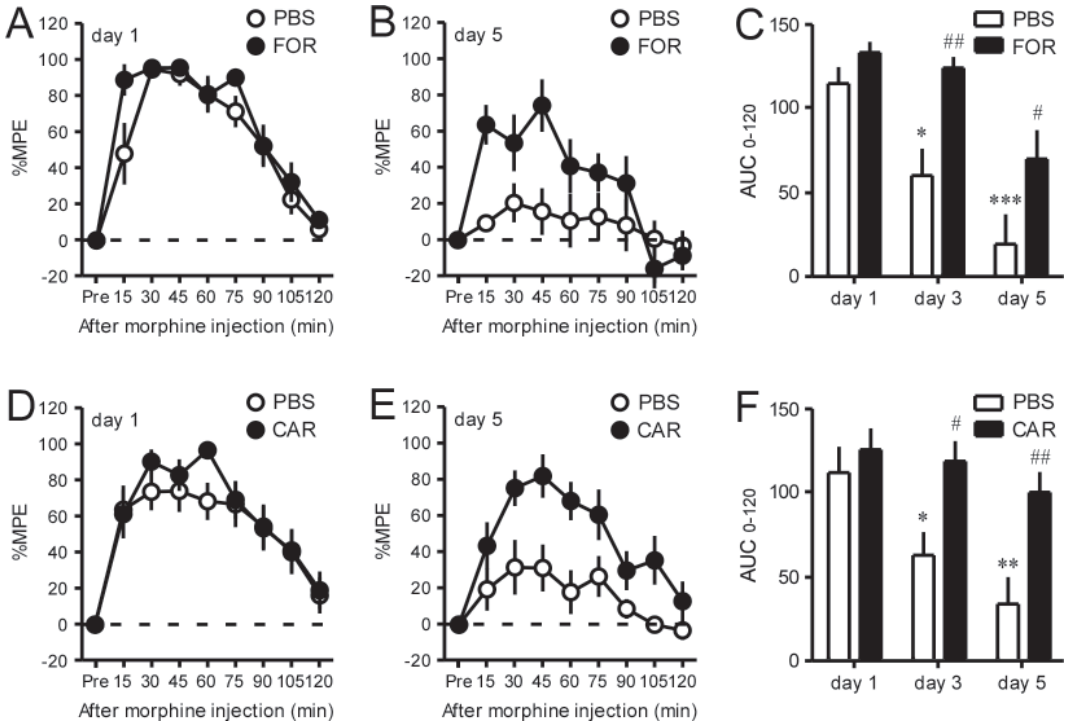

Figure 3. Inhibition of morphine analgesic tolerance by formalin- or carrageenan-induced inflammatory pain. 2% formalin (FOR; **A**-**C**) or 1% carrageenan (CAR; **D**-**F**) was *i.pl.* injected 2 h or 3 h before morphine administration on day 1, respectively. As vehicle control, PBS was injected. Morphine (10 mg/kg, *s.c.*) was administered once a day for 5 days, and morphine-induced analgesia was evaluated for 120 min on days 1, 3, and 5. Analgesic effects of morphine in FOR- or CAR-treated group on days 1 (**A**, **D**) and 5 (**B**, **E**) are shown as time course of %MPE (**A**, **B**, **D**, **E**), and AUC (**C**, **F**). Data are presented as the mean ± S.E.M. of 8-9 mice. %MPE: the percentage of maximum possible effect; AUC: area under the curve. * $p < 0.05$, ** $p < 0.01$, *** $p < 0.001$ *vs*. day 1. # $p < 0.05$, ## $p < 0.01$ *vs*. PBS.

inflammatory pain on days 3 and 5 (Figure 3C). Second, as another inflammatory pain model, 1% carrageenan was *i.pl.* injected into mice 3 h before the first morphine administration. On day 1, there was no difference between morphine (10 mg/kg)-induced analgesia in carrageenan-treated mice and that in PBS-treated control mice, suggesting that carrageenan injection also had no effect on morphine-induced analgesia on day 1 (Figure 3D). On day 3 and 5, the analgesic effect in carrageenan-treated mice was greater than that in PBS-treated mice (Figures 3E and 3F).

3.4. *Effects of formalin-induced inflammatory pain on tolerance to SCS elevation by morphine*

Morphine produces not only analgesia but also SCS elevation. To confirm the inhibition of morphine analgesic tolerance by inflammatory pain, we examined the effect of formalin-induced inflammatory pain on tolerance to SCS elevation by repeated morphine administration. Morphine (10 mg/kg) was administered once a day for 5 days, and the SCS level was evaluated 1 h after morphine injection (10 mg/kg) on day 6. Basal SCS level was 6.8 ± 1.3 μg/dL (n = 5) in naive mice. After repeated saline injection for 5 days, SCS was markedly elevated by morphine. The morphine-induced SCS elevation was significantly suppressed after repeated morphine administration for 5 days, while tolerance was developed following *i.pl.* administration of PBS. The repeated morphine-induced suppression of SCS elevation was reversed by formalin *i.pl.*, indicating the inhibition of tolerance by formalin-induced inflammatory pain (Figure 4).

3.5. *Inhibition of tolerance to intracerebroventricular or intrathecal morphine analgesia by carrageenan-induced inflammatory pain*

Generally, it is believed that morphine develops analgesic tolerance through a central mechanism, although morphine acts on both the peripheral and central nervous systems. To investigate the key region, *i.e.*, supraspinal or spinal sites, of the inhibitory effects of painful stimuli on tolerance to morphine analgesia, we examined the effects of carrageenan-induced inflammatory pain on tolerance to *i.c.v.* or *i.t.* morphine. The analgesic tolerance to morphine was developed by the administration of morphine (10 mg/kg, *s.c.*) once a day for 3 days (on days 2, 3, and 4), and morphine *i.c.v.* or *i.t.*-induced analgesia was evaluated on days 1 and 5. On day 1, there was no effect of carrageenan *i.pl.* injection on the time course of morphine *i.c.v.* (10 nmol)-induced analgesia (Figure 5A). In PBS *i.pl.*-treated mice, the analgesic effect of *i.c.v.* morphine on day 5 was significantly diminished in comparison with that on day 1 by repeated morphine *s.c.* administration, which indicated the development of analgesic tolerance to *i.c.v.* morphine. However, on day 5, the analgesic effect of morphine *i.c.v.* in carrageenan *i.pl.*-treated mice was greater than that in PBS-treated mice (Figures 5B and 5C). On day 1, there was no effect of carrageenan *i.pl.* injection on morphine *i.t.* (5 nmol)-induced analgesia (Figure 5D). However, on day 5, the analgesic effect of morphine *i.t.* in carrageenan *i.pl*.-treated mice was greater than that in PBS-treated mice (Figures 5E and 5F). These results suggest that the development of tolerance to *i.c.v.* or *i.t.* morphine analgesia was significantly inhibited by carrageenan-induced inflammatory pain on day 5.

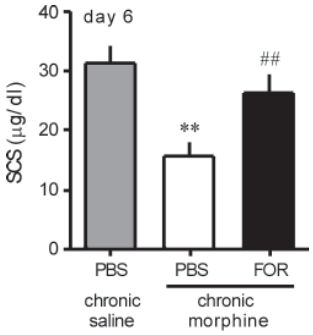

Figure 4. Inhibitory effect of intraplanter formalin on tolerance to morphine-induced corticosterone elevation. 2% formalin (FOR) was *i.pl.* injected 2 h before morphine administration on day 1. As vehicle control, PBS was injected. Morphine (10 mg/kg, *s.c.*) or saline was administered once a day for 5 days, and SCS elevation at 1 h after morphine (10 mg/kg, *s.c.*) administration was evaluated on day 6. Data are presented as the mean ± S.E.M. of 5-6 mice. ** $p < 0.01$ *vs.* chronic saline. $^{\#\#}$ $p < 0.01$ *vs.* PBS.

4. Discussion

It is generally considered that opioid tolerance may be antagonized under painful conditions in clinic (*1,8*). Here, we demonstrated that morphine-induced analgesia was gradually decreased by repeated morphine administration in mice. This indicated the development of tolerance to morphine analgesia, which is consistent with previous reports (*20,21*). Therefore, we examined the effect of neuropathic and inflammatory pain on the development of tolerance to morphine analgesia in mice. PSL-induced neuropathic pain (*i.e.*, allodynia and thermal hyperalgesia) is usually observed on the next day of PSL, and lasts for at least 14 days (*22*). After *i.pl.* injection of formalin or carrageenan, hyperalgesia and edema were observed, which are typical prognostics of inflammation, and these phenomena lasted for 7-14 days (*18,19*). On day 1, morphine analgesia evaluated by the time-course and AUC was not affected by both PSL-induced neuropathic pain and formalin- or carrageenan-induced inflammatory pain. We found that tolerance to morphine analgesia was inhibited by not only PSL-induced neuropathic pain, but also formalin- or carrageenan-induced inflammatory pain.

To confirm the inhibitory effects of pain stimuli on morphine tolerance, we focused on SCS elevation, which is one of characteristic effects of morphine. Normally, acute administration of morphine increases

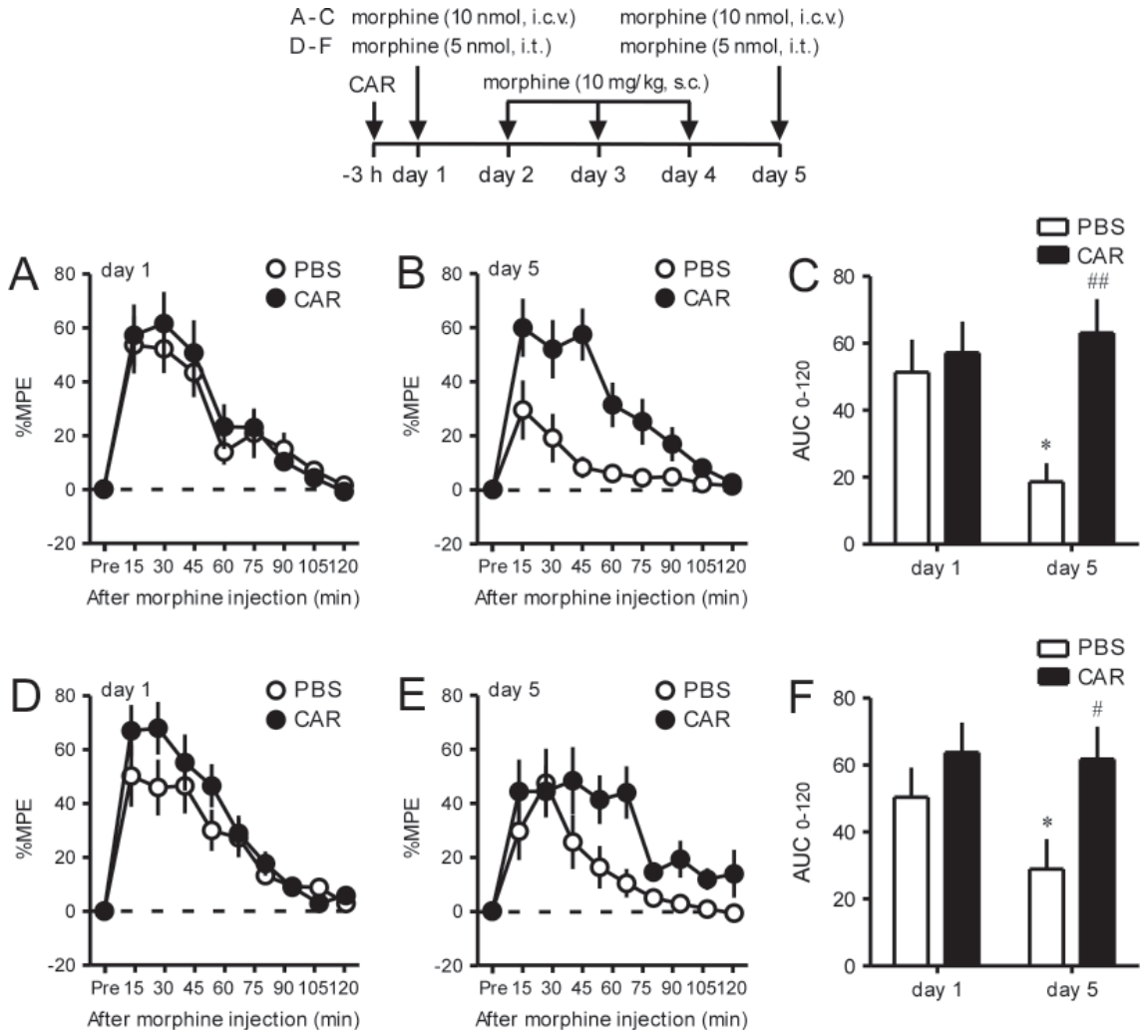

Figure 5. Inhibition of intracerebroventricular or intrathecal morphine tolerance by carrageenan-induced inflammatory pain. 1% carrageenan (CAR) was *i.pl.* injected 3 h before morphine administration on day 1. As vehicle control, PBS was injected. Morphine was administered *i.c.v.* (10 nmol, **A-C**) or *i.t.* (5 nmol, **D-F**) on days 1 and 5. For the development of tolerance, morphine (10 mg/kg) was *s.c.* administered on days 2, 3, and 4. Morphine-induced analgesia was evaluated for 120 min on days 1 and 5. Experimental schedules are indicated above. Analgesic effects of *i.c.v.* or *i.t.* morphine on days 1 (**A**, **D**) and 5 (**B**, **E**) are shown as time course of %MPE, respectively, and AUC (**C**, **F**) was calculated from time course of %MPE. Data are presented as the mean ± S.E.M. of 11-13 mice. *i.c.v.*: intracerebroventricular; *i.t.*: intrathecal; %MPE: the percentage of maximum possible effect; AUC: area under the curve. * $p < 0.05$ *vs*. day 1. $^{\#}p < 0.05$, $^{\#\#}p < 0.01$ *vs*. PBS.

the SCS level in a dose-dependent manner. This effect is also diminished by repeated administration of morphine, indicating the development of tolerance (*23*). The tolerance to SCS elevation was also suppressed by formalin-induced inflammatory pain, strongly suggesting that painful stimuli might affect the mechanism of tolerance through not only an analgesic effect, but also an endocrine effect. It is well known that morphine acts on the hypothalamus to release corticotropin-releasing factor, which then releases adrenocorticotropic hormone (ACTH) from the pituitary. The released ACTH works on the adrenal cortex and results in the elevation of SCS (*24*). These observations indicate that tolerance to SCS elevation by morphine may be mediated by a supraspinal site, and are consistent with analgesic tolerance.

Several lines of evidence indicate the potential molecular mechanisms of opioid tolerance. It is well known that opioid receptors are 7-transmembrane G protein-coupled receptors that are classified in three types, μ, δ, and κ (*25*). All of the opioid receptors are associated with an intracellular Gαi protein, and are thought to produce analgesic effects through the activation of Gαi-related pathways (*26*). Notably, the μ-opioid receptor largely contributes to opioid analgesia, and desensitization of the μ-opioid receptor may be responsible for opioid tolerance (*27*). According to the cAMP hypothesis reported previously (*28*), opioid tolerance develops due to receptor internalization and subsequent desensitization at the single cell level (*29*). The relative activity versus endocytosis hypothesis was also suggested as a mechanism to explain the receptor internalization-dependent desensitization (*3,28*). Furthermore, the relationship between the activation of protein kinase C (PKC) and receptor desensitization was reported. Indeed, blockade of the

PKC pathway inhibited the development of morphine tolerance (*30*). Recently, growing evidence suggests that opioid tolerance is mediated by anti-opioidergic neural networks in the CNS, *i.e.*, the midbrain (*6*). Namely, anti-opioidergic neural networks in the CNS were enhanced by chronic morphine treatment, and cholecystokinin, neuropeptide, and glutamate, which are candidates of typical anti-opioid mediators, prevented the opioid effects (*31-33*). For example, concomitant treatment with MK801 (NMDA glutamatergic receptor antagonist) suppressed the development of tolerance to morphine analgesia. Furthermore, chronic morphine exposure activates microglia and astrocytes in the CNS (*5*). These cells express μ-opioid receptor and produce several inflammatory mediators following morphine treatment (*34*). For instance, the critical roles of interleukin (IL)-1β and IL-6 in morphine tolerance were identified (*21,35*). Taken together, anti-opioidergic neural networks and inflammation in the CNS largely participate in the opioid tolerance.

It was reported that analgesic effects were produced through not only the CNS but also the peripheral nervous system, *e.g.* primary afferents (*36*). To clarify a key region underlying inhibition of morphine tolerance by painful stimuli, we evaluated the effect of carrageenan-induced inflammatory pain on the analgesia and its tolerance by *i.c.v.*- or *i.t.*- administered morphine. In these experiments, analgesic tests after morphine *i.c.v.* or *i.t.* administration were performed on days 1, and 5. To avoid excess tissue damage by the manipulation of *i.c.v.* and *i.t.*, morphine was systemically (*s.c.*) administered on days 2, 3, and 4 for the development of tolerance. Tolerances to both *i.c.v.*- and *i.t.*-administered morphine were inhibited by carrageenan-induced inflammatory pain. These results indicate that interaction between opioid actions and pain stimuli in the CNS (midbrain and spinal cord) is crucial for the inhibition of opioid tolerance mediated by painful stimuli.

Although we could not determine the exact mechanisms underlying the inhibition of morphine tolerance by painful stimuli in this study, a possible mechanism is suggested. Previous reports showed that the inhibition of morphine tolerance and dependence by painful stimuli was partially mediated by activation of the endogenous κ opioid system (*10,37*). Therefore, this mechanism our observations in the midbrain and spinal cord presented here. However, further research into the mechanisms is still required.

In conclusion, morphine analgesic tolerance is inhibited by several pain stimuli, including neuropathic and inflammatory pain, through central mechanisms. The mechanistic details remain to be established, but these findings suggest that the clinical use of opioids should not be limited by its adverse tolerance, and we hope that these findings may lead to the development of more efficacious therapeutics for patients suffering from severe pain.

Acknowledgements

The authors appreciate the valuable advice given by Dr. Takehiko Maeda (Niigata University of Pharmacy and Applied Life Sciences) in this study.

References

1. Davis MP, Walsh D, Lagman R, LeGrand SB. Controversies in pharmacotherapy of pain management. Lancet Oncol. 2005; 6:696-704.
2. Bell RF, Wisløff T, Eccleston C, Kalso E. Controlled clinical trials in cancer pain. How controlled should they be? A qualitative systematic review. Br J Cancer. 2006; 94:1559-1567.
3. Taylor DA, Fleming WW. Unifying perspectives of the mechanisms underlying the development of tolerance and physical dependence to opioids. J Pharmacol Exp Ther. 2001; 297:11-18.
4. Inoue M, Mishina M, Ueda H. Locus-specific rescue of GluRepsilon1 NMDA receptors in mutant mice identifies the brain regions important for morphine tolerance and dependence. J Neurosci. 2003; 23:6529-6536.
5. Watkins LR, Hutchinson MR, Johnston IN, Maier SF. Glia: Novel counter-regulators of opioid analgesia. Trends Neurosci. 2005; 28:661-669.
6. Williams JT, Christie MJ, Manzoni O. Cellular and synaptic adaptations mediating opioid dependence. Physiol Rev. 2001; 81:299-343.
7. Vaccarino AL, Couret LC Jr. Formalin-induced pain antagonizes the development of opiate dependence in the rat. Neurosci Lett. 1993; 161:195-198.
8. Liang DY, Guo T, Liao G, Kingery WS, Peltz G, Clark JD. Chronic pain and genetic background interact and influence opioid analgesia, tolerance, and physical dependence. Pain. 2006; 121:232-240.
9. Ho ST, Wang JJ, Liaw WJ, Lee HK, Lee SC. Surgical pain attenuates acute morphine tolerance in rats. Br J Anaesth. 1999; 82:112-116.
10. Tokuyama S, Nagae R, Mashida E, Hamabe W. Involvement of kappa opioid receptors in formalin-induced inhibition of analgesic tolerance to morphine in mice. J Pharm Pharmacol. 2007; 59:1109-1115.
11. Zimmermann M. Ethical guidelines for investigations of experimental pain in conscious animals. Pain. 1983; 16:109-110.
12. Haley TJ, McCormick WG. Pharmacological effects produced by intracerebral injection of drugs in the conscious mouse. Br J Pharmacol Chemother. 1957; 12:12-15.
13. Hylden JL, Wilcox GL. Intrathecal morphine in mice: A new technique. Eur J Pharmacol. 1980; 67:313-316.
14. Kiguchi N, Maeda T, Tsuruga M, Yamamoto A, Yamamoto C, Ozaki M, Kishioka S. Involvement of spinal Met-enkephalin in nicotine-induced antinociception in mice. Brain Res. 2008; 1189:70-77.
15. Zenker N, Bernstein DE. The estimation of small amounts of corticosterone in rat plasma. J Biol Chem. 1958; 231:695-701.
16. Seltzer Z, Dubner R, Shir Y. A novel behavioral model of neuropathic pain disorders produced in rats by partial sciatic nerve injury. Pain. 1990; 43:205-218.
17. Iwai S, Maeda T, Kiguchi N, Kobayashi Y, Fukazawa Y, Ozaki M, Kishioka S. Pioglitazone attenuates tactile

allodynia and microglial activation in mice with nerve injury. Drug Discov Ther. 2008; 2:353-356.
18. Kowaluk EA, Mikusa J, Wismer CT, *et al*. ABT-702 (4-amino-5-(3-bromophenyl)-7-(6-morpholino-pyridin-3-yl)pyrido[2,3-d]pyrimidine), a novel orally effective adenosine kinase inhibitor with analgesic and anti-inflammatory properties. II. *In vivo* characterization in the rat. J Pharmacol Exp Ther. 2000; 295:1165-1174.
19. Porreca F, Vanderah TW, Guo W, Barth M, Dodey P, Peyrou V, Luccarini JM, Junien JL, Pruneau D. Antinociceptive pharmacology of N-[[4-(4,5-dihydro-1H-imidazol-2-yl)phenyl]methyl]-2-[2-[[(4-methoxy-2,6-dimethylphenyl) sulfonyl]methylamino]ethoxy]-N-methylacetamide, fumarate (LF22-0542), a novel nonpeptidic bradykinin B1 receptor antagonist. J Pharmacol Exp Ther. 2006; 318:195-205.
20. Johnston IN, Milligan ED, Wieseler-Frank J, Frank MG, Zapata V, Campisi J, Langer S, Martin D, Green P, Fleshner M, Leinwand L, Maier SF, Watkins LR. A role for proinflammatory cytokines and fractalkine in analgesia, tolerance, and subsequent pain facilitation induced by chronic intrathecal morphine. J Neurosci. 2004; 24:7353-7365.
21. Shavit Y, Wolf G, Goshen I, Livshits D, Yirmiya R. Interleukin-1 antagonizes morphine analgesia and underlies morphine tolerance. Pain. 2005; 115:50-59.
22. Kiguchi N, Maeda T, Kobayashi Y, Fukazawa Y, Kishioka S. Macrophage inflammatory protein-1α mediates the development of neuropathic pain following peripheral nerve injury through interleukin-1β up-regulation. Pain. 2010; 149:305-315.
23. Yamamoto A, Kiguchi N, Kobayashi Y, Maeda T, Ueno K, Yamamoto C, Kishioka S. Pharmacological relationship between nicotinic and opioid systems in analgesia and corticosterone elevation. Life Sci. 2011; 89:956-961.
24. Armario A. Activation of the hypothalamic-pituitary-adrenal axis by addictive drugs: Different pathways, common outcome. Trends Pharmacol Sci. 2010; 31:318-325.
25. Kieffer BL. Opioids: First lessons from knockout mice. Trends Pharmacol Sci. 1999; 20:19-26.
26. Ueda H, Harada H, Nozaki M, Katada T, Ui M, Satoh M, Takagi H. Reconstitution of rat brain mu opioid receptors with purified guanine nucleotide-binding regulatory proteins, Gi and Go. Proc Natl Acad Sci U S A. 1988; 85:7013-7017.
27. He L, Fong J, von Zastrow M, Whistler JL. Regulation of opioid receptor trafficking and morphine tolerance by receptor oligomerization. Cell. 2002; 108:271-282.
28. Kieffer BL, Evans CJ. Opioid tolerance-in search of the holy grail. Cell. 2002; 108:587-590.
29. Whistler JL, Chuang HH, Chu P, Jan LY, von Zastrow M. Functional dissociation of mu opioid receptor signaling and endocytosis: Implications for the biology of opiate tolerance and addiction. Neuron. 1999; 23:737-746.
30. Ueda H, Inoue M, Matsumoto T. Protein kinase C-mediated inhibition of mu-opioid receptor internalization and its involvement in the development of acute tolerance to peripheral mu-agonist analgesia. J Neurosci. 2001; 21:2967-2973.
31. Trujillo KA, Akil H. Inhibition of morphine tolerance and dependence by the NMDA receptor antagonist MK-801. Science. 1991; 251:85-87.
32. Stinus L, Allard M, Gold L, Simonnet G. Changes in CNS neuropeptide FF-like material, pain sensitivity, and opiate dependence following chronic morphine treatment. Peptides. 1995; 16:1235-1241.
33. Pommier B, Beslot F, Simon A, Pophillat M, Matsui T, Dauge V, Roques BP, Noble F. Deletion of CCK2 receptor in mice results in an upregulation of the endogenous opioid system. J Neurosci. 2002; 22:2005-2011.
34. Watkins LR, Hutchinson MR, Rice KC, Maier SF. The "toll" of opioid-induced glial activation: Improving the clinical efficacy of opioids by targeting glia. Trends Pharmacol Sci. 2009; 30:581-591.
35. Wang Z, Ma W, Chabot JG, Quirion R. Cell-type specific activation of p38 and ERK mediates calcitonin gene-related peptide involvement in tolerance to morphine-induced analgesia. FASEB J. 2009; 23:2576-2586.
36. Rashid MH, Inoue M, Toda K, Ueda H. Loss of peripheral morphine analgesia contributes to the reduced effectiveness of systemic morphine in neuropathic pain. J Pharmacol Exp Ther. 2004; 309:380-387.
37. Suzuki T, Kishimoto Y, Misawa M, Nagase H, Takeda F. Role of the kappa-opioid system in the attenuation of the morphine-induced place preference under chronic pain. Life Sci. 1999; 64:PL1-7.

(Received January 10, 2012; Revised January 24, 2012; Accepted January 25, 2012)

Original Article

DOI: 10.5582/ddt.2012.v6.1.38

Comparison of antioxidant activity of compounds isolated from guava leaves and a stability study of the most active compound

Witayapan Nantitanon, Siriporn Okonogi*

Faculty of Pharmacy, Chiang Mai University, Chiang Mai, Thailand.

ABSTRACT: In the present study, quercetin (QT), morin (MR), and quercetin-3-*O*-glucopyranoside (QG) isolated from guava leaves were comparatively tested for antioxidant activity using DPPH, ABTS, and FRAP methods. QT was the most active among them. The free radical scavenging activity of QT was approximately four times higher than MR and two times higher than QG. The reducing power of QT was eight times higher than MR and two times higher than QG. A mixture of QT with MR or QG showed interesting combination effect. The synergistic antioxidant activity was obtained when QT was mixed with MR whereas the antagonistic effect was found when mixed with QG. The stability study of QT in liquid preparations indicated that the decomposition reaction rate of QT could be explained by a kinetic model assuming a first-order chemical reaction. The aqueous solution of QT was rapidly decomposed with $t_{1/2}$ of approximately five days whereas QT entrapped in chitosan nanoparticles was five times longer. It was concluded that QT was the most active antioxidant from guava leaves. Entrapment of QT in chitosan nanoparticles could significantly enhance its stability.

Keywords: Guava, quercetin, antioxidant, combination effect, stability, chitosan nanoparticles

1. Introduction

Guava (*Psidium guajava* L.), a plant of the Myrtaceae family, is found widespread in hot climate countries including Thailand. Traditional healers of different countries use its leaves to treat diarrhea, one of the leading causes of mortality and morbidity especially in developing countries (*1*). The scientific evaluation of guava with respect to diarrhea has been well studied (*2-5*). The extract of guava leaves has been reported to have narcotic-like activity (*6*), antinociceptive (*7*), antimutagenic (*8*), anticough (*9*), and central nervous system (CNS) depressant activity (*10*). Our previous study on the screening for biological actions of several plants commonly grown in Thailand reported that fruits and leaves of many edible plants possess high antioxidant activity (*11*). Among these, guava leaf extract has shown the highest antioxidant capacity (*12*). It was reported that the antioxidant activity of guava leaves is higher than its fruit (*13*). A phytochemical study of guava leaves has demonstrated many compounds including lipids, carbohydrates, proteins, vitamins, essential oils, tannins, saponins, flavonoids, sterols and triterpenes (*14,15*). Those polyphenolic compounds are believed to be the major principles that provide the plant with high antioxidant properties (*16-19*). However, a literature survey revealed that no data has been made to compare the potency of the active compounds as well as the interaction effects among them. The present study aimed to compare the antioxidant capacity of the active compounds isolated from guava leaves. Moreover, the interaction of the most active compound in combination with others as well as its stability was also our interest.

**Address correspondence to:*
Dr. Siriporn Okonogi, Department of Pharmaceutical Science, Faculty of Pharmacy, Chiang Mai University, Chiang Mai 50200, Thailand.
E-mail: sirioko@chiangmai.ac.th

2. Materials and Methods

2.1. *Plant materials*

Mature leaves of guava (*P. guajava*) were collected during January-February from the botanical garden of Chiang Mai University, Thailand. The leaves were washed with clean water then dried in a hot air oven at 50°C for 48 h. After drying, they were pulverized into fine powder. The guava leaf powder obtained which passed a No. 60 sieve was collected for further study.

2.2. *Chemicals*

Potassium persulfate, ferrous sulfate ($FeSO_4 \cdot 7H_2O$), ferric chloride ($FeCl_3 \cdot 6H_2O$), 2-diphenyl-1-picrylhydrazyl (DPPH), and 2,2'-azinobis-(3-ethylbenzothiazoline-6-sulfonic acid) diammonium salt (ABTS) were purchased from Sigma-Aldrich (St. Louis, MO, USA). Trolox was from Aldrich Chemical Company (Steinheim, Germany) and 2,4,6-tri (2-pyridyl)-S-triazine (TPTZ) was

from Fluka Chemicals (Buchs, Switzerland). Column chromatography were carried out on Cosmosil 75 µm C_{18}-OPN (Nacalai Tesque, Kyoto, Japan), Sephadex LH-20 (GE Healthcare Biosciences AB, Uppsala, Sweden), Silica gel 60 (230-400 mesh) (Merck, Darmstadt, Germany), Toyopearl HW-40C (TOSOH, Tokyo, Japan) and MCI-gel (Mitsubishi chemical corporation, Tokyo, Japan). Pre-coated RP-18 F_{254} (0.25 mm) and organic solvents (AR grade) were from Merck (Darmstadt, Germany). Water was deionized and purified using a Milli-Q system (Millipore, Bedford, MA, USA). Sodium alginate was from Sigma-Aldrich (St. Louis, MO, USA), chitosan (95% DD, MW 22 kDa) was a gift from Seafresh Industrial PCL, Thailand. Other chemicals were of the highest available grade and used as obtained.

2.3. *Compound extraction*

Three active compounds, quercetin (QT), morin (MR), and quercetin-3-*O*-glucopyranoside (QG), were isolated according to the description in our previous report (*20*). Briefly, the methanol (MeOH) extract from the dried powder of guava leaves was subjected to column chromatography (Cosmosil C18-OPN, 75 µm, 6.0 cm (i.d.) × 40 cm) and eluted stepwise with MeOH-aqueous mixtures of different polarity (5 to 100% aqueous MeOH). Fractions were collected and subjected to chemical analysis using thin-layer chromatography (TLC) and antioxidant activity was evaluated by the DPPH method. The most active fractions were further isolated by column chromatography using Sephadex LH-20 and silica gel 60 columns to obtain QT, Toyopearl HW-40C and Cosmosil 75 µm C18-OPN columns to obtain MR, and Cosmosil 75 µm C18-OPN and MCI-gel columns to yield QG.

2.4. *DPPH assay*

The DPPH assay is considered to be a good *in vitro* model widely used to assess free radical scavenging efficacy in a relatively short time. In the present study, this method was used to screen the antioxidant power of the extracted fractions and the isolated bioactive pure compounds of guava leaves. In its free radical form, DPPH has an absorbance at 515 nm which disappears upon reduction by an antioxidant compound to become a stable diamagnetic molecule with a result of a color change from purple to yellow (*21*). The test could be taken as an indication of the hydrogen donating ability of the tested compounds. The assay was done using the method described previously by Gamez *et al*. (*22*) with some modification. Briefly, a sample in MeOH (100 µL) was added to a solution of 200 µM DPPH radicals in 100 µL. The reaction mixture was left to stand for 30 min at room temperature in the dark. The scavenging activity of samples was estimated by measuring the absorption of the mixture at 515 nm, which reflected to the amount of DPPH radicals remaining in the solution. The scavenging activity was expressed as the IC_{50}, the concentration of samples required for scavenging 50% of DPPH radicals in the solution.

2.5. *ABTS assay*

The ABTS assay is an excellent method used for determining the antioxidant activity of a broad diversity of substances, such as hydrogen-donating antioxidants or scavengers of aqueous phase radicals and of chain-breaking antioxidants or scavengers of lipid peroxyl radicals (*23*). In the present study, it was used for confirmation on the free radical scavenging potential of the pure and combined compounds isolated from guava leaves. The assay was done in the same manner as previously described by Okonogi *et al*. (*11*). Briefly, the pre-formed radical monocation of ABTS was generated by reacting ABTS solution (7 mM) with 2.45 mM potassium persulfate ($K_2S_2O_8$). The mixture was allowed to stand for 15 h in the dark at room temperature. The solution was diluted with ethanol to obtain an absorbance of 0.7 ± 0.2 units at 750 nm. The test samples were separately dissolved in ethanol to yield an appropriate concentration. An aliquot of 20 µL of an ethanolic test solution of each sample was added to 180 µL of ABTS free radical cation solution. The absorbance, monitored for 5 min, was measured spectrophotometrically at 750 nm using a microtitre plate reader. The free radical scavenging activity of each sample was expressed as trolox equivalent antioxidant capacity (TEAC), which was obtained by comparing the absorbance change at 750 nm in a reaction mixture containing a test material with that containing trolox. This index is defined as the millimolar concentration of a trolox solution whose antioxidant capacity is equivalent to 1.0 mg of the test sample (*24*).

2.6. *Ferric reducing ability of plasma (FRAP) method*

This method was used to confirm antioxidant activity by mechanism of reducing action of the pure and combined compounds isolated from guava leaves. The reducing power of the test samples was determined by using a FRAP assay described by Benzie & Strain (*25*) with some modification. Briefly, the FRAP reagent containing 2.5 mL of 10 mM TPTZ solution in 40 mM HCl plus 2.5 mL of 20 mM $FeCl_3$ and 25 mL of 0.3 M acetate buffer, pH 3.6, was freshly prepared. The test samples were dissolved in ethanol to an optimal concentration. An aliquot of 20 µL test solution was mixed with 180 µL of FRAP reagent. The absorption of the reaction mixture was measured at 595 nm by a microtitre plate reader. Ethanolic solutions of known Fe (II) concentration, in the range of 50-500 µM ($FeSO_4$), were used as a calibration curve. The reducing power was expressed as equivalent concentration (EC). This parameter was defined as the concentration of the test

sample having a ferric reducing ability equivalent to that of 1 mM $FeSO_4$.

2.7. *Interaction effect on antioxidant activity*

The mixture of QT and MR or QT and QG at a weight ratio of 1:1 was subjected to antioxidant test using ABTS and FRAP assays. The experimental antioxidant activity (*E*) of the mixture expressed as TEAC or EC values respectively was determined as described in Sections 2.5 and 2.6, respectively. The theoretical antioxidant activity (*T*) is the sum of the experimental activity of each compound fraction, calculated using individual antioxidant activity in the following equation: $T = [(X_A \times E_A) + (X_B \times E_B)]$, where X_A and X_B represent the mole fraction of compound A and compound B, respectively, and E_A and E_B represent the antioxidant activity of 100% A and B, respectively (*26*).

2.8. *Preparation and characterization of QT loaded chitosan nanoparticles*

QT loaded chitosan nanoparticles were prepared according to the ionic gelation principle described previously by Sarmento *et al*. (*27*) with some modification. Chitosan at 0.5 mg/mL in 1% (v/v) acetic aqueous solution was prepared. A portion of 1 mL of 0.1 mg/mL QT in water-propylene glycol mixture was mixed with 10 mL of 0.03% (w/v) sodium alginate solution. Under magnetic stirring at room temperature, 0.3 mL of 0.18 mM calcium chloride solution was added followed by 1 mL of chitosan solution. Opalescent colloidal dispersion was formed spontaneously. The hydrodynamic diameter and zeta potential of the nanoparticles were measured by dynamic light scattering (DLS) using a Malvern system (Zetasizer, version 5.00, Malvern Instruments Ltd., Malvern, UK) consisting of computerized auto-titrate and DLS software. Measurements were taken at an angle of 173°. For entrapment efficiency determination, the dispersion was subjected to ultra centrifugation at 20,000 g, 4°C for 30 min. The separated nanoparticles obtained were dissolved in DMSO prior to analysis by HPLC using a C-18 column (150 mm × 4.6 mm, 5 µm; Agilent, USA) with a mobile phase of acetonitrile/0.1% (w/v) phosphoric acid solution (30:70, v/v) and detected by UV detector at 373 nm.

2.9. *Stability testing*

The aqueous solution of QT (0.1 mg/mL) and colloidal dispersion of QT loaded nanoparticles of equivalent QT concentration were kept in light protected and non-protected containers for 4 weeks. The amount of QT remaining in each sample during the storage time was determined periodically by HPLC as described in Section 2.8.

3. Results and Discussion

3.1. *Antioxidant activity of the isolated compounds*

The antioxidant activity can be evaluated by different methods depending on the mechanism of antioxidant action. In this study, three compounds, *i.e.* QT, MR, and QG, structures as shown in Figure 1, were isolated from guava leaves and subsequently subjected to the comparative antioxidant test using DPPH and ABTS methods for the free radical scavenging mechanism and the FRAP method for reducing action. The results as shown in Table 1 indicated that QT was the most active antioxidant with an IC_{50} value of 1.20 ± 0.02 µg/mL. The results from ABTS confirmed that QT possessed excellent free radical scavenging activity with a TEAC value of 57.54 ± 0.07 mM/mg. It was noticed from the IC_{50} and the TEAC values that the free radical scavenging potential of QT was approximately four times higher than MR and two times higher than QG. The principle of the FRAP method is based on the reduction of a ferric-tripyridyltriazine complex to its ferrous colored form in the presence of antioxidants. The reducing power property indicates that the antioxidant compounds are electron donors and can reduce the oxidized intermediates of the lipid peroxidation process, so that they can act as primary and secondary antioxidants (*28*). The results indicated that QT, MR, and QG possessed reducing activity but not at the same level. These results clearly indicated

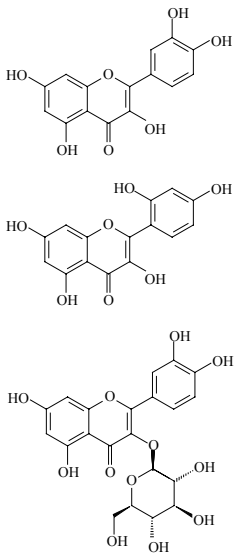

Figure 1. Chemical structure of quercetin (QT), morin (MR), and quercetin-3-*O*-glucopyranoside (QG).

Table 1. Antioxidant activity of the isolated compounds

Isolated compound	IC_{50} (µg/mL)	TEAC (mM/mg)	EC (mM/mg)
QT	1.20 ± 0.02	57.54 ± 0.07	72.69 ± 1.06
MR	5.41 ± 0.20	14.59 ± 0.62	8.56 ± 0.33
QG	3.58 ± 0.05	32.35 ± 0.12	42.52 ± 1.08

that QT was the most potent reducing substance with an EC value of 72.69 ± 1.06 mM/mg. This value was eight and two times higher than MR and QG, respctively. From this point of view, it was confirmed that QT was the most active antioxidant compound among them. According to its obviously high EC value, QT was considered to be a good electron donor and could terminate oxidation chain reactions by reducing the oxidized intermediates into a stable form.

3.2. *Effect of compound combination on antioxidant power*

As QT showed the strongest antioxidant activity among the three active compounds isolated from guava leaves, this compound was combined with each of the other two in order to examine interaction effects. The calculated theoretical antioxidant activities (*T*) of the mixtures were compared with the experimental activity (*E*). If *E* is greater than *T* (*E*/*T* > 1), then a positive interaction happened among the compounds, thus displaying synergism. On the other hand, if *E* is less than *T* (*E*/*T* < 1) a negative interaction happened, thus displaying antagonism. An additive effect was obtained when no reaction occurred and the ratio of *E/T* showed a value of 1. The results of QT in combination with MR or QG are shown in Table 2. It was found that the combination of QT with MR yielded a significant synergistic antioxidant effect, whereas the combination with QG gave an antagonistic antioxidant action. Synergistic effects of complex mixtures are thought to be important in plant defenses against a harmful environment. Plants usually present defenses as a set of compounds, not as individual ones, and it is thought that the minor constituents may act as synergists, enhancing the effect of the major constituents through a variety of mechanisms (*29*). In the present study, our results demonstrated that the antioxidant activity of QT as a major active component was synergized by a minor component, MR.

3.3. *Stability study*

This experiment was done in order to examine the effect of light and aging on the chemical stability of QT extracted from guava leaves. The results revealed that QT decreased rapidly during the first week of storage and further gradually decomposed according to the exponential degradation profiles demonstrated in Figure 2. A high reduction within one week of approximately 70% of QT was found in the samples without light protection as shown in Figure 2A and 30% in the light protection samples as demonstrated in Figure 2B. The result suggested that QT degradation was enhanced by photolysis. This result of light-induced decomposition of QT in our study was in agreement with the report of Smith *et al*. (*30*). The results provided valuable information about the degradation aspect of QT. This revealed the relevance to the real conditions of QT encountered in pharmaceutical or cosmetic products that is limited. To overcome this drawback, in the present investigation, QT was encapsulated in nanoparticles of chitosan. It was found that QT loaded chitosan nanoparticles were formed successfully by the gelation method. The hydrodynamic diameter and zeta potential of the nanoparticles obtained were found to be 310.1 ± 7.1 nm and –35.9 ± 0.5 mV, respectively. This confirmed that QT loaded particles obtained were in the nanometer size range. The resulting zeta potential value, from the viewpoint of the DLVO theory (*31,32*), indicated the high stability of the QT loaded nanoparticle colloidal system obtained. The entrapment efficiency was found to be 96.26 ± 0.1% indicating that QT was quantitatively encapsulated in the nanoparticles. The degradation profile of QT in the nanoparticles was demonstrated to be an exponential curve as shown in Figure 3. It was noted that the degradation of QT entrapped in the nanoparticles was also enhanced by light. However, the amount of QT entrapped in the nanoparticles when compared with that of non-entrapped samples, was found to be significantly higher at the same time of storage. This result indicated that the degradation of QT in the nanoparticles was obviously reduced.

Table 2. Antioxidant activity of the combined isolated compounds

Antioxidant activity	T	E	E/T	Interaction effect
TEAC (mM/mg)				
QT + MR	36.06	57.72	1.60	Synergism
QT + QG	44.95	35.91	0.79	Antagonism
EC (mM/mg)				
QT + MR	40.62	67.54	1.66	Synergism
QT + QG	60.79	40.84	0.67	Antagonism

Mixture of 1:1 weight ratio.

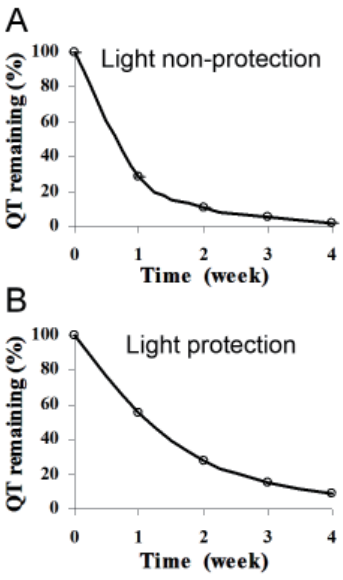

Figure 2. Effect of aging on QT solution kept in light non-protected (A) and light protected (B) containers.

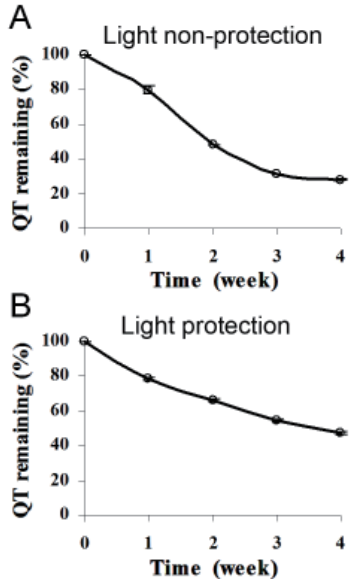

Figure 3. Effect of aging on QT loaded chitosan nanoparticles kept in light non-protected (A) and light protected (B) containers.

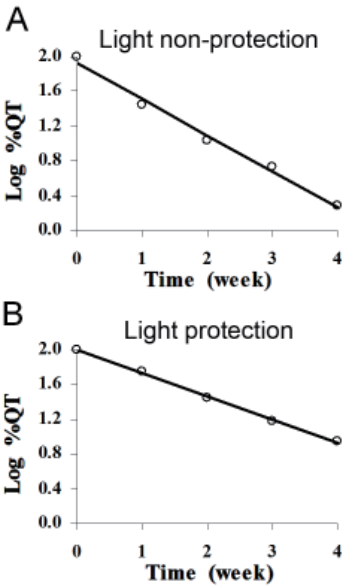

Figure 4. Plot of the logarithm concentration of QT remaining in light non-protected (A) and light protected (B) containers versus time of storage.

The relation of logarithm concentration of the remaining QT and the storage time showed a linear regression of $y = 1.93 – 0.42x$ ($r^2 = 0.991$) and $y = 1.99 – 0.27x$ ($r^2 = 0.998$) for the light non-protected and protected samples, respectively as shown in Figure 4. This result suggested that the decomposition of QT could be explained by a kinetic model assuming a first-order chemical reaction in the following equation: $dC/C = –kdt$ where C is the remaining amount of QT at time t, k is the degradation rate constant, and t is the time point of storage. Similarly with the non-entrapped QT, the linear relationship, of $y = 2.00 – 0.15x$ ($r^2 = 0.967$) and $y = 1.99 – 0.08x$ ($r^2 = 0.993$), was obtained from the light non-protected and protected

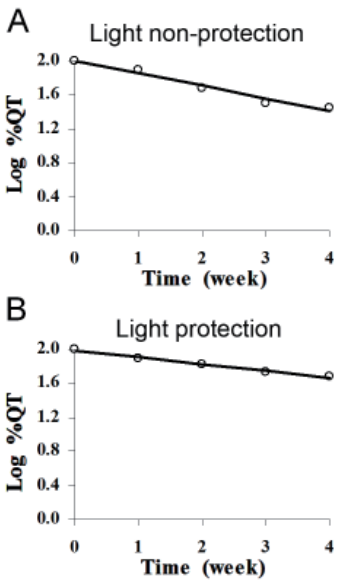

Figure 5. Plot of the logarithm concentration of QT loaded chitosan nanoparticles remaining in light non-protected (A) and light protected (B) containers versus time of storage.

Table 3. Experimental first order kinetic parameters and correlation coefficient of the degradation of QT in different samples

QT samples	r^2	$k_{(OBS)}$(week^{-1})	$t_{1/2}$ (days)
NE-QT-L	0.991	0.961	5.049
NE-QT-NL	0.998	0.612	9.704
NN-QT-L	0.967	0.347	13.966
NN-QT-NL	0.993	0.187	25.995

NE-QT-L: non-entrapped QT solution in light non-protected container; NE-QT-NL: non-entrapped QT solution in light protected container; NN-QT-L: QT entrapped in nanoparticles dispersion in light non-protected container; NN-QT-NL: QT entrapped in nanoparticles dispersion in light protected container.

nanoparticles, respectively as shown in Figure 5. This indicated that the degradation kinetics of QT entrapped in the nanoparticles also followed a first-order kinetic reaction. The degradation rate of QT from each sample could be simply observed from the slope of the straight lines, the higher the slope the higher the decomposition rate. The experimental kinetic parameters of QT degradation are provided in Table 3. The observed first order kinetic rate constant, $k_{(OBS)}$, was obtained from the slope value multiplied by 2.303. The half-life, $t_{1/2}$, of QT from each sample was calculated from the $k_{(OBS)}$. It was found that QT entrapped in chitosan nanoparticles and protected from light was the most stable. The $t_{1/2}$ of QT from this sample was approximately five times longer than that of the non-entrapped sample kept in the light non-protected container.

4. Conclusion

QT, MR, and QG were isolated from guava leaves. Among these three compounds, QT was found to have the most active antioxidant activity through free radical scavenging and reducing mechanisms. The antioxidant activity of QT was synergized by MR and antagonized by QG. The

stability study of QT in liquid preparations revealed that QT was unstable. The degradation of QT was enhanced by light and through a first-order kinetic reaction. Entrapment of QT in chitosan nanoparticles could significantly improve the stability of QT.

Acknowledgement

Financial support from the Commission on Higher Education and the Thailand Research Fund through DBR-MC Grant is gratefully acknowledged. The authors also thank the Graduate School, Chiang Mai University for their partial support.

References

1. Black RE, Brown KH, Becker S, Yunus M. Longitudinal studies of infectious diseases and physical growth of children in rural area of Bangladesh. I. Patterns of morbidity. Am J Epidemiol. 1982; 115:305-314.
2. Lutterodt GD. Inhibition of gastrointestinal release of acetylcholine by quercetin as a possible mode of action of *Psidium guajava* leaf extract in the treatment of acute diarrhoea. J Ethnopharmacol. 1989; 25:235-247.
3. Ghosh TK, Sen T, Das A, Dutta AS, Nag Chaudhuri AK. Antidiarrhoeal activity of the methanolic fraction of the extract of unripe fruits of *Psidium guajava* Linn. Phytother Res. 1993; 7:431-433.
4. Lozoya X, Meckes M, Abou-Zaid M, Tortoriello J, Nozzolillo C, Arnason JT. Quercetin glycosides in *Psidium guajava* L. leaves and determination of spasmolytic principle. Arch Med Res. 1994; 25:11-15.
5. Morales MA, Trotoriello J, Meckes M, Paz D, Lozoya X. Calcium-antagonist effect of quercetin and its relation with the spasmolytic properties of *Psidium guajava* L. Arch Med Res. 1994; 25:17-21.
6. Lutterodt GD, Maleque A. Effects on mice locomotor activity of a narcotic-like principle from *Psidium guajava* leaves. J Ethnopharmacol. 1988; 24:219-231.
7. Santos FA, Rao VSN, Silveira ER. Investigations on the antinociceptive effect of *Psidium guajava* leaf essential oil and its major constituents. Phytother Res. 1998; 12:24-27.
8. Matsuo T, Hanamure N, Shimoi K, Nakamura Y, Tomita I. Identification of (+)- galoocatechin as a bio-antimutagenic compound in *Psidium guajava* leaves. Phytochem. 1994; 36:1027-1029.
9. Jaiarj P, Khoohaswan P, Wongkrajang Y, Peungvicha P, Suriyawong P, Sumal Saraya ML, Ruangsomboon O. Anticough and antimicrobial activities of *Psidium guajava* Linn. leaf extract. J Ethnopharmacol. 1999; 67:203-212.
10. Shaheen HM, Ali BH, Alqarawi AA, Bashir AK. Effect of *Psidium guajava* leaves on some aspects of the central nervous system in mice. Phytother Res. 2000; 14: 107-111.
11. Okonogi S, Duangrat C, Anuchpreeda S, Tachakittirungrod S, Chowwanapoonpohn S. Comparison of antioxidant capacities and cytotoxicities of certain fruit peels. Food Chem. 2007; 103:839-846.
12. Tachakittirungrod S, Okonogi S, Chowwanapoonpohn S. Study on antioxidant activity of certain plants in Thailand: Mechanism of antioxidant action of guava leaf extract. Food Chem. 2007; 103:381-388.
13. Chen HY, Yen GC. Antioxidant activity and free radical-scavenging capacity of extracts from guava (*Psidium guajava* L.) leaves. Food Chem. 2007; 101:686-694.
14. Okuda T, Yoshida T, Hatano T, Yazaki K, Ikegami Y, Shingu T. Guavins A, C and D, complex tannins from *Psidium guajava*. Chem Pharm Bull. 1987; 35:443-446.
15. Abdel Wahab SM, Hifawy MS, El Gohary HM, Isak M. Study of carbohydrates, lipids, protein, flavonoids, vitamin C and biological activity of *Psidium guajava* L. growing in Egypt. Egypt J Biomed Sci. 2004; 16:35-52.
16. Muir AD. Antioxidative activity of condensed tannins. In: Natural Antioxidants: Chemistry, Health effects, and Applications (Shahidi F, ed.). AOCS Press, Champaign, IL, USA, 1997; pp. 204-212.
17. Wang W. Study on antioxidant activity of natural edible flavonoid pigment. Shipin Kexue (Beijing). 2001; 22:26-28.
18. Bors W, Michel C, Stettmaier K. Antioxidant effects of flavonoids. Biofactors. 1997; 6:399-402.
19. Faure M, Lissi E, Torres R, Videla LA. Antioxidant activities of lignans and flavonoids. Phytochem. 1990; 29:3773-3775.
20. Tachakittirungrod S, Ikegami F, Okonogi S. Antioxidant active principles isolated from *Psidium guajava* grown in Thailand. Sci Pharm. 2007; 75:179-193.
21. Brand-Williams W, Cuvelier ME, Berset C. Use of a free radical method to evaluate antioxidant activity. Food Sci Technol. 1995; 28:25-30.
22. Gamez EJ, Luyengi L, Lee SK, Zhu LF, Zhou BN, Fong HH, Pezzuto JM, Kinghorn AD. Antioxidant flavonoid glycosides from *Daphniphyllum calycinum*. J Nat Prod. 1998; 61:706-708.
23. Re R, Pellegrini N, Proteggente A, Pannala A, Yang M, Rice-Evans C. Antioxidant activity applying an improved ABTS radical cation decolorization assay. Free Radic Biol Med. 1999; 26:1231-1237.
24. Antolovich M, Prenzler PD, Patsalides E, McDonald S, Robards K. Methods for testing antioxidant activity. Analyst. 2002; 127:183-198.
25. Benzie IF, Strain JJ. The ferric reducing ability of plasma (FRAP) as a measure of "antioxidant power": The FRAP assay. Anal Biochem. 1996; 239:70-76.
26. Liu D, Shi J, Colina Ibarra A, Kakuda Y, Jun Xue S. The scavenging capacity and synergistic effects of lycopene, vitamin E, vitamin C, and [β]-carotene mixtures on the DPPH free radical. LWT-Food Sci Technol. 2008; 41:1344-1349.
27. Sarmento B, Ferreira D, Veiga F, Ribeiro A. Characterization of insulin-loaded alginate nanoparticles produced by ionotropic pre-gelation through DSC and FTIR studies. Carbohyd Polym. 2006; 66:1-7.
28. Yen GC, Chen HY. Antioxidant activity of various tea extracts in relation to their antimutagenicity. J Agri Food Chem. 1995; 43:27-32.
29. Hummelbrunner LA, Isman MB. Acute, sublethal, antifeedant, and synergistic effects of monoterpenoid essential oil compounds on the tobacco cutworm, *Spodoptera litura* (Lep., Noctuidae). J Agri Food Chem. 2001; 49:715-720.
30. Smith GJ, Thomsen SJ, Markham KR, Andary C, Cardon D. The photostabilities of naturally occurring 5-hydroxyflavones, flavonols, their glycosides and their aluminium complexes. J Photochem Photobiol A Chem. 2000; 136: 87-91.
31. Missana T, Adell A. On the applicability of DLVO theory to the prediction of clay colloids stability. J Colloid Interf Sci. 2000; 230:150-156.
32. Mohanraj VJ, Chen Y. Nanoparticles – A Review. Trop J Pharm Res. 2006; 5:561-573.

(Received October 13, 2011; Revised February 3, 2012; Accepted February 6, 2012)

Original Article

DOI: 10.5582/ddt.2012.v6.1.44

A novel flow-injection analysis system for evaluation of antioxidants by using sodium dichloroisocyanurate as a source of hypochlorite anion

Hideaki Ichiba, Katsuya Hanami, Keiko Yagasaki, Misa Tanaka, Hiroko Ito, Takeshi Fukushima*

Department of Analytical Chemistry, Faculty of Pharmaceutical Sciences, Toho University, Chiba, Japan.

ABSTRACT: A flow injection analysis (FIA) system for evaluation of the antioxidant activity of a compound capable of scavenging a hypochlorite anion (OCl^-), one of the reactive oxygen species (ROS), was developed. Aminophenyl fluorescein (APF), a fluorescence indicator of ROS, was mixed manually with the test compounds and the mixed solution was injected into the FIA system. The injected solution was reacted in-line with OCl^-, that was produced by using sodium dichloroisocyanurate in the presence of 0.1 M CH_3CO_2Na in H_2O. The fluorescence intensity of fluorescein generated from non-fluorescent APF was significantly attenuated in compounds that had a scavenging effect on OCl^-. The precision obtained by the FIA system was satisfactory (relative standard deviation < 5.0%) and a rapid assay within 0.5 min per sample was achieved. The proposed FIA system was used to demonstrate that reduced glutathione, dithiothreitol, and 3-methyl-1-phenyl-5-pyrazolone (edaravone) showed a significant scavenging effect on OCl^-. Therefore, the proposed FIA system can be used as a screening assay for OCl^--scavenging compounds.

Keywords: Screening assay, reactive oxygen species, aminophenyl fluorescein, fluorescence, reduced glutathione

1. Introduction

Reactive oxygen species (ROS) such as hydroxyl radicals, superoxide anion, and hypochlorite anion have attracted considerable attention in the post-genome era because they are involved in posttranslational modification of proteins (*1-3*). It has been suggested that these posttranslational modifications lead to dysfunctions in biological systems, thus causing diseases such as diabetes and cancer (*4,5*). Recently, we reported that hydroxyl radicals could oxidize specifically ^{27}Met of glucagon (*6*), and furthermore that the ability of ^{27}Met sulfoxide of glucagon to produce cAMP was reduced to approximately 25% of that of native glucagon in HepG2 cells (*6*). A similar phenomenon has been observed in the case of cholecystokinin octapeptide (CCK8) (*7*), in which the oxidized CCK8 revealed *in vitro*-altered bioactivity in the LOVO cells (*8*). Similarly, oxidation of functionalized proteins or bioactive peptides by ROS could deteriorate their original and regular functions (*9,10*). Therefore, it is crucial to prevent ROS-induced oxidative stress by providing an anti-oxidant supplied from exogenous origins such as food or supplements. Research has focused on a variety of candidates for anti-oxidants capable of preventing oxidation from ROS, such as catechins, ascorbic acid, and quercetin (*11-17*).

Considering this background on the importance of anti-oxidants *in vivo*, a novel screening assay system is needed for the discovery and evaluation of compounds that can scavenge ROS. In most studies concerning ROS, Fenton's or Fenton-like reactions, which utilize Fe^{2+} or Cu^{2+} and H_2O_2 as a tool for ROS production, have been employed for *in vitro*-generation of hydroxyl radical (HO·) (*18,19*). In Fenton's reaction, however, it is difficult to regulate the concentration of hydroxyl radicals generated from Fenton's solution. Therefore, Fenton's reaction has a disadvantage in that a constant concentration of hydroxyl radical could not be provided. In order to evaluate precisely the anti-oxidant activity of a compound, it is preferable that the amount of generated ROS should remain unchanged in the reaction system. In the present study, therefore, hypochlorous acid (HOCl) was selected as the ROS. In aqueous solution, HOCl is released as hypochlorite anion (OCl^-), which is involved in the etiology of atherosclerosis (*20*). As a source of HOCl and OCl^-, sodium dichloroisocyanurate (DCCA, Figure 1)

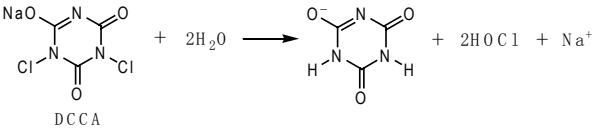

Figure 1. Reaction scheme of DCCA with H_2O.

**Address correspondence to:*
Dr. Takeshi Fukushima, Department of Analytical Chemistry, Faculty of Pharmaceutical Sciences, Toho University, 2-2-1 Miyama, Funabashi-shi, Chiba 274-8510, Japan.
E-mail: t-fukushima@phar.toho-u.ac.jp

was used because an accurate concentration of the DCCA solution is easy to prepare due to the fact that it is a solid compound. As shown in Figure 1, DCCA can be released as OCl^- in aqueous solution (*21*). Until now, DCCA has been used for the production of OCl^-, which has in turn been utilized for chemiluminescent detection of sulfide ion in spring water (*21*). To evaluate the scavenging effect of ROS, aminophenyl fluorescein (APF) (*22*) was employed in this study. It has been reported that APF can emit fluorescence originating from fluorescein in the presence of OCl^- (*22*).

Taking these reagents together, we constructed a flow-injection analysis (FIA) system (Figure 2) in order to develop a reliable, simple, and rapid whole assay operation method. APF was mixed manually with each test compound and the mixed solution was injected into the FIA system. The injected solution was reacted in-line with OCl^- produced from DCCA. The fluorescence intensity of fluorescein generated from non-fluorescent APF would be significantly attenuated if the test compound had a scavenging effect on the OCl^-. Thus, the change of the fluorescence intensity can be used to estimate the anti-oxidant activity of the test compounds. In the present study, several compounds known as anti-oxidants were assayed by the proposed FIA system and the feasibility of the FIA system was verified.

2. Materials and Methods

2.1. *Materials*

Aminophenyl fluorescein (APF) was purchased from Sekisui Medical Co., Ltd. (Tokyo, Japan). Dichloroisocyanuric acid, sodium salt (DCCA) was purchased from Sigma-Aldrich (St. Louis, MO, USA). *N,N*-Dimethylformamide (DMF) was purchased from Nacalai Tesque, Inc. (Kyoto, Japan). Sodium hypochlorite containing 6% active chlorine was purchased from Koso Chemical (Tokyo, Japan). Water used throughout this investigation was processed by a Milli-Q Water Purification System (Millipore Corporation, Milford, MA, USA).

2.2. *Sample preparations*

A commercially available 5.0 mM APF solution (in DMF) was diluted with additional DMF to create a 10 μM APF stock solution. The APF stock solution was stable for several months in a refrigerator. Each sample solution was prepared by mixing a test compound in 500 μL of 0.1 M sodium acetate (in H_2O) with 500 μL of 10 μM APF. The blank solution was a mixture of 500 μL of 0.1 M sodium acetate and the same volume of 10 μM APF. Twenty microliters of either a sample or the blank solution were injected manually into the FIA system through a Rheodyne 7125 injector equipped with a 20 μL sample loop.

2.3. *FIA system*

A schematic diagram of the FIA system constructed in this experiment is shown in Figure 2. The two elution pumps were Shimadzu LC-10AS (Shimadzu Corp., Kyoto, Japan). All elution tubing and connectors used were of PEEK™ materials. Fluorescence intensity was monitored using a Shimadzu RF-535 fluorescence detector and the excitation and emission wavelengths were set at a constant 490 and 515 nm, respectively. The mobile phase solutions A and B were 0.1 M sodium acetate and 50 μM DCCA in H_2O, respectively. The flow rate for both solutions was 2.0 mL/min.

2.4. *Preparation of test compounds*

The test compounds dithiothreitol, reduced glutathione, and 3-methyl-1-phenyl-5-pyrazolone (MPP) were all purchased from Nacalai Tesque, Inc.

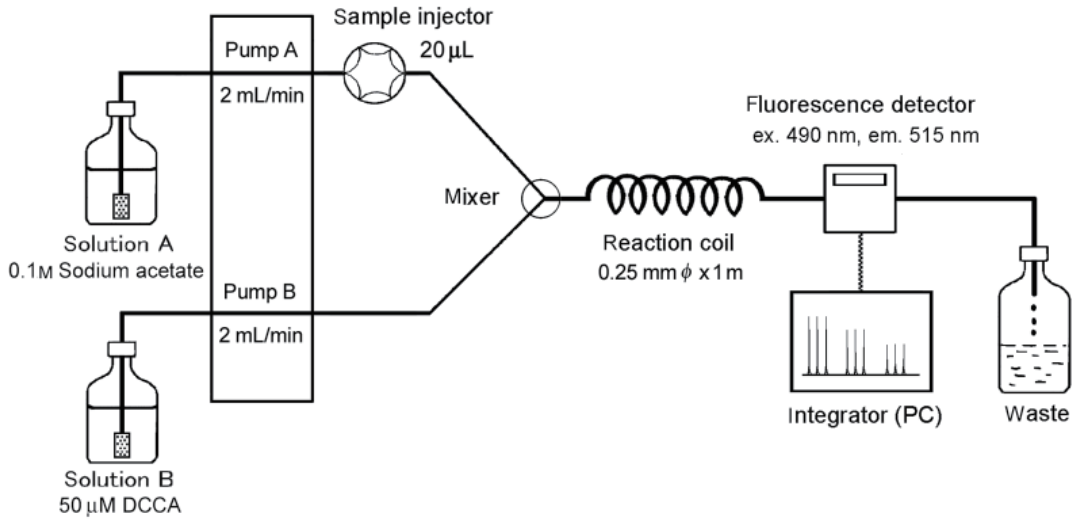

Figure 2. Block diagram of the proposed FIA system.

Quercetin dihydrate was purchased from Wako Pure Chemical Industries, Ltd. (Osaka, Japan). Melatonin, quinolinic acid, and kynurenine were purchased from Sigma-Aldrich (St. Louis, MO, USA). These compounds were dissolved in H_2O to prepare a 1.0 mM stock solution. In the case of the lipophilic compounds such as the pyrazolone derivatives, a water-soluble organic solvent such as DMF was used. The stock solution was diluted with 0.1 M sodium acetate in H_2O to prepare a 0.05-20 μM solution, and 500 μL of the aliquot was used for the evaluation of anti-oxidant activity by the FIA system described above.

2.5. *Evaluation of anti-oxidant activity*

In the absence of a test compound, the fluorescence peak height obtained in the FIA chart was designated as the blank value (100%) (n = 5). Subsequently, a dose-response curve for each test compound was drawn by plotting the fluorescence peak height at each concentration of test compound against the concentration of the test compound (n = 5). The concentration of the test compound indicating 50% of the blank value was regarded as the EC_{50} of the compound according to previous papers (*23,24*). Thus, in the present study, the EC_{50} value (μM) was evaluated as the anti-oxidant activity of the test compound.

3. Results and Discussion

3.1. *Source of hypochlorite anion*

Among several kinds of ROS such as $HO^{\cdot}$, $O_2^{\cdot -}$, $^1O_2$, H_2O_2, $ONOO^-$, HOCl, and $ROO^{\cdot}$, in the present study, we chose HOCl as the ROS for the present FIA assay. As a source of OCl^-, we first investigated the use of sodium hypochlorite (NaOCl); however, the relative standard deviation (RSD) value of the sample was too large, and therefore stable precise data could not be obtained (data not shown). For this reason, it was speculated that the poor precision may have arisen from the physical properties of NaOCl, because NaOCl is a liquid compound. Commercially available NaOCl is a 5-7% solution, and therefore the concentration is not exact. Thus, DCCA was chosen as the source of OCl^-, because although DCCA is a solid compound, it can release OCl^- in aqueous solution (Figure 1).

3.2. *Effect of pH and kinds of base*

In the present study, APF was used for the ROS indicator. APF fluoresces, which originates from fluorescein in the presence of a hydroxyl radical or HOCl, although APF itself shows no fluorescence (*22*). The responsiveness of APF to HOCl was three times higher than it was to a hydroxyl radical, and therefore a subtle scavenging effect of OCl^- by a test compound could be detected using APF. APF can react with OCl^- to emit intense fluorescence at 515 nm in a basic solution. A pH range for the carrier solution of 8.0-11.0 was therefore recommended. For preparing the carrier solution at pH 8.0-11.0, several bases were examined as to whether sufficient data could be obtained. Table 1 lists the fluorescence peak height and the RSD of each base examined in the present study. As listed in Table 1, the use of 0.1 M sodium acetate (CH_3CO_2Na) in H_2O gave the highest peak height and the smallest RSD values. Therefore, 0.1 M CH_3CO_2Na was used as the carrier solution.

3.3. *Effect of concentrations of APF and DCCA*

Figures 3A and 3B show the change of fluorescence intensity (peak height) as a function of the concentrations of DCCA and APF, respectively. The observed fluorescence peak height increased with increasing concentration of both DCCA and APF. In the preliminary experiment, a decrease of fluorescence peak height was not dependent on the concentration of the test compound at DCCA concentrations above 50 μM in carrier solution B (Figure 2) (data not shown); therefore, the DCCA concentration was set at 50 μM. The obtained peak height was 7.0×10^5 at 5.0 μM APF; therefore, the concentration of 5.0 μM APF was sufficient for the evaluation of EC_{50} values for each test compound. Reproducibility of the FIA system was estimated using relative standard deviations of peak height for each measured point, RSD < 4.5% for DCCA (Figure 3A) and RSD < 4.4% for APF (Figure 3B).

3.4. *Effect of flow rate*

Figure 4 shows a representative FIA chart of reduced glutathione obtained at a flow rate of 2.0 mL/min. The observed peak heights apparently decreased with increasing concentration of reduced glutathione, indicating that the anti-oxidant activity of reduced glutathione could also be evaluated by the present FIA

Table 1. Effects of carrier solution on the fluorescence peak height and RSD (%)

Carrier solution	Mean value of peak height	RSD (%)
0.01 M Sodium phosphate buffer in H_2O (pH 7.4)	3,200	5.3-19.7
0.1 M Sodium acetate in H_2O (pH 8.5)	531,689	0.2-2.7
0.1 M Sodium bicarbonate in H_2O (pH 8.7)	40,700	1.5-8.7
0.1 M Sodium carbonate in H_2O (pH 10.5)	7,250	0.7-5.2

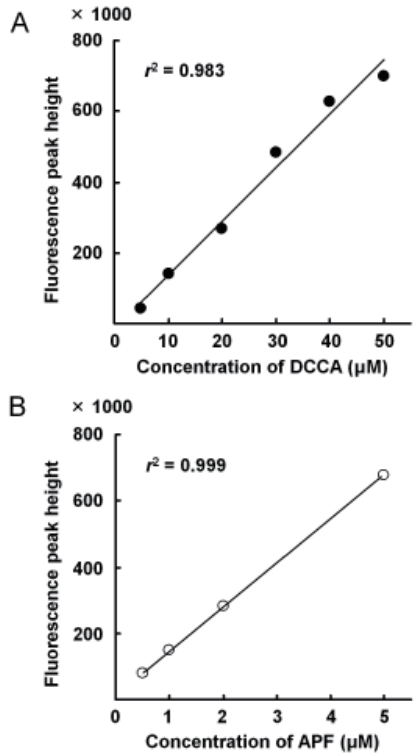

Figure 3. Fluorescence intensity of fluorescein produced from APF as a function of concentration by the present FIA system. Concentration of DCCA **(A)** and APF **(B)**.

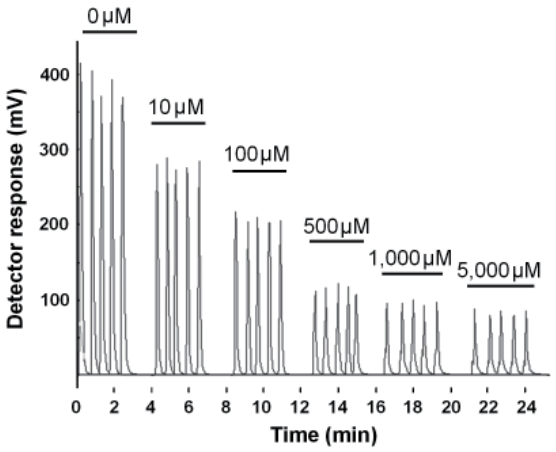

Figure 4. Representative FIA chart of 0, 10, 100, 500, 1,000, and 5,000 μM reduced glutathione, obtained at a flow rate of 2.0 mL/min. Numerals in this figure represent the concentrations of reduced glutathione.

system. When the flow rate was slow (0.5 mL/min), the peak top was divided. Although the reason why the peak shape deteriorated is not yet understood, a clear peak shape would be required for an accurate evaluation. In addition, a higher flow rate can contribute to a reduced analysis time. Thus, considering the peak shape and total analysis time, a flow rate of 2.0 mL/min was chosen in this study.

3.5. *Anti-oxidant activity of test compounds*

Figure 5 shows a representative dose-response curve

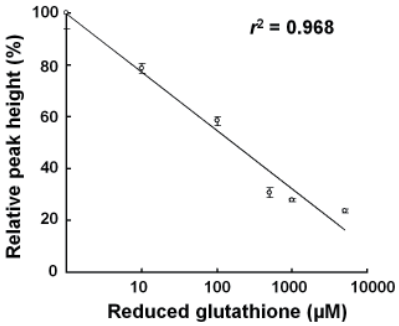

Figure 5. Dose-response curve of reduced glutathione evaluated by the present FIA system.

Table 2. EC_{50} values of test compounds, obtained by the proposed method

Test compounds	EC_{50} (μM)
Ascorbic acid	307.2
Reduced glutathione	162.6
Quercetin dihydrate	1,024
Dithiothreitol	211.1
Edaravone (3-methyl-1-phenyl-5-pyrazolone)	203.1
Quinolinic acid	1,723
Kynurenine	934.2
Melatonin	1,517

of reduced glutathione evaluated by the present FIA system. At concentrations of reduced glutathione above 1,000 μM, the plotted point was excluded from the linear regression line; therefore, only the points within the linear regression line were adopted to determine the EC_{50} value. Similarly, several compounds were tested for anti-oxidant activity using the present FIA system.

In the present study, the test compounds other than reduced glutathione were ascorbic acid, quercetin dihydrate, dithiothreitol, edaravone, quinolinic acid, kynurenine, and melatonin. The EC_{50} values for each compound were calculated and are listed in Table 2. Among them, reduced glutathione exhibited the smallest EC_{50} value. To our knowledge, thus far there have been no reports revealing that the anti-oxidant activity against OCl^- of reduced glutathione was more effective than that of ascorbic acid, which is a well-known antioxidant. In the case of scavenging OCl^- in an *in vitro* experiment, our studies indicated that reduced glutathione might be more effective than ascorbic acid. Based on these studies, it is speculated that reduced glutathione might also be efficacious for scavenging OCl^- *in vivo*.

4. Conclusion

By using APF as an ROS indicator, an FIA system for the evaluation of antioxidants using DCCA as a source of OCl^- was developed. The anti-oxidant activity of several compounds was satisfactorily evaluated by the present FIA system, demonstrating that it can be useful as a screening assay for anti-oxidant activity against OCl^-.

Acknowledgements

The authors gratefully thank Dr. Ishigami, Toho University, for his valuable comments in this study, and Miss Rie Ikeda, Miss Ayako Tsutiya, Miss Kahori Kobayashi, and Mr. Takahisa Kanayama for their technical assistance.

References

1. Davies MJ. The oxidative environment and protein damage. Biochim Biophys Acta. 2005; 1703:93-109.
2. Cadet J, Douki T, Ravanat JL. Oxidatively generated damage to the guanine moiety of DNA: Mechanistic aspects and formation in cells. Acc Chem Res. 2008; 41:1075-1083.
3. Fonseca C, Domingues P, Reis A, Domingues MR. Identification of leucine-enkephalin radical oxidation products by liquid chromatography tandem mass spectrometry. Biomed Chromatogr. 2008; 22:947-959.
4. Sayre LM, Perry G, Smith MA. Oxidative stress and neurotoxicity. Chem Res Toxicol. 2008; 21:172-188.
5. Bonomini F, Tengattini S, Fabiano A, Bianchi R, Rezzani R. Atherosclerosis and oxidative stress. Histol Histopathol. 2008; 23:381-390.
6. Ichiba H, Ogawa T, Yajima T, Fukushima T. Analysis of hydroxyl radical-induced oxidation process of glucagon by reversed-phase HPLC and ESI-MS/MS. Biomed Chromatogr. 2009; 23:1051-1058.
7. Ichiba H, Nakamoto M, Yajima T, Takayama M, Fukushima T. Analysis of oxidation process of cholecystokinin octapeptide with reactive oxygen species by high-performance liquid chromatography and subsequent electrospray ionization mass spectrometry. Biomed Chromatogr. 2010; 24:140-147.
8. Ichiba H, Nakamoto M, Yajima T, Fukushima T. *In vitro* binding assay of ^{31}methionine-oxidized cholecystokinin octapeptide to the CCK_B receptor. J Health Sci. 2009; 55: 636-640.
9. Hoepken HH, Gispert S, Morales B, Wingerter O, Del Turco D, Mülsch A, Nussbaum RL, Müller K, Dröse S, Brandt U, Deller T, Wirth B, Kudin AP, Kunz WS, Auburger G. Mitochondrial dysfunction, peroxidation damage and changes in glutathione metabolism in PARK6. Neurobiol Dis. 2007; 25:401-411.
10. Edwards AM, Ruiz M, Silva E, Lissi E. Lysozyme modification by the Fenton reaction and γ radiation. Free Radic Res. 2002; 36:277-284.
11. Damianaki A, Bakogeorgou E, Kampa M, Notas G, Hatzoglou A, Panagiotou S, Gemetzi C, Kouroumalis E, Martin PM, Castanas E. Potent inhibitory action of red wine polyphenols on human breast cancer cells. J Cell Biochem. 2000; 78:429-441.
12. Kim YJ, Chung JE, Kurisawa M, Uyama H, Kobayashi S. Superoxide Anion scavenging and xanthine oxidase inhibition of (+)-catechin-aldehyde polycondensates. Amplification of the antioxidant property of (+)-catechin by polycondensation with aldehydes. Biomacromolecules. 2004; 5:547-552.
13. Tian B, Sun Z, Xu Z, Hua Y. Chemiluminescence analysis of the prooxidant and antioxidant effects of epigallocatechin-3-gallate. Asia Pac J Clin Nutr. 2007; 16(Suppl 1):153-157.
14. Duarte TL, Jones GD. Vitamin C modulation of H_2O_2-induced damage and iron homeostasis in human cells. Free Radic Biol Med. 2007; 43:1165-1175.
15. Bodannes RS, Chan PC. Ascorbic acid as a scavenger of singlet oxygen. FEBS Lett. 1979; 105:195-196.
16. Nishikimi M. Oxidation of ascorbic acid with superoxide anion generated by the xanthine-xanthine oxidase system. Biochem Biophys Res Commun. 1975; 63:463-468.
17. Rice ME. Ascorbate regulation and its neuroprotective role in the brain. Trends Neurosci. 2000; 23:209-216.
18. Neyens E, Baeyens J. A review of classic Fenton's peroxidation as an advanced oxidation technique. J Hazard Mater. 2003; 98:33-50.
19. Halliwell B, Whiteman M. Measuring reactive species and oxidative damage *in vivo* and in cell culture: How should you do it and what do the results mean? Br J Pharmacol. 2004; 142:231-255.
20. Hazell LJ, Baernthaler G, Stocker R. Correlation between intima-to-media ratio, apolipoprotein B-100, myeloperoxidase, and hypochlorite-oxidized proteins in human atherosclerosis. Free Radic Biol Med. 2001; 31:1254-1262.
21. Afsaneh S, Mohammad AK, Mohammad RH. Flow injection chemiluminescence determination of sulfide by oxidation with chlorinated isocyanurates. Anal Lett. 2002; 35: 2023-2037.
22. Setsukinai K, Urano Y, Kakinuma K, Hideyuki J, Majima HJ, Nagano T. Development of novel fluorescence probes that can reliably detect reactive oxygen species and distinguish specific species. J Biol Chem. 2003; 278:3170-3175.
23. Nakamura K, Oba Y, Kishikawa N, Kuroda N. Measurement of antioxidative activity against hypochlorite ion by sequential injection analysis with luminol chemiluminescence detection. Bunseki Kagaku. 2004; 53:925-930.
24. Wada M, Kido H, Ohyama K, Ichibangase T, Kishikawa N, Ohba Y, Nakashima MN, Kuroda N, Nakashima K. Chemiluminescent screening of quenching effects of natural colorants against reactive oxygen species: Evaluation of grape seed, monascus, gardenia and red radish extracts as multi-functional food additives. Food Chem. 2007; 101:980-986.

(Received January 6, 2012; Revised January 27, 2012; Accepted January 28, 2012)

Original Article

DOI: 10.5582/ddt.2012.v6.1.49

Stability-indicating HPLC method for the determination of the stability of oxytocin parenteral solutions prepared in polyolefin bags

Gagan Kaushal[1,*], Brian E. Sayre[2], Terrence Prettyman[2]

[1] *Department of Pharmaceutics and Administrative Sciences, University of Charleston School of Pharmacy, Charleston, WV, USA;*
[2] *Charleston Area Medical Center, Department of Pharmacy and Drug Information, Charleston, WV, USA.*

ABSTRACT: Oxytocin is very commonly used in clinical settings and is a nonapeptide hormone that stimulates the contraction of uterine smooth muscles. In this study the stability of extemporaneously compounded oxytocin solutions was investigated in polyolefin bags. The sterile preparations of oxytocin were compounded to the strength of 0.02 U/mL in accordance with United States Pharmacopeia (USP) <797> standards. In order to carry out the stability testing of these parenteral products, the solutions were stored under three different temperature conditions of −20°C (frozen), 2-6°C (refrigerated), and 22-25°C (room temperature). Three solutions from each temperature were withdrawn and were assessed for stability on days 0, 7, 15, 21, and 30 as per the USP guidelines. The assay of oxytocin was examined by an HPLC method at each time point. No precipitation, cloudiness or color change was observed during this study at all temperatures. The assay content by HPLC revealed that oxytocin retains greater than at least 90% of the initial concentrations for 21 days. There was no significant change in pH and absorbance values for 21 days under all the conditions of storage. Oxytocin parenteral solutions in the final concentration of 0.02 U/mL and diluted in normal saline are stable for at least 30 days under frozen and refrigerated conditions for 30 days. At the room temperature, the oxytocin solutions were stable for at least 21 days. The stability analysis results show that the shelf-life of 21 days observed in this study was far better than their recommended expiration dates.

Keywords: Oxytocin, stability, parenteral, compounding, HPLC

**Address correspondence to:*
Dr. Gagan Kaushal, Department of Pharmaceutics and Administrative Sciences, University of Charleston School of Pharmacy (UCSOP) , 2300 MacCorkle Ave. S.E., Charleston, WV-25304, USA.
E-mail: gagankaushal@ucwv.edu

1. Introduction

Oxytocin, a nonapeptide hormone, stimulates the contraction of uterine smooth muscles. It is commonly used in the clinical settings for the induction and augmentation of the first stage of labor, mid trimester abortion, and the cessation or prevention of postpartum hemorrhage (*1-4*). The recommended doses of oxytocin are as follows; for the induction of labor: 10 units per 1,000 mL, for the control of post-partum bleeding: 10 to 40 units per 1,000 mL, and for the treatment of inevitable absorption: 10 units in 500 mL (*5*). For these purposes, oxytocin is most often used as parenteral solutions and the recommended solvents are saline or 5% dextrose in saline solution (Product Insert, Teva Parenteral Medicines, 2004). The intravenous forms are diluted from the commercially available oxytocin vials, since the final recommended concentrations are commercially unavailable. These intravenous solutions are prepared using aseptic conditions under the laminar flow hood and should be stored suitably until further used.

There are few studies which provide the guidance regarding the short-term stability of these compounded syringes (*3,6*). In a study by Boothby *et al*. (*7*), the stability of oxytocin solution was examined in Ringer's lactate solution at 4 and 25°C for over 31 days. In another study by Trissel *et al*. (*8*), the stability was done for 90 days at room temperature in 5% dextrose injection, normal saline, and lactated Ringer's solution. However, no stability-indicating study has evaluated the stability of oxytocin stored for a period of 30 days under different temperature conditions in normal saline (the most commonly used diluent for oxytocin). Thus, the hospital pharmacy is placed in a unique situation in determining how to prepare the solutions, how long the product should be stored, and how to improve compounding efficiency while at the same time reducing waste in any health-care model.

The objective of the present study was to determine the physical and chemical stability of extemporaneously compounded oxytocin to 0.02 U/mL in normal saline and stored in polyolefin bags. Three different temperature conditions were used for this study; room temperature (22-25°C), frozen (−20°C) or under refrigeration (2-6°C) for up to 30 days.

2. Materials and Methods

2.1. *Materials*

All chemicals were of analytical grade. Oxytocin, sodium phosphate, sodium chloride, sodium hydroxide, hydrochloric acid, and all other chemicals were purchased from Sigma Chemical Co. (St. Louis, MO, USA). Acetonitrile (HPLC grade) was purchased from Fisher Chemicals (Fair Lawn, NJ, USA). Oxytocin vials of 100 U/10 mL (10 U/mL), 10 mL Multiple Dose Vial was purchased from Teva Pharmaceuticals (Teva Pharmaceuticals USA, Inc., Sellersville, PA, USA) and normal saline bags were purchased from B. Braun (Bethlehem, PA, USA).

2.2. *HPLC sample preparation using solid phase extraction (SPE) method*

All the samples for the HPLC analysis were prepared using Oasis HLB cartridges (60 mg-3 mL; Product No. WAT094226) obtained from Waters Corporation (Milford, MA, USA). The cartridges were pre-washed with 3 mL of acetonitrile and 1.5 mL of water, then conditioned with 1.5 mL of 10 mM phosphate buffer (pH 7.5). The cartridge was not permitted to run dry during the whole conditioning procedure. The sample (3 mL) of oxytocin solution was loaded on the cartridge and was eluted with 0.75 mL 50% of 10 mM phosphate buffer (pH 7.5) and 50% acetonitrile. This sample was immediately centrifuged at 9,000 × g for 3.5 min and 500 µL of supernatant was transferred to an HPLC vial with a micro-insert.

2.3. *HPLC system*

All the chromatographic studies were performed on a Dionex Ultimate 3000 HPLC system connected with an absorbance detector. The separations were done on X Bridge™ C8 cartridge column (250 × 4.6 mm I.D., Waters Associates, Milford, MA, USA) with the column particle diameter of 3.5 µm. The column effluents were monitored at wavelength of 214 nm for a run time of 16 min at the temperature of 30°C. The absorbance value was selected based on the full range scan of an oxytocin sample that was carried under the same conditions in the HPLC system. The mobile phase was 50% of 10 mM phosphate buffer (pH 7.5) and 50% acetonitrile. The mobile phase was filtered and degassed before use. The flow rate was 0.2 mL/min and the injection volume was 50 µL.

2.4. *Stability-indicating HPLC assay*

The suitability of the present HPLC conditions to be used as a stability-indicating method was tested by accelerating the degradation of oxytocin. The stability-indicating capability of the assay was examined by degradation of 0.02 U/mL oxytocin in 1 M HCl and 1 M NaOH solutions and these solutions were heated at 90°C for 1 h. The samples were withdrawn before and after heating each of the solutions and were subjected to SPE. Each sample was analysed by HPLC using the conditions as explained above.

2.5. *Oxytocin standard curve*

The calibration of HPLC system was performed by constructing a standard curve using five known concentrations of oxytocin. In order to prepare standard curve, fixed amounts (0.01, 0.015, 0.02, 0.03, and 0.04 U/mL) of standard oxytocin were respectively added to the normal saline solutions and these samples were analyzed by subjecting them to SPE and then using the standardized HPLC conditions.

All the samples were analyzed three times (intra-day variation) on three different days (inter-days variation). The accuracy was calculated at each concentration as the ratio of the measured concentration to the nominal concentration multiplied by 100%.

The limit of quantitation (LOQ) of the method was defined as the lowest concentration of that could be quantitatively determined with acceptable precision and accuracy. Acceptance limits were defined as accuracy of 80-120% and precision of ≤ 20%.

2.6. *Preparation of oxytocin parenteral solutions*

Dilutions of the oxytocin parenteral solutions to nominal concentrations of 0.02 U/mL were performed by the Charleston Area Medical Center (CAMC Solutions, Charleston, WV, USA) under aseptic conditions. All the solutions were prepared on the same day. Briefly, 2 mL of solution was withdrawn from a 1,000 mL normal saline bag and was replaced by 2 mL of oxytocin stock (10 U/mL). The bag was then agitated for couple of seconds to ensure uniform mixing.

The solutions were frozen (−20°C), refrigerated (2-6°C), or stored at room temperature (22-25°C). The solutions at room temperature were exposed to normal fluorescent light. Frozen and refrigerated samples were kept in a dark refrigerator and were exposed to light only during sampling. These samples were allowed to warm at room temperature and no external source of heat was used to warm these parenteral solution bags. Three bags for each of the storage conditions were assessed for physical and chemical stability over 30 days. Stability was assessed on days 0, 7, 15, 21, and 30. The storage temperatures were closely monitored throughout the study.

2.7. *Physical evaluation*

Physical stability of oxytocin parenteral solutions was assessed by visual examination. The solutions were evaluated against black and white backgrounds for visible particulate matter, cloudiness, and color changes.

To complement the visual inspection of the syringes, absorbance was also measured at the wavelength of 600 nm using spectrophotometer (Hitachi High Technologies America, Inc., CA, USA).

The pH was measured at each sampling point with Corning Pinnacle pH meter (Model 530, Cole-Parmer, IL, USA) fitted with Orion 9102BNWP electrode (single junction Ag/AgCl refillable combination pH), using three-point standardization with buffer solutions (pH of 4.0, 7.0, and 10.0). The pH of each sample was read at least two times. pH is defined as an important parameter that governs the stability of the product as the change in pH can cause the precipitation of the product. Thus pH along with spectroscopy can be a valuable tool for evaluating the stability.

2.8. *Oxytocin stability assay*

Chromatogram peak heights were used to determine oxytocin concentrations in the parenteral solutions. Three samples were withdrawn on each of the sampling day from each of the storage temperature and each sample was injected at least two times. The percentage of oxytocin remaining in each of the infusion after day zero was calculated based on the oxytocin content at day zero. The drug concentration was considered stable if its concentration was more than 90% of the initial concentration.

2.9. *Data Analysis*

Student's *t*-test was used to compare the difference between the data of interest with $\alpha = 0.05$ as the minimal level of significance. Wherever possible, the data is presented as mean ± standard deviation.

3. Results

3.1. *Standard curve and method validation*

The chromatogram of oxytocin standards in normal saline showed a peak at retention time of 11.6 min (Figure 1). A blank sample (normal saline only) was also injected to the HPLC system and a peak at 5.4 min was observed from this sample. No peak was observed when sterile water or mobile phase was injected to the HPLC system. Thus the first peak in the chromatogram is because of normal saline and the second peak at 11.6 min is for oxytocin. As shown in Figure 2, a good linearity was exhibited in the concentration range (0.01-0.04 U/mL) by using the presently developed HPLC method. The average coefficient of determination of 0.99 was observed for the standard curve. The slopes of the curves illustrated an excellent agreement with coefficient of variability.

The intra- and inter-day relative standard deviations (RSD) were calculated to be 1.83% and 1.67%, respectively. For each concentration studied, a relative error (RE) of less than 10% was obtained. An acceptable precision and accuracy was acquired by this method for all the standards and quality controls based on the recommended criteria (*9*). The percentage recovery of oxytocin using the present HPLC method was also calculated from the peak areas obtained. As shown from the data in Table 1, an admirable recovery was accomplished at each of the added concentration. In accordance to the official requirements the LOQ was 0.005 U/mL.

3.2. *Stability-indicating HPLC method characterization*

Figures 3A and 3B show the degradation of oxytocin after heating at 90°C for 1 h in the presence of 1 M HCl and 1 M NaOH, respectively. As is clear from the chromatograms, multiple degradation product peaks were observed. Under both the conditions, acidic and alkaline, there was significant loss of

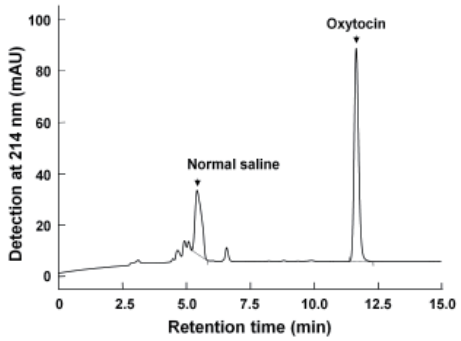

Figure 1. A representative HPLC chromatogram of oxytocin sample (0.02 U/mL) in the saline solution. The chromatogram showed a displacement peak originating from the saline solution at 5.4 min and oxytocin peak at 11.6 min.

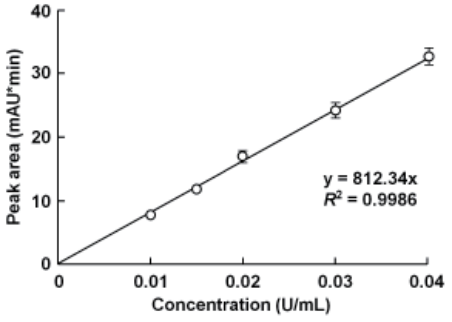

Figure 2. Standard curve of oxytocin assay. The samples were processed by HPLC as described in Section 2.3. For each concentration point 3 set of samples were prepared and this study was done on three different days.

Table 1. Recovery of oxytocin from the standard samples (*n* = 3)

Concentration added (U/mL)	Concentration obtained (U/mL)	Recovery (%)
0.01	0.012 ± 0.0008	100.2
0.03	0.032 ± 0.0011	100.2
0.05	0.053 ± 0.002	100.3

oxytocin after heating at 90°C for 1 h. There was no interference of the degradation products as these peaks were seen at retention times other than the retention time for oxytocin (11.6 min, arrowhead in Figure 3). These results suggest that the present method is sufficiently specific to the drug and that, based on the chromatograms of forced degradation of oxytocin, this method can simultaneously analyze oxytocin and its degradation products in a sample.

3.3. *Physical evaluation*

The oxytocin parenteral solution remained clear throughout the study when kept frozen, under refrigeration, or at room temperature. No precipitation was observed. No significant increase ($p > 0.05$) in absorbance was observed as compared to the freshly read sample of the distilled water at the wavelength of 600 nm (data not shown).

The pH value of normal saline before addition of oxytocin was around 4.40. After the addition of oxytocin this value increases to 5.48 ± 0.18. As shown in Table 2, there was no significant increase or decrease ($p > 0.05$) in this pH value under all the three temperatures used in this study over a period of 30 days.

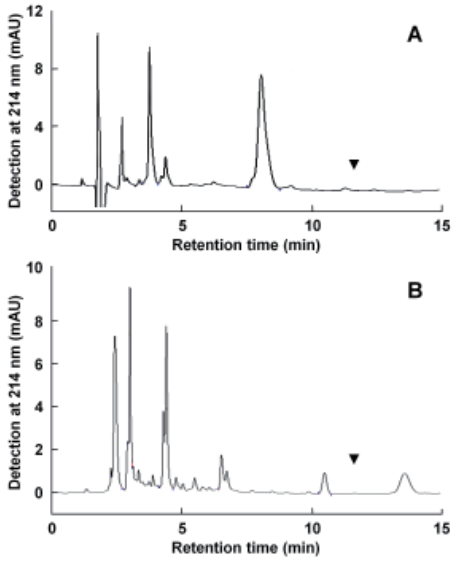

Figure 3. Chromatograms of oxytocin after accelerated degradation. Oxytocin was treated under **(A)** acidic and **(B)** alkaline conditions and the samples were processed by HPLC as described in Section 2.3. Arrowhead: expected elution position of oxytocin (11.6 min).

3.4. *Drug content*

As shown in Figure 4, all the oxytocin parenteral solutions were in the range of 90-110% of the labeled drug amount under frozen (−20°C) and refrigerated (2-6°C) conditions for 30 days; at room temperature (22-25°C) the oxytocin solutions were stable for at least 21 days. Minimal to no degradation was observed and no new degradation peaks were observed in the stable samples (data not shown).

4. Discussion

The stability data of the routinely used large volume parenteral in the final working condition are unavailable as they are commercially not available. Knowing the stability of these preparations would minimize compounding them just before the administration. A concentration of 0.02 U/mL is commonly used in the clinical setting.

The parent drug stability test guideline Q1A (R2) issued by the International Conference on Harmonization (ICH) suggest that stress studies should be carried out on a drug to ascertain its inherent stability characteristics (*10*). A proper identification of degradation products would hence support the suitability of the proposed analytical procedures. It also requires that analytical test procedures for stability samples should be stability-indicating and be fully validated. In order to analyze the concentration of oxytocin, a stability-indicating HPLC method was validated and used for the present study.

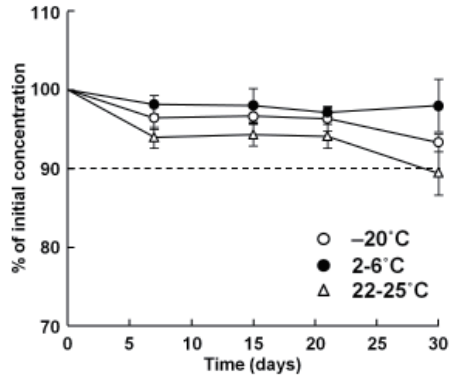

Figure 4. Percentage of initial concentration *versus* time profile for oxytocin parenteral solutions ($n = 9$). Open circle, −20°C; closed circle, 2-6°C; open triangle, 22-25°C. Dashed line indicates 90% of initial concentration of oxytocin.

Table 2. The results of pH analysis ($n = 9$)

Storage temperature	Day 0	Day 7	Day 15	Day 21	Day 30
−20°C	5.48 ± 0.18	5.17 ± 0.15	5.16 ± 0.07	5.16 ± 0.06	5.10 ± 0.13
2-6°C	5.48 ± 0.18	5.22 ± 0.10	5.21 ± 0.04	5.20 ± 0.13	5.08 ± 0.03
22-25°C	5.48 ± 0.18	5.36 ± 0.16	5.33 ± 0.06	5.20 ± 0.04	5.28 ± 0.17

The present HPLC method met with all the acceptance criteria and was sensitive and reproducible enough for the acceptable study of oxytocin in unknown samples. As reported by Trissel (*11*), the failure to recognize the degradation products is the most common point that leads to erroneous reporting of the data on the stability studies.

There are some published studies in the literature that do report the short-term stability of oxytocin (*3,6*). Gard *et al*. (*3*) have reported oxytocin is stable in lactated Ringer's solution and lactated Ringer's-dextrose 5% solution over a 24-hour period at 25°C and over a 7-day period at 5°C. In an attempt to measure long term stability, Boothby *et al*. (*7*) published that oxytocin in lactated Ringer's solution is stable for 31 days at 4 and 25°C. Another comprehensive study done by Trissel *et al*. (*8*) have examined the extended stability of oxytocin in 5% dextrose injection, 0.9% sodium chloride injection, lactated Ringer's injection bags for 90 days at room temperature. Based on their results they have reported that oxytocin diluted in 5% dextrose or 0.9% sodium chloride is stable to be used for 90 days at room temperature. However, when diluted in lactated Ringer's solution it is advisable to be used only for 28 days when stored at room temperature. The most commonly recommended solvent for the dilution of oxytocin for clinical use is 0.9% sodium chloride. It is very pertinent to establish the stability of commonly used concentration of oxytocin solution at three normally used storage temperatures for parenteral products in the hospitals. Thus for the present study we have used all the three different temperature conditions of room temperature (22-25°C), refrigeration (2-6°C), and frozen (−20°C) and done the stability studies for 30 days.

Based on our results, oxytocin parenteral solutions are stable for at least 30 days when stored under refrigerated or frozen conditions. At room temperature, these solutions were observed to be stable for at least 21 days. Trissel *et al*. (*8*) have recommended that the use of oxytocin parenteral solutions should be restricted to no greater than 28 days at room temperature, regardless of the diluent used. The recommendation based on our present study is reasonably more than what is presently used.

A major driver of operations within the pharmacy department in a hospital setting is increasing efficiency and reducing waste. Therefore, Charleston Area Medical Center (CAMC) utilizes a consolidated intravenous medication preparation model where a central, USP <797> compliant clean room prepares many compounded sterile products in batches for use within our organization. Thus, the pharmacy is able to mass produce extemporaneously compound parenteral solutions from this facility and ship the finished products to each hospital of our health system, thus allowing the organization to free up its pharmacy team to provide more direct patient care while improving operational efficiencies. One of the challenges to this model is expiration dating of medications. The aim of the compounding pharmacy is to prepare sterile products that can be compounded in large batches and with long expiration dates. Based on the present study, oxytocin solutions are stable for at least 21 days under different temperature conditions. By consolidating with the pharmacy in a hospital, workload can be removed from each facility thus shortening the turnaround time for the pharmacy to send medications to the patients.

The results of this study show that extended stability for oxytocin parenteral solutions can be assigned. However, assigned stability data should not exceed the mandates from USP <797> in the absence of end product sterility testing according to USP <71>.

5. Conclusion

A stability-indicating method was developed, which separates all the degradation products formed. The present HPLC method meets all the acceptance criteria and was sensitive and reproducible enough for the acceptable study of oxytocin in unknown samples. A good linearity of the standard curves with reproducible slopes was observed with this method. Hence it is recommended for analysis of the drug and degradation products in stability samples. The present method proved to be rapid and simple, and its precision is sufficient for routine quality control of oxytocin.

The oxytocin solutions were stable for at least 21 days under all the temperatures studied in the concentrations normally used in clinical setting when prepared in 0.9% sodium chloride (normal saline) for parenteral use. The extended stability of this preparation can improve operational efficiency, reduce waste, and reduce medication delivery delays.

Acknowledgements

This project was supported by the CAMC Health Education and Research Institute, Inc. and Charleston Area Medical Center Foundation, Inc. of Charleston, WV, USA.

References

1. Balki M, Ronayne M, Davies S, Fallah S, Kingdom J, Windrim R, Carvalho JC. Minimum oxytocin dose requirement after cesarean delivery for labor arrest. Obstet Gynecol. 2006; 107:45-50.
2 Elbourne D, Prendiville W, Chalmers I. Choice of oxytocic preparation for routine use in the management of the third stage of labour: An overview of the evidence from controlled trials. Brit J Obstet Gynecol. 1988; 95:17-30.
3 Gard JW, Alexander JM, Bawdon RE, Albrecht JT. Oxytocin preparation stability in several common obstetric intravenous solutions. Am J Obstet Gynecol. 2002; 186:496-498.
4 Nordström L, Fogelstam K, Fridman G, Larsson A,

Rydhstroem H. Routine oxytocin in the third stage of labour: A placebo controlled randomised trial. Brit J Obstet Gynecol. 1997; 104:781-786.
5 McEvoy GK. AHFS Drug Information. AHFS Drug Information 2005, Bethesda, MD: American Society of Health-System Pharmacists.
6 Chang CH, Ashford WR, Ives DA, *et al*. Stability of oxytocin in various infusion solutions. Can J Hosp Pharm. 1972; 25:152.
7 Boothby LA, Madabushi R, Kumar V, Breland BD, Hatton RC, Doering PL, Derendorf H. Extended Stability of Oxytocin in Ringer's Lactate Solution at 4° and 25°C. Hosp Pharm. 2006; 41:437-441.
8 Trissel LA, Zhang Y, Douglass K, Kastango E. Extended stability of oxytoc in common infusion solutions. Int J Pharm Comp. 2006; 10:156-158.
9 Karnes HT, March C. Precision, accuracy, and data acceptance criteria in biopharmaceutical analysis. Pharm Res. 1993; 10:1420-1426.
10 Food and Drug Administration, HHS. International Conference on Harmonisation; Stability Data Package for Registration Applications in Climatic Zones III and IV; Stability Testing of New Drug Substances and Products; availability. Notice. Fed Regist. 2003; 68:65717-65718.
11 Trissel LA. Avoiding common flaws in stability and compatibility studies of injectable drugs. Am J Hosp Pharm. 1983; 40:1159-1160.

(*Received September 29, 2011; Revised November 13, 2011; Re-revised January 20, 2012; Accepted January 21, 2012****)***

DD&T
Drug Discoveries & Therapeutics

Guide for Authors

1. Scope of Articles

Drug Discoveries & Therapeutics welcomes contributions in all fields of pharmaceutical and therapeutic research such as medicinal chemistry, pharmacology, pharmaceutical analysis, pharmaceutics, pharmaceutical administration, and experimental and clinical studies of effects, mechanisms, or uses of various treatments. Studies in drug-related fields such as biology, biochemistry, physiology, microbiology, and immunology are also within the scope of this journal.

2. Submission Types

Original Articles should be well-documented, novel, and significant to the field as a whole. An Original Article should be arranged into the following sections: Title page, Abstract, Introduction, Materials and Methods, Results, Discussion, Acknowledgments, and References. Original articles should not exceed 5,000 words in length (excluding references) and should be limited to a maximum of 50 references. Articles may contain a maximum of 10 figures and/or tables.

Brief Reports definitively documenting either experimental results or informative clinical observations will be considered for publication in this category. Brief Reports are not intended for publication of incomplete or preliminary findings. Brief Reports should not exceed 3,000 words in length (excluding references) and should be limited to a maximum of 4 figures and/or tables and 30 references. A Brief Report contains the same sections as an Original Article, but the Results and Discussion sections should be combined.

Reviews should present a full and up-to-date account of recent developments within an area of research. Normally, reviews should not exceed 8,000 words in length (excluding references) and should be limited to a maximum of 100 references. Mini reviews are also accepted.

Policy Forum articles discuss research and policy issues in areas related to life science such as public health, the medical care system, and social science and may address governmental issues at district, national, and international levels of discourse. Policy Forum articles should not exceed 2,000 words in length (excluding references).

Case Reports should be detailed reports of the symptoms, signs, diagnosis, treatment, and follow-up of an individual patient. Case reports may contain a demographic profile of the patient but usually describe an unusual or novel occurrence. Unreported or unusual side effects or adverse interactions involving medications will also be considered. Case Reports should not exceed 3,000 words in length (excluding references).

News articles should report the latest events in health sciences and medical research from around the world. News should not exceed 500 words in length.

Letters should present considered opinions in response to articles published in Drug Discoveries & Therapeutics in the last 6 months or issues of general interest. Letters should not exceed 800 words in length and may contain a maximum of 10 references.

3. Editorial Policies

Ethics: Drug Discoveries & Therapeutics requires that authors of reports of investigations in humans or animals indicate that those studies were formally approved by a relevant ethics committee or review board.

Conflict of Interest: All authors are required to disclose any actual or potential conflict of interest including financial interests or relationships with other people or organizations that might raise questions of bias in the work reported. If no conflict of interest exists for each author, please state "There is no conflict of interest to disclose".

Submission Declaration: When a manuscript is considered for submission to Drug Discoveries & Therapeutics, the authors should confirm that 1) no part of this manuscript is currently under consideration for publication elsewhere; 2) this manuscript does not contain the same information in whole or in part as manuscripts that have been published, accepted, or are under review elsewhere, except in the form of an abstract, a letter to the editor, or part of a published lecture or academic thesis; 3) authorization for publication has been obtained from the authors' employer or institution; and 4) all contributing authors have agreed to submit this manuscript.

Cover Letter: The manuscript must be accompanied by a cover letter signed by the corresponding author on behalf of all authors. The letter should indicate the basic findings of the work and their significance. The letter should also include a statement affirming that all authors concur with the submission and that the material submitted for publication has not been published previously or is not under consideration for publication elsewhere. The cover letter should be submitted in PDF format. For example of Cover Letter, please visit http://www.ddtjournal.com/downcentre.php (Download Centre).

Copyright: A signed JOURNAL PUBLISHING AGREEMENT (JPA) must be provided by post, fax, or as a scanned file before acceptance of the article. Only forms with a hand-written signature are accepted. This copyright will ensure the widest possible dissemination of information. A form facilitating transfer of copyright can be downloaded by clicking the appropriate link and can be returned to the e-mail address or fax number noted on the form (Please visit Download Centre). Please note that your manuscript will not proceed to the next step in publication until the JPA form is received. In addition, if excerpts from other copyrighted works are included, the author(s) must obtain written permission from the copyright owners and credit the source(s) in the article.

Suggested Reviewers: A list of up to 3 reviewers who are qualified to assess the scientific merit of the study is welcomed. Reviewer information including names, affiliations, addresses, and e-mail should be provided at the same time the manuscript is submitted online. Please do not suggest reviewers with known conflicts of interest, including participants or anyone with a stake in the proposed research; anyone from the same institution; former students, advisors, or research collaborators (within the last three years); or close personal contacts. Please note that the Editor-in-Chief may accept one or more of the proposed reviewers or may request a review by other qualified persons.

Language Editing: Manuscripts prepared by authors whose native language is not English should have their work proofread by a native English speaker before submission. If not, this might delay the publication of your manuscript in Drug Discoveries & Therapeutics.

The Editing Support Organization can provide English proofreading, Japanese-English translation, and Chinese-English translation services to authors who want to publish in Drug Discoveries & Therapeutics and need assistance before submitting a manuscript. Authors can visit this organization directly at http://www.iacmhr.com/iac-eso/support.php?lang=en. IAC-ESO was established to facilitate manuscript preparation by researchers whose native language is not English and to help edit works intended for international academic journals.

4. Manuscript Preparation

Manuscripts should be written in clear, grammatically correct English and submitted as a Microsoft Word file in a single-column format. Manuscripts must be paginated and typed in 12-point Times New Roman font with 24-point line spacing. Please do not embed figures in the text. Abbreviations should be used as little as possible and should be explained at first mention unless the term is a well-known abbreviation (*e.g.* DNA). Single words should not be abbreviated.

Title page: The title page must include 1) the title of the paper (Please note the title should be short, informative, and contain the major key words); 2) full name(s) and affiliation(s) of the author(s), 3) abbreviated names of the author(s), 4) full name, mailing address, telephone/fax numbers, and e-mail address of the corresponding author; and 5) conflicts of interest (if you have an actual or potential conflict of interest to disclose, it must be included as a footnote on the title page of the manuscript; if no conflict of interest exists for each author, please state "There is no conflict of interest to disclose"). Please visit Download Centre and refer to the title page of the manuscript sample.

Abstract: A one-paragraph abstract consisting of no more than 250 words must be included. The abstract should briefly state the purpose of the study, methods, main findings, and conclusions. Abbreviations must be kept to a minimum and non-standard abbreviations explained in brackets at first mention. References should be avoided in the abstract. Key words or phrases that do not occur in the title should be included in the Abstract page.

Introduction: The introduction should be a concise statement of the basis for the study and its scientific context.

Materials and Methods: The description should be brief but with sufficient detail to enable others to reproduce the experiments. Procedures that have been published previously should not be described in detail but appropriate references should simply be cited. Only new and significant modifications of previously published procedures require complete description. Names of products and manufacturers with their locations (city and state/country) should be given and sources of animals and cell lines should always be indicated. All clinical investigations must have been conducted in accordance with Declaration of Helsinki principles. All human and animal studies must have been approved by the appropriate institutional review board(s) and a specific declaration of approval must be made within this section.

Results: The description of the experimental results should be succinct but in sufficient detail to allow the experiments to be analyzed and interpreted by an independent reader. If necessary, subheadings may be used for an orderly presentation. All figures and tables must be referred to in the text.

Discussion: The data should be interpreted concisely without repeating material already presented in the Results section. Speculation is permissible, but it must be well-founded, and discussion of the wider implications of the findings is encouraged. Conclusions derived from the study should be included in this section.

Acknowledgments: All funding sources should be credited in the Acknowledgments section. In addition, people who contributed to the work but who do not meet the criteria for authors should be listed along with their contributions.

References: References should be numbered in the order in which they appear in the text. Citing of unpublished results, personal communications, conference abstracts, and theses in the reference list is not recommended but these sources may be mentioned in the text. In the reference list, cite the names of all authors when there are fifteen or fewer authors; if there are sixteen or more authors, list the first three followed by *et al*. Names of journals should be abbreviated in the style used in PubMed. Authors are responsible for the accuracy of the references. Examples are given below:

Example 1 (Sample journal reference):
Nakata M, Tang W. Japan-China Joint Medical Workshop on Drug Discoveries and Therapeutics 2008: The need of Asian pharmaceutical researchers' cooperation. Drug Discov Ther. 2008; 2:262-263.

Example 2 (Sample journal reference with more than 15 authors):
Darby S, Hill D, Auvinen A, *et al*. Radon in homes and risk of lung cancer: Collaborative analysis of individual data from 13 European case-control studies. BMJ. 2005; 330:223.

Example 3 (Sample book reference):
Shalev AY. Post-traumatic stress disorder: Diagnosis, history and life course. In: Post-traumatic Stress Disorder, Diagnosis, Management and Treatment (Nutt DJ, Davidson JR, Zohar J, eds.). Martin Dunitz, London, UK, 2000; pp. 1-15.

Example 4 (Sample web page reference):
World Health Organization. The World Health Report 2008 – primary health care: Now more than ever. *http://www.who.int/whr/2008/whr08_en.pdf* (accessed September 23, 2010).

Tables: All tables should be prepared in Microsoft Word or Excel and should be arranged at the end of the manuscript after the References section. Please note that tables should not in image format. All tables should have a concise title and should be numbered consecutively with Arabic numerals. If necessary, additional information should be given below the table.

Figure Legend: The figure legend should be typed on a separate page of the main manuscript and should include a short title and explanation. The legend should be concise but comprehensive and should be understood without referring to the text. Symbols used in figures must be explained.

Figure Preparation: All figures should be clear and cited in numerical order in the text. Figures must fit a one- or two-column format on the journal page: 8.3 cm (3.3 in.) wide for a single column, 17.3 cm (6.8 in.) wide for a double column; maximum height: 24.0 cm (9.5 in.). Please make sure that artwork files are in an acceptable format (TIFF or JPEG) at minimum resolution (600 dpi for illustrations, graphs, and annotated artwork, and 300 dpi for micrographs and photographs). Please provide all figures as separate files. Please note that low-resolution images are one of the leading causes of article resubmission and schedule delays. All color figures will be reproduced in full color in the online edition of the journal at no cost to authors.

Units and Symbols: Units and symbols conforming to the International System of Units (SI) should be used for physicochemical quantities. Solidus notation (*e.g.* mg/kg, mg/mL, mol/mm^2/min) should be used. Please refer to the SI Guide www.bipm.org/en/si/ for standard units.

Supplemental data: Supplemental data might be useful for supporting and enhancing your scientific research and Drug Discoveries & Therapeutics accepts the submission of these materials which will be only published online alongside the electronic version of your article. Supplemental files (figures, tables, and other text materials) should be prepared according to the above guidelines, numbered in Arabic numerals (*e.g.*, Figure S1, Figure S2, and Table S1, Table S2) and referred to in the text. All figures and tables should have titles and legends. All figure legends, tables and supplemental text materials should be placed at the end of the paper. Please note all of these supplemental data should be provided at the time of initial submission and note that the editors reserve the right to limit the size and length of Supplemental Data.

5. Submission Checklist

The Submission Checklist will be useful during the final checking of a manuscript prior to sending it to Drug Discoveries & Therapeutics for review. Please visit Download Centre and download the Submission Checklist file.

6. Online submission

Manuscripts should be submitted to Drug Discoveries & Therapeutics online at http://www.ddtjournal.com. The manuscript file should be smaller than 5 MB in size. If for any reason you are unable to submit a file online, please contact the Editorial Office by e-mail at office@ddtjournal.com

7. Accepted manuscripts

Proofs: Galley proofs in PDF format will be sent to the corresponding author *via* e-mail. Corrections must be returned to the editor (proof-editing@ddtjournal.com) within 3 working days.

Offprints: Authors will be provided with electronic offprints of their article. Paper offprints can be ordered at prices quoted on the order form that accompanies the proofs.

Page Charge: A page charge of $140 will be assessed for each printed page of an accepted manuscript. The charge for printing color figures is $340 for each page. Under exceptional circumstances, the author(s) may apply to the editorial office for a waiver of the publication charges at the time of submission.

(Revised October 2011)

Editorial and Head Office:

Pearl City Koishikawa 603
2-4-5 Kasuga, Bunkyo-ku
Tokyo 112-0003
Japan
Tel: +81-3-5840-9697
Fax: +81-3-5840-9698
E-mail: office@ddtjournal.com

DD&T
Drug Discoveries & Therapeutics

JOURNAL PUBLISHING AGREEMENT (JPA)

Manuscript No.:

Title:

Corresponding author:

The International Advancement Center for Medicine & Health Research Co., Ltd. (IACMHR Co., Ltd.) is pleased to accept the above article for publication in Drug Discoveries & Therapeutics. The International Research and Cooperation Association for Bio & Socio-Sciences Advancement (IRCA-BSSA) reserves all rights to the published article. Your written acceptance of this JOURNAL PUBLISHING AGREEMENT is required before the article can be published. Please read this form carefully and sign it if you agree to its terms. The signed JOURNAL PUBLISHING AGREEMENT should be sent to the Drug Discoveries & Therapeutics office (Pearl City Koishikawa 603, 2-4-5 Kasuga, Bunkyo-ku, Tokyo 112-0003, Japan; E-mail: office@ddtjournal.com; Tel: +81-3-5840-9697; Fax: +81-3-5840-9698).

1. Authorship Criteria

As the corresponding author, I certify on behalf of all of the authors that:

1) The article is an original work and does not involve fraud, fabrication, or plagiarism.
2) The article has not been published previously and is not currently under consideration for publication elsewhere. If accepted by Drug Discoveries & Therapeutics, the article will not be submitted for publication to any other journal.
3) The article contains no libelous or other unlawful statements and does not contain any materials that infringes upon individual privacy or proprietary rights or any statutory copyright.
4) I have obtained written permission from copyright owners for any excerpts from copyrighted works that are included and have credited the sources in my article.
5) All authors have made significant contributions to the study including the conception and design of this work, the analysis of the data, and the writing of the manuscript.
6) All authors have reviewed this manuscript and take responsibility for its content and approve its publication.
7) I have informed all of the authors of the terms of this publishing agreement and I am signing on their behalf as their agent.

2. Copyright Transfer Agreement

I hereby assign and transfer to IACMHR Co., Ltd. all exclusive rights of copyright ownership to the above work in the journal Drug Discoveries & Therapeutics, including but not limited to the right 1) to publish, republish, derivate, distribute, transmit, sell, and otherwise use the work and other related material worldwide, in whole or in part, in all languages, in electronic, printed, or any other forms of media now known or hereafter developed and the right 2) to authorize or license third parties to do any of the above.

I understand that these exclusive rights will become the property of IACMHR Co., Ltd., from the date the article is accepted for publication in the journal Drug Discoveries & Therapeutics. I also understand that IACMHR Co., Ltd. as a copyright owner has sole authority to license and permit reproductions of the article.

I understand that except for copyright, other proprietary rights related to the Work (*e.g.* patent or other rights to any process or procedure) shall be retained by the authors. To reproduce any text, figures, tables, or illustrations from this Work in future works of their own, the authors must obtain written permission from IACMHR Co., Ltd.; such permission cannot be unreasonably withheld by IACMHR Co., Ltd.

3. Conflict of Interest Disclosure

I confirm that all funding sources supporting the work and all institutions or people who contributed to the work but who do not meet the criteria for authors are acknowledged. I also confirm that all commercial affiliations, stock ownership, equity interests, or patent-licensing arrangements that could be considered to pose a financial conflict of interest in connection with the article have been disclosed.

Corresponding Author's Name (Signature):

Date: